Energy Storage System (ES...

H$_2$ production

H$_2$ storage

H$_2$

NH$_3$ production

NH... sto...

N$_2$

MVC

water

air

N$_2$ production

electricity

power from NH$_3$

electricity

...MAND ...OFILE

Analysis of Islanded Ammonia-based Energy Storage Systems

Analysis of Islanded Ammonia-based Energy Storage Systems

René Bañares-Alcántara [1]
Gerard Dericks III [2]
Maurizio Fiaschetti [2]
Philipp Grünewald [3]
Joaquín Masa Lopez [1]
Edman Tsang [4]
Aidong Yang [1]
Lin Ye [4]
Shangyi Zhao [1]

[1] Department of Engineering Science
[2] Smith School of Enterprise and the Environment
[3] Environmental Change Institute
[4] Department of Chemistry

University of Oxford

Oxford, September 2015

Executive Summary

With the expectation for accelerated penetration of renewable energy in the global energy market, energy storage is becoming an increasingly important component to effectively cope with the intermittent nature of renewable energy supply. This report addresses the techno-economics of an ammonia-based energy storage system (ESS) integrated with renewable electricity generation on an island system (a power network which is not connected to the grid). The ammonia-assisted renewable energy system satisfies specific power (and possibly ammonia) demands. This study reviews the options for the technical components of such a system. We present a mathematical model developed for evaluating the technical performance and economic costs of the system configured with various options at the individual components level. A techno-economic assessment is subsequently presented by applying the model to a number of scenarios. A broader market analysis is also given to place ammonia-based energy storage in the business landscape of renewable energy, energy storage, and ammonia demand and supply. The key observations and conclusions derived from the literature review, model-based assessment and market analysis include:

- Electrolysis and the conversion of stored ammonia to power account for most of the energy losses and for the largest percentage of capital and operating costs of the ESS. Improvement of current technologies or adoption of more advanced ones in the future can have a large impact in making an NH₃-based ESS economically attractive.

- The electrochemical synthesis of ammonia would eliminate the need for electrolysis. However, the reported production rates are very far away from those using heterogeneous catalysts.

- The levelised cost of ammonia (LCOA) via water electrolysis was estimated, using conservative assumptions, to be between 1.5 and 3 times more expensive than that of ammonia produced via natural gas steam reforming.

- There is significant potential for ammonia to bypass electrical grid construction in the exploitation of stranded renewable energy resources. There may also be a market for an NH₃-based ESS in 'islanded' locations which

simultaneously require both energy storage and anhydrous ammonia fertiliser and where simplicity is valued.

- The market potential for the different combinations of {islanded / non-islanded} operation which produce ammonia {as an energy storage medium / as a chemical commodity / for a dual purpose} varies dramatically.

- Decreasing the concentration of impurities in the ammonia production feedstocks increases the number of suitable ammonia synthesis catalysts.

Acknowledgements

Table of Contents

5

List of Figures

List of Tables

1.   Introduction

Renewable energy is playing an increasingly important role in addressing some of the key challenges facing today's global society, such as energy security and climate change. One of the challenges emerging from the large scale integration of renewable energy technologies into energy systems is their variable output profiles, which may require added system flexibility, for instance in the form of energy storage (IMechE, 2014). To date, a number of mechanical, electrical, thermal, and chemical approaches have been developed for storing electrical energy from renewable sources (IMechE, 2014), (Evans et al., 2012) and (Chen et al., 2009). These approaches vary broadly in terms of efficiency, capacity, cost, response time as well as technical maturity.

1.1 Aim and objectives

Our work focuses on renewable electrical energy storage with ammonia. This approach has previously not been assessed comprehensively except in the recent work by Morgan (Morgan, 2013). Ammonia has received considerable attention in the past as a potential energy storage medium (see http://nh3fuelassociation.org).
This work considers an "islanded" system (a power network which is not connected to the grid), in which a renewable electricity generation facility (e.g. a wind farm) is integrated with an ammonia-based energy storage system, such that the whole "energy island" can provide power output to meet a specified power demand profile, with or without additionally supplying ammonia as a separate product to meet other needs, e.g. local agriculture.

Five objectives will be addressed in this report:

1. Produce a preliminary assessment of the key technology options for ammonia production in connection with intermittent renewable electricity generation, ammonia-based energy storage, and its integration to ammonia fuelled power generation (or to be used as a raw material for fertiliser production).

2. Produce a techno-economic assessment for each of the key options and scenarios identified with an indication of optimum configurations.

3. Assess the interaction of ammonia production and conversion with islanded electricity markets at various operating conditions.

4. Characterise the key performance criteria of different options and actions for the improvement of the overall system.

5. Derive key sensitivities and risks in the development of technology options.

1.2 Project approach and report structure

A range of concerted research activities have been carried out to address the above objectives. These include a literature review of existing technologies and systems, the development of a quantitative technical and costing model, a techno-economic assessment based on the model, and a market analysis. The outcomes are documented in the following parts of the report.

Section 2: Existing literature on the technologies involved in the components of the ammonia-based energy storage system is reviewed. These include options for electrolysis for producing hydrogen (H$_2$), air separation for producing nitrogen (N$_2$), ammonia (NH$_3$) synthesis, as well as storage of H$_2$, N$_2$ and NH$_3$. This review focuses particularly on the technical specifications of these options, hence providing technical parameters for the model reported in Section 4.

Section 3: A critical review is presented on the catalytic chemical conversion involved in the Haber-Bosch (HB) synthesis of ammonia, particularly the characteristics and performance of a range of catalysts. A review is also conducted on the chemistry of non-conventional ammonia synthesis and that of ammonia decomposition processes potentially involved in ammonia to power conversion.

Section 4: The technical and costing model is presented. Part (a) quantifies the performance and economic cost of each technical component of the NH$_3$-based energy storage system, and part (b) quantifies technically and economically the entire system for a given wind power availability, a set of selected system components, and a demand to be met.

Section 5: Based on the model described in Section 4, a techno-economic assessment is reported to reveal how the options in technology selection affect the efficiencies and economic costs of the entire system.

Section 6: A broad market analysis is presented to place NH$_3$-based energy storage in the business landscape of renewable energy, energy storage, and ammonia demand and supply.

Section 7: Concluding the report, a list of key observations and suggestions is presented to highlight future opportunities in technological and business development.

2. State of the art and emerging technologies

The nature of this project, which integrates wind power with ammonia production, gives rise to special technical requirements and considerations in order to successfully merge these two technologies. The following challenges were identified:

- An all-electric ammonia production process will have intrinsic differences to the conventional natural gas driven Haber-Bosch (HB) process, impacting energy and purity requirements amongst other performance indicators.
- The variability of wind loads means the process should be as flexible as possible, influencing technology decisions.
- The scalability of compatible technologies with an all-electric process is a matter not widely discussed in literature.

For these reasons, and to gain a scope of the feasible scenarios our model can portray, a technical assessment of available technologies is detailed in the following sub-sections.

Section 2.1 is an overview of the main aspects of conventional ammonia production, commonly known as the Haber-Bosch process. In Section 2.2 a description of our ammonia-based Energy Storage System (ESS) is introduced. A review and analysis of each of the modules that make up our ESS, namely hydrogen production, nitrogen production, and ammonia synthesis, follows in sections 2.2.1, 2.2.2, and 0 respectively, along with a comparison of the available technology options.

2.1 State of the Art: the Haber-Bosch process

The Haber-Bosch process was developed in the early 20th century and accounts for 90% of the total current ammonia production (Appl, 1999). An overview of the process is shown in Figure 2-1.
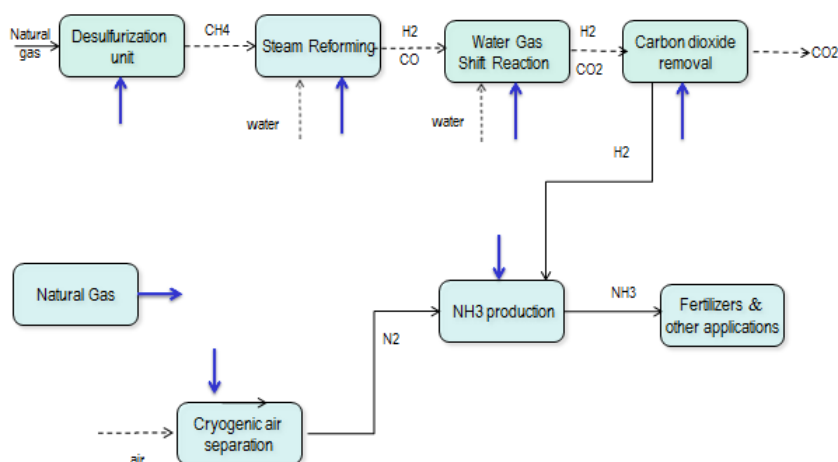
Figure 2-1: Main steps for the conventional production of ammonia (Haber-Bosch process).

The process reaction is shown in Eqn. 2-1:

Eqn. 2-1: $$N_2 + 3H_2 \leftrightarrow 2NH_3 \quad \Delta H = -46.22 \; kJ/mol$$
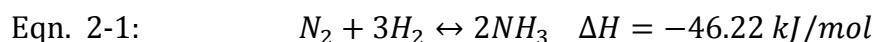
A mixture of hydrogen and nitrogen, also called synthesis gas, reacts in stoichiometric amounts over a Fe-based catalyst at temperatures of 400-500 C and pressures above 100 bars. The unfavourable kinetics at STP, combined with the strong thermodynamic barrier the nitrogen triple bond dissociation poses (941 kJ/mol, (Morgan, 2013)), force these conditions as a prerequisite for reasonable ammonia production rates.

The HB process is a commercially mature technology that has experimented very little changes in the past 50 years. This is because synthetic gas production represents the highest proportion of total ammonia production costs (Appl, 2012). Around 80% of total ammonia synthesis uses natural gas as feedstock; less popular alternatives are coal gasification, methanol cracking and partial oxidation (Morgan et al., 2014).

This traditional natural gas ammonia synthesis involves a series of steps for the formation and purification of hydrogen. As appreciated in Figure 2-1, these include desulphurisation of the initial feedstock, steam reforming of natural gas to produce CO and hydrogen, shift conversion of CO into CO_2 and, finally, absorption and subsequent removal of the CO_2 formed. Nitrogen is usually produced through cryogenic distillation, though in some cases air is fed to a secondary reformer where oxygen will react with the produced hydrogen to create a stoichiometric mixture of synthesis gas (Bartels, 2008). This gas then enters a synthesis loop where it reacts to form ammonia.

This process is very energy intensive; (Benner et al., 2012) reports a consumption of 22.1 GJ/ton_NH$_3$ for the feed, plus a consumption of 7.2-9.0 GJ/ton_NH$_3$ for fuel. The CO$_2$ emission associated with these energy demands is reported to be 1.2 ton_CO$_2$/ ton_NH$_3$ and 0.4-0.5 ton_CO$_2$/ton_ NH$_3$ respectively. Based on the lower heating value of ammonia, taken to be 18.7 MJ/kg, the efficiency of this process is around 60-64 % (Morgan et al., 2014).

2.2 Emerging technologies

There are various criteria on which we can assess the feasibility of merging ammonia production with wind power; an intermittent, electric source of energy. The feasibility of an ammonia-based energy storage system will be heavily dependent on various factors:

- The selection of technologies, which will determine the overall power requirements and efficiency. Key parameters from the literature review will be implemented on the model to assess the various scenarios contemplated.
- The flexibility of the various processes to power fluctuations. This can be seen from two perspectives: (a) the resilience of the catalyst to varying temperature and pressure cycles, and (b) the variation of efficiency with load. These will have an influence on the logic behind the model.
- The production rates achievable by different technologies will influence the scenarios we will regard as competitive.

In the conclusion of every sub-section a table with the parameters taken by the model is shown, along with a discussion on the issues mentioned above.
Figure 2-2 shows a schematic overview of the different units in our process.
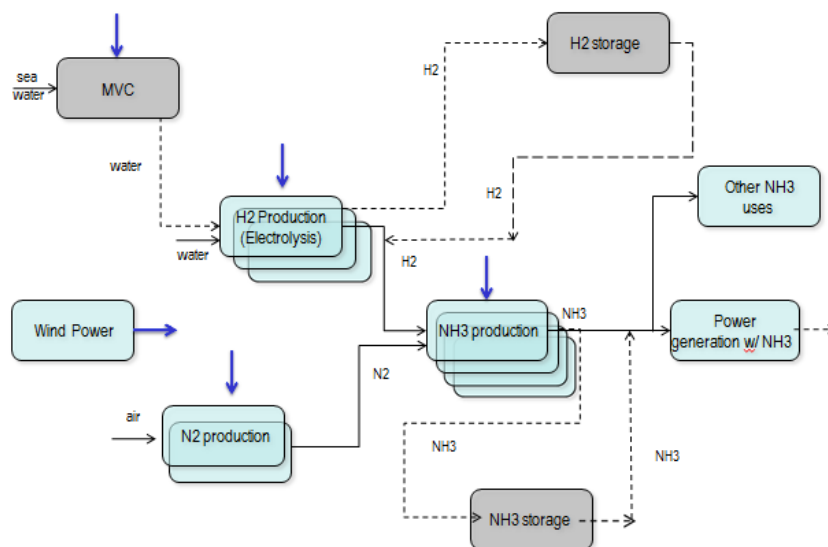
Figure 2-2: Breakdown of the ammonia-based Energy Storage System.

Relating back to Figure 2-1 we can appreciate two main differences, the production of H_2 via an electrolytic route, as opposed to steam reforming, and the number of options considered for H_2, N_2 and NH_3 production.

Regarding the former, the introduction of Section 2.2.1, Hydrogen production, compares these two processes and their influence on the main parameters of the overall ESS. Regarding the latter, there is a critical review on three different catalytic options detailed in Section 3; these are the conventional Fe-based catalyst and two alternatives: Ru- and CoMoN-based catalysts with the conventional HB synthesis loop as the framework of analysis. Section 0, Ammonia production, focuses on the main features of the synthesis loop and states the main operating parameters of the three catalysts explored.

2.2.1 Hydrogen production

The economic feasibility of the conventional HB process relies on the cheap cost of natural gas, as 70-90% of total ammonia production costs are natural gas purchasing costs (Benner et al., 2012). The sensitivity of this process to natural gas prices and availability has driven research to more sustainable and independent ways to produce synthesis gas, particularly hydrogen.

An electric current will split water into its two components, oxygen and hydrogen; this is the principle of electrolysis. For ammonia production purposes electrolysis represents less than 0.5% of world production (Morgan, 2013). It is the only

process that complies with an all-electric ammonia production and that can achieve reasonable rates of production.

Figure 2-3 from (Stoll and von Linde, 2000) shows how the cost per m^3 of hydrogen varies with plant capacity for both the fossil fuel based ammonia synthesis technologies and for electrolysis. Electrolysis curves 4 and 5 correspond to electricity prices of 0.04 $/kWh and 0.08 $/kWh respectively.
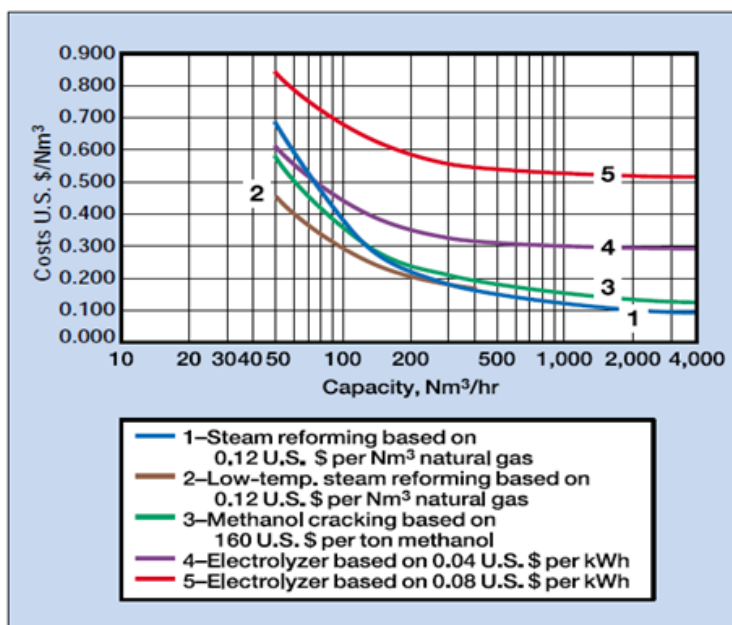
Figure 2-3: Cost of hydrogen production for different technologies. Source: (Stoll and von Linde, 2000).

Figure 2-3 shows that electrolysis-based NH$_3$ production is less competitive for nearly all capacities. There are two main reasons for this: the first one is the higher energy requirements of electrolysis due to the thermodynamic barrier of splitting water, theoretically 39.4 kWh/kg_H$_2$ (Morgan, 2013). (Giddey et al., 2013) reports a consumption of 43.2 GJ/ton_NH$_3$ if electrolysis is used as the hydrogen production route, compared to 34.2 GJ/ton_NH$_3$ via steam reforming. (Appl, 2012), on the other hand, argues that water electrolysis consumes 34 GJ/ton_NH$_3$ just considering the caloric equivalent, i.e. if fossil fuels were to supply this energy with an efficiency of 40%, the consumption would be driven up to 85 GJ/ton_NH$_3$, three times as much as the best value of 28 GJ/ton_NH$_3$ for steam reforming production. As a final comparison figure, (Stoll and von Linde, 2000) reports a CO$_2$ emission of 2.4 ton_CO$_2$/ton_H$_2$ if the energy demands of the electrolysers where supplied with natural gas, compared to emissions of 0.8 ton_CO$_2$/ton_H$_2$ for natural gas based production.

23

The second reason for this disparity comes from scale of current ammonia plants. Most of them produce 1000-1500 tons /day (Morgan, 2013), whilst electrolysis units tend to be modular in nature and hence do not benefit from economies of scale. This can be appreciated in Figure 2-3; beyond 400 Nm³/hr the slope of curves 4 and 5 is practically flat.

It is clear from the above discussion that applications involving large-scale ammonia production based on electrolysis are not competitive at present. However, the reliance of the HB process on natural gas costs both as a feed material and a fuel means this could change in the future. Furthermore, assessment of this process may need to consider other factors, such as CO_2 emissions.

There are various electrolytic configurations available. Table 2-1 shows various commercial units along with their operation parameters.

Manufacturer	Technology	← Operating Range Available Today →			
		System Energy Requirement (kWh/kg)	H₂ Production Rate (kg/yr)	Power Required for Max. H₂ Production Rate (kW)	H₂ Product Pressure (psig)
Avalence	Unipolar Alkaline	56.4 – 60.5	320 – 3,600	2-25	Up to 10,000
Proton	PEM	62.3 – 70.1	400 - 7,900	3-63	~200
Teledyne	Bipolar Alkaline	59.0 – 67.9	2,200 - 33,000	17-240	60-115
Stuart	Bipolar Alkaline	53.4 – 54.5	2,400 - 71,000	15-360	360
Norsk Hydro	Bipolar Alkaline (high pressure)	53.4	7,900 - 47,000	48-290	~230
	Bipolar Alkaline (atmospheric)	53.4	39,000 - 380,000	240-2,300	0.3

Table 2-1: Commercially available electrolysis units. Source: NREL Technology Brief: Analysis of Current-Day Commercial Electrolyzers (http://www.nrel.gov/docs/fy04osti/36705.pdf)

The main types of electrolysers available are Atmospheric Alkaline, High Pressure Alkaline, Proton Exchange Membranes (PEM) and Solid Oxide fuel cells. The first three are mature established technologies, whilst Solid Oxide fuel cells are still under development and thus will not be discussed further.

The following subsections will discuss the main features and parameters of these three types of electrolysers. All of them are constrained by the thermodynamic energy requirement of 39.4 kWh /kg_H₂. Additionally, electrolysers have a very high water purity requirement, as well as requiring softening to a specific resistance of 1-2 MΩ/cm (Benner et al., 2012). These stringent requirements

create the need for a mechanical vapour compression unit (MVC) prior to the electrolysis unit. Its specifications are detailed in Section 2.2.1.4.

2.2.1.1 Alkaline electrolysis

Alkaline electrolysis is the most mature and commercially employed electrolytic technology at present, especially for large scale systems (Jensen et al., 2008). A cross section of the electrolytic cell is shown in Figure 2-4. These electrolysers typically employ an aqueous solution containing KOH as the electrolyte with a weight of 20-30% in the solution (Jensen et al., 2008). The current applied will transfer ions through the NiO diaphragm.
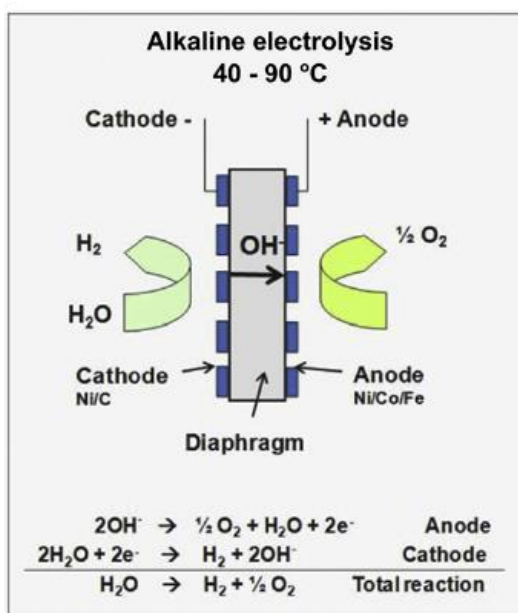
Figure 2-4: Alkaline electrolysis system model. Source: (Carmo et al., 2013).

As seen in Table 2-1, the lowest power requirement for atmospheric alkaline electrolysers is reported to be 53.4 KWh/ kg_H$_2$. This implies a maximum efficiency of 73.8% (based on a minimum energy requirement of 39.4 KWh/Kg_H$_2$). This device operates with DC current, so the overall efficiency must take into account the transformer/rectifier efficiency, stated commonly as 95% x 95%. The current density range of operation is 200-600 mA/ cm^2 (Morgan, 2013).

The load range at which these units can operate is 20-100%. It is possible to increase this load range by arranging, in parallel, various electrolysers of different magnitudes (Gutiérrez-Martín et al., 2010). (Morgan et al., 2014) states that once the electrolysers are hot their dynamic response to sudden changes in power is good, assuming an advanced thermal control system. As mentioned before,

atmospheric electrolysis produces very high purity hydrogen, only containing residual amounts of oxygen. Oxygen is poisonous to the catalyst in the HB synthesis loop, so these impurities are normally removed in a catalytic converter where they react with minimal amounts of hydrogen to produce water (Grundt and Christiansen, 1982).

Figure 2-5 shows the variation of current density and cost with load, in this case named utilisation factor. Gutierrez-Martin et al. (Gutiérrez-Martín et al., 2009) state that the energy consumption per unit of product increases linearly with the current density. It is clear from the graph that electrolysers are more efficient at higher loads. There are also results that efficiency decreases 5-10% as the utilization factor decreases from 1.0 to 0.25 (Gutiérrez-Martín et al., 2009) and (Ursúa et al., 2009).
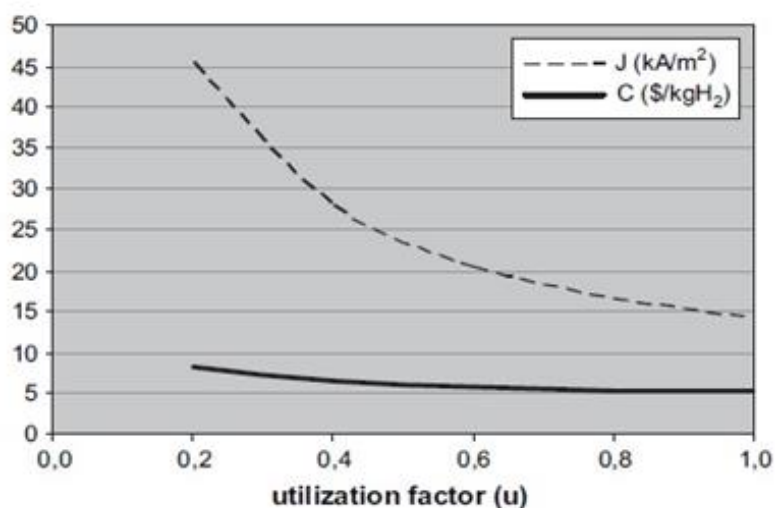
Figure 2-5: Current density and unit cost variation with utilisation factor, Source: (Gutiérrez-Martín et al., 2009).

One disadvantage of this type of electrolyser is that the product must be dried and rinsed before it is mixed with nitrogen prior to being fed to the synthesis loop. This is partly because of the inability of the NiO diaphragm to prevent cross diffusing, combined with the fact that output hydrogen is at low pressure, configurations of this type tend to be bulky in nature (Carmo et al., 2013). The low maximum current density the system can handle means the scope of improvement of this technology is handicapped.

2.2.1.2   High Pressure Alkaline electrolysis

The main operating characteristics of HP alkaline electrolysers are similar to those of the atmospheric alkaline electrolyser described in Section 2.2.1.1, however with an elevated outlet pressure of the product H_2. The impact of a higher operating pressure on the efficiency of the electrolyser appears to be complex. The reversible (ideal) thermodynamics favours lower pressures. A higher operating pressure may reduce certain losses in the electrolyser (Jensen et al., 2008), but may affect in various ways the other parts of an electrolysis plant (Roy et al., 2006), (Bensmann et al., 2013). Nevertheless, based on the data of an existing industrial unit, as shown in Table 2-1, it seems to be possible that the energy requirement of this unit is the same as for the atmospheric alkaline electrolyser counterpart, with two differences; lower attainable production rates, and the fact that high pressure operation will reduce downstream compression requirements. The trade-off between these two factors is explored in Section 5, and is the reason for the inclusion of this unit in the review.

2.2.1.3   Proton Exchange Membrane (PEM) electrolysis

PEM electrolysers are often presented as the best alternative to the commercially established alkaline electrolysers. Their characteristics are inherently different, which gives a wider range of scenarios relating to technology choices. However, their limited production rates imply their cost effectiveness may decrease substantially for high ammonia plant outputs. A schematic diagram of the structure is shown in Figure 2-6. PEMs operate at 30 bar, using an electrolyte membrane (usually Nafion) which has a thickness of 20-300 micro-meters, giving high proton conductivity.

Referring back to Table 2-1, PEMs have a power requirement of around 62-70 KWh/kg, which implies an efficiency of 56-63%. As with alkaline electrolysers, the transformation from AC to DC power will decrease this efficiency by a small amount. These devices operate at current densities from 1500-2000 mA / cm², around an order of magnitude higher than their alkaline counterparts (Harrison et al., 2009).

PEMs have a load range of 0-100% (Carmo et al., 2013). Additionally, they show an almost immediate response to load changes, as they are not delayed by inertia like liquid electrolytes (Carmo et al., 2013), giving them a really good synergy with wind systems. As with alkaline electrolysers, their efficiency tends to be lower at lower production rates.

PEM electrolysis
20 - 100 °C

Cathode -   + Anode

H_2 H^+ ½ O_2

          H_2O

Cathode   Anode
Pt   Ir

Membrane

H_2O	$\rightarrow$	$2H^+ + \frac{1}{2} O_2 + 2e^-$	Anode
$2H^+ + 2e^-$	$\rightarrow$	H_2	Cathode
H_2O	$\rightarrow$	$H_2 + \frac{1}{2} O_2$	Total reaction
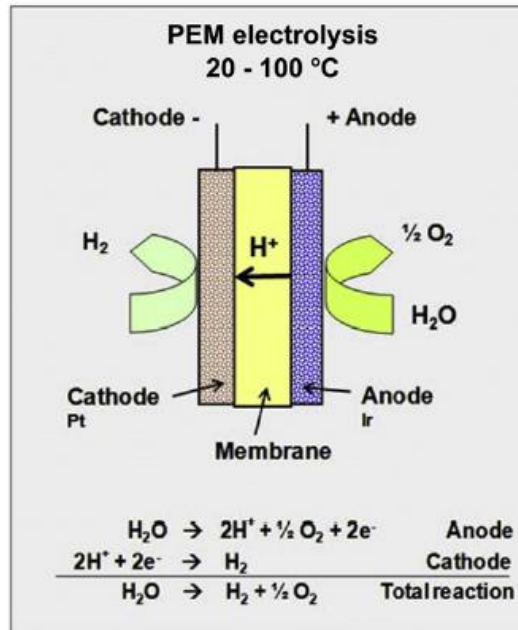
Figure 2-6: PEM electrolysis system model. Source: (Carmo et al., 2013).

The purity output of this system is 99.998%, which eliminates the necessity for any further purification, nor for drying or rinsing. However, according to Table 2-1, the maximum production rate achievable by a PEM electrolyser is 7.9 tons/year. For plants producing around 250 tons of ammonia per day, it is very likely the number of electrolysers needed will quickly make the cost of producing hydrogen via this route uneconomical.

The lack of scalability shown by electrolysers affects PEMs to a higher extent since their production rates are orders of magnitude lower. Additionally, the high cost of the components and the lower durability further makes the cost per unit produced less competitive. However, their operation at high current densities means there is potential to improve the process overall efficiency in the future.

2.2.1.4   Mechanical Vapour Compression (MVC)

As mentioned before, both alkaline and PEM electrolysers have stringent water purity requirements, both in terms of purity and specific resistance. Table 2-2 shows different electrical options for desalination of water, along with some important performance indicators.

If sea water is the input to the desalination plant, electrodialysis would not be able to cope with this feed water quality, as sea water averages 35000 ppm TDS

(Morgan, 2013). Reverse osmosis cannot provide a sufficient purity for successful electrolyser operation, so mechanical vapour compression is the only feasible technology to purify water.

Process	Mechanical power input (kWh/m3 of product)	Feed water quality (ppm TDS)	Product water purity (ppm TDS)
Vapor compression	8–16 (16)	Any	<20
Reverse osmosis	5–13 (10)	Any	250-700
Electrodialysis	12	3000-11000	20-700

Table 2-2: Options for desalination of water. Source: (Morgan, 2013).

The power input, as seen in Table 2-2, is 16 KWh/m^3 of water. The adiabatic efficiency of this process is 75%, and taking the transformer/rectifier efficiency to be 95% the total power input comes down to 22.45 kWh/m^3 of water (Morgan, 2013).

The indifference of MVCs to water purity levels, their high load ranges and their little maintenance requirements makes them a suitable candidate for this process.

2.2.1.5   Hydrogen storage

Hydrogen storage enhances the flexibility of the system; its absence would constraint the logic behind the model to feed all produced hydrogen to the synthesis loop for ammonia production. A short term storage solution combined with an overproduction of hydrogen from stoichiometric levels will allow the system to take advantage of high wind power inputs to satisfy the energy demand of the electrolysers and maintain the ability to produce ammonia, bypassing hydrogen production when wind power inputs are low.

Hydrogen has a density of 0.090 Kg/m^3 at STP, and a volumetric energy density of 10.05 MJ/m^3 at these conditions, based on the LHV (Staffell, 2011). In order to store the required quantities of hydrogen without a large compromise on capital costs derived from high-volume tanks, hydrogen must either be compressed to 200-700 bars or liquefied to -253 C (Bartels, 2008). Both options are very energy

demanding, but in general liquid hydrogen storage is advantageous both in terms of density and volumetric energy density, as can be appreciated in Table 2-3.

Storage Conditions	Density (Kg/m^3)	(Vol.) Energy Density(MJ/L)
Hydrogen at -253 C	72.41	8.685
Hydrogen at 350 bar	23.65	2.837
Hydrogen at 700 bar	39.69	4.761

Table 2-3: Density and volumetric energy density at different storage conditions. Source: (Staffell, 2011).

Additionally, the pressure of operation limits the maximum size of these containers, as well as setting a lower bound on the amount of steel necessary to successfully maintain the storage tanks at the required pressure. Low temperature storage tanks can hold up to 900 tonnes of hydrogen (Bartels, 2008), at least an order of magnitude higher than its high pressure counterparts (Morgan, 2013).

The major drawback of low temperature storage is the need of a refrigerating system to prevent the continuous boil off of the stored hydrogen. Bartels reports an energy consumption of 36 MJ/Kg_H$_2$ for liquefaction and an additional 6.552 MJ/kg_H$_2$ for storage (182 days), with an efficiency of 76.9% based on the HHV (Bartels, 2008).

2.2.1.6   Comparison of hydrogen production technologies

In this section various electrolytic configurations have been explored; Table 2-4 shows the parameters taken by the model for analysis.

From the above discussion, there are intrinsic differences between the electrolytic options displayed in this section. Alkaline electrolysers are a well stablished technology, with good long term stability, which operate at low current densities. HP alkaline electrolysers produce hydrogen at a higher pressure than their atmospheric counterparts. PEMs are less mature and smaller in nature, operate at higher current densities and have a better load range.

Referring to Table 2-4, we can start to envisage the various scenarios for which different configurations will be competitive, in the context of the overall system. For large wind power outputs, alkaline electrolysers are likely to be the only units which can realistically achieve reasonable rates of production without a significant compromise on capital costs.

Main Parameters	Electrolyser Technology		
	Atmospheric Alkaline	High Pressure Alkaline	Proton Exchange Membrane
Power Requirements(KWh/Kg)	53.4	53.4	62.3 - 70.1
Load Range (%)	20 - 100	20 - 100	0 - 100
Production range (tons_H$_2$ /day)	0.1182 - 1.1515	0.0239 - 0.1424	0.0012 - 0.9
Power requirements at load range (GJ/ton)	224.86* - 192.24	** - 192.24	** - 238.32***

(*An efficiency reduction of 10% was applied, for a load range of 20%;

 ** No data; *** Average value of power requirements.)

Table 2-4: Main performance indicators for the electrolytic options explored in this section.

For a smaller energy input all three options are potential candidates for the process. The flexibility and dynamic response of PEMs could prove to be an attractive option for certain wind profiles; the high pressure output of the hydrogen product from the HP alkaline electrolyser could make this option more economical from an overall energy consumption perspective.

As a concluding comment, given the high energy requirements and relatively low production rate of electrolysers, this type of unit will likely dominate the overall capital cost of the system.

2.2.2 Nitrogen production

In terms of cost and energy consumption, nitrogen production is the cheapest and least energy intensive process of all the modules that make up the ammonia production process. Conventional plants will typically use air liquefaction and separation to separate nitrogen from air (Smith and Klosek, 2001). (Morgan, 2013) reports cryogenic distillation accounts for around 90% of total world nitrogen production. In this section this process will be reviewed along with pressure swing absorption, presented in literature as an interesting alternative.

There are two main performance indicators to assess the competitiveness of nitrogen production technology; these are production capacity and product purity. Figure 2-7 shows these two criteria for different technologies.

Membranes are based on a selective barrier that separates high pressure and low pressure process streams based on the different rates of diffusion oxygen and nitrogen exhibit (Smith and Klosek, 2001). Their purity output is on the lower bound of the requirements of the synthesis loop, and at present it is an immature technology that cannot achieve commercial rates of production, as seen in Figure 2-7. Hence it will not be explored further.
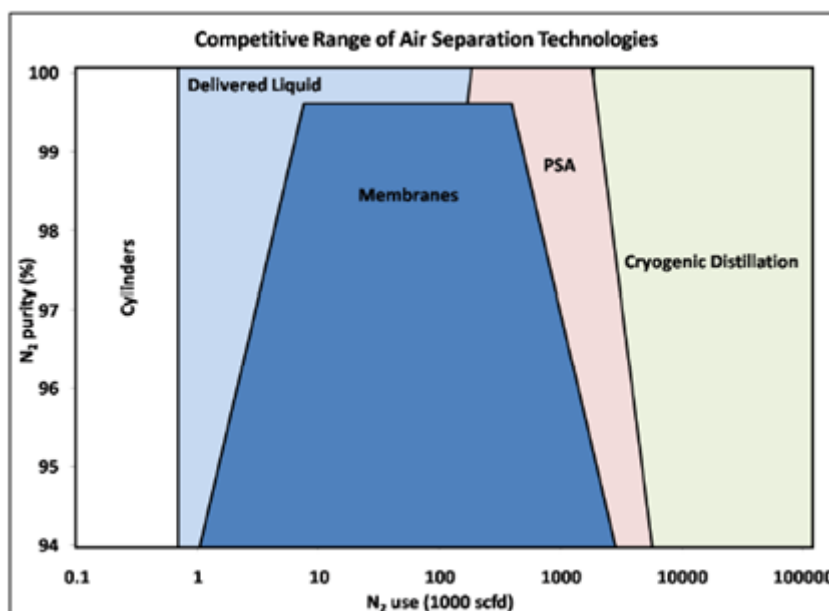
Figure 2-7: Product purity and production rates of various technologies for N$_2$ production from air. Source: (Morgan, 2013).

2.2.2.1   Cryogenic air separation

Cryogenic distillation is a mature technology that uses a two or three distillation column process, making use of the difference in boiling points between nitrogen, oxygen and argon. Figure 2-8 shows a flowsheet of the process.

Referring to Figure 2-8, the main steps for cryogenic separation are as follows: Air is compressed to about 8 bas, and re-cooled to ambient temperature with condensing of water and carbon dioxide through the molecular sieve absorbers. The air then enters a heat exchanger where it is partially liquefied by residual gases. Finally, the remaining mixture is fed to a distillation column which gives a close to pure nitrogen top product and an oxygen rich mixture as the bottom product (Castle, 2002), (Grundt and Christiansen, 1982). If a three-column design

is used it is possible to reduce the argon content of the nitrogen top product to residual levels. This would imply higher capital costs for the ASU, but these could be offset by savings using a very small purge rate, since the products from electrolysis are also extremely pure.
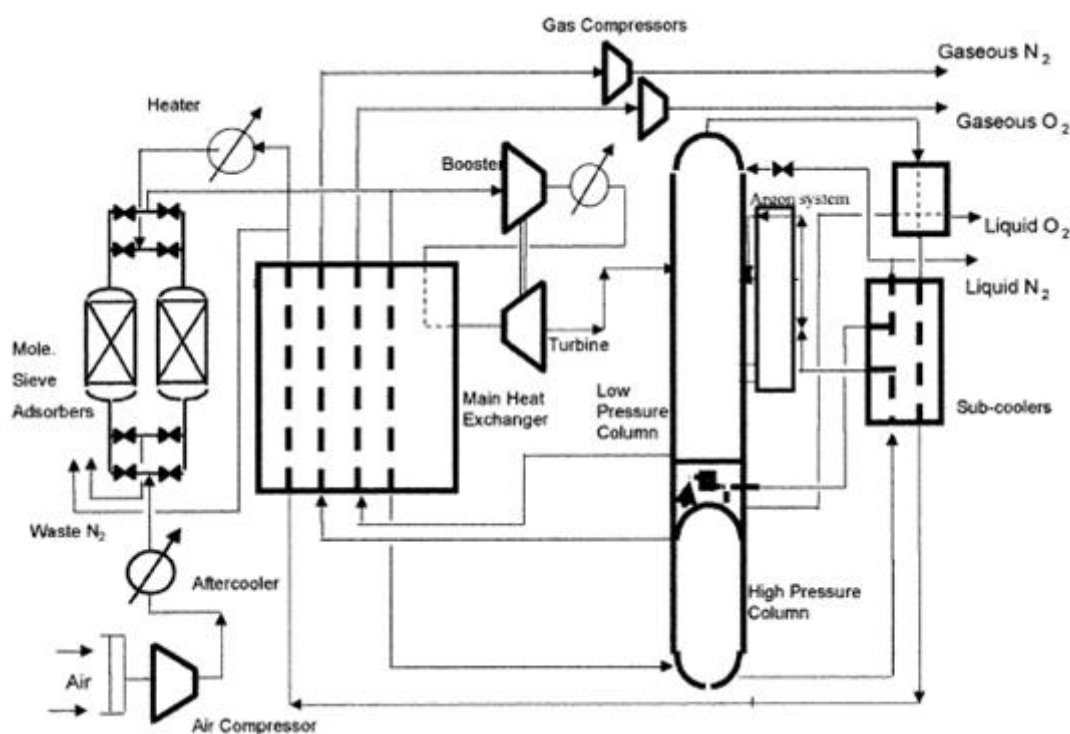
Figure 2-8: Simplified flowsheet of an air separation unit. Source: (Castle, 2002).

From Figure 2-7 it can be appreciated that cryogenic distillation is the only process that can provide high flowrates of nitrogen at the required purity. (Castle, 2002) claims these plants can produce up to 10000 tonnes of nitrogen per day. The main energy requirements for this process come from its compressors and coolers; the power consumption is reported to be 0.11 kWh/kg_N_2 (Morgan et al., 2014). The standard nature of the equipment makes ASUs benefit from economies of scale; hence larger plants have a lower unit cost.

(Morgan, 2013) reports the load range of this process is around 60%-100%, with a very slow dynamic response, in the order of hours. This constraint is an impediment to flexible ammonia production, but the low power requirements of this unit means one can probably afford to run it continuously for most wind power outputs.

2.2.2.2   Pressure Swing Adsorption (PSA)

For applications involving large production levels, cryogenic distillation is the only technology that can commercially supply this at present. However, in cases of small scale production, PSA has been successfully implemented in many countries over the past few decades (Wiessner, 1988). This system can be described in four steps: pressurisation, adsorption, depressurisation and desorption (Chung et al., 1998). Figure 2-9 shows a simplified diagram of the process.
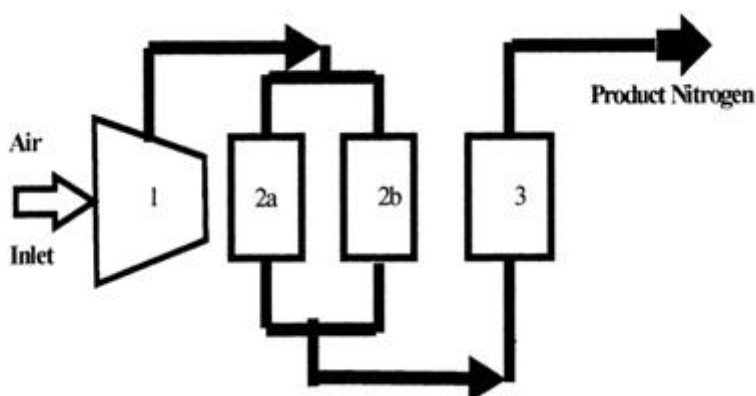
Figure 2-9: Block diagram of the main subunits in a PSA system, Source: (Castle, 2002).

1 – Air Compressor. 2a, 2b – PSA adsorber vessels. 3 – Product surge drum.

Referring to Figure 2-9, air is compressed (1) to a few bars (Sankararao and Gupta, 2007), prior to entering the bed of absorbers (2a and 2b), usually CMS (Carbon Molecular Sieve) (Castle, 2002). PSA works on the principle that at higher pressures oxygen binds more strongly to the adsorbent. The two beds work in conjunction; whilst one bed is pressurised for flow intake the other one will desorb oxygen at lower pressures leaving a pure nitrogen product, awaiting re-pressurisation. There is a surge drum (3) which smooth's out variations in pressure and composition (Castle, 2002).

A critical parameter of this process is the contact time (Morgan, 2013), or how long this absorption process takes to reach equilibrium. A large contact time will influence positively purity levels, but there is a trade off with production rates. Referring back to Figure 2-7, this is the main reason why PSAs are limited in the purity they can achieve after rates of production of 2000-5000 Nm³/ hr (Wiessner, 1988), (Morgan, 2013).

The power requirements for this process are 0.29 kWh/kg_N_2 (Wiessner, 1988); (Morgan, 2013) reports a value of 0.11 kWh/kg_N_2, which is the value used in the

model developed in this work. The load range at which PSA can operate is 30–100 % (Morgan, 2013), wider than their cryogenic counterparts. (Ivanova and Lewis, 2012) reports PSAs operate best a full or close to full load; there is a reduction in efficiency as the system is ramped down. However, one can expect the dynamic response to be effective, as there is little risk of the apparatus clogging (Step and Petrovichev, 2002). On a final note, these units require little maintenance, short start up times and are compact, offering several advantages in an islanded production scenario.

2.2.2.3 Nitrogen storage

Given the low energy requirements of nitrogen production (air separation) in relation to those of hydrogen (electrolysis) and ammonia (Haber-Bosch), the model matches stoichiometrically the production of nitrogen to that of ammonia, bypassing the need for nitrogen storage in the Energy Storage System (ESS).

2.2.2.4 Comparison of nitrogen production technologies

In this section the two main technologies for the production of nitrogen from air were described; Table 2-5 shows the data taken by the model for analysis.

As explained above, cryogenic distillation is a mature technology that complies with both the purity and production requirements needed for our process. PSA is a technology that inherently cannot provide both high production outputs and the required purity levels. However, referring to Table 2-5, the production rates of PSA are good enough for potential smaller-scale scenarios in which economies of scale do not yet favour ASUs over them. Furthermore, their higher load range gives them an edge when assessing the response of the system to certain wind loads.

Main Parameters	Nitrogen Technology	
	Cryogenic air separation	Pressure Swing Adsorption
Power Requirements(KWh/kg)	0.119	(0.29) 0.11
Load Range (%)	60-100	30-100
Production range (tons_N$_2$ /day)	7.5 - 63000	1.5 – 89.94
Power requirements at load range (GJ / ton)	(*) – 0.428	(*) – 0.396

(* No data.)

Table 2-5: Main performance indicators for the nitrogen production options explored in this section.

2.2.3 Ammonia production

The following section explores the main features of the conventional synthesis loop and storage system, reviews the progress of electrochemical synthesis and explores the feasibility of mini-ammonia plants.

As mentioned before, three catalysts are explored in Section 3; their influence on the energy and economic requirements of both the synthesis loop and the overall system is detailed in Section 5. The conclusion of this section will show the operating conditions of each catalyst.

2.2.3.1 Ammonia synthesis loop

Whilst the synthesis loop configuration might be unique to every plant, the general process for the production of ammonia from synthesis gas is well-established, consisting of compressors, a reactor, a flash drum to separate the ammonia from the unreacted synthesis gas and a heat exchanger network. A flowsheet for the process is shown in Figure 2-10.

The synthesis gas enters a compressor train where its pressure is raised to the required operating conditions through a number of stages with inter-stage cooling to minimise compressor work.

The feed gas entering the loop has a very high purity requirement, close to 99.99% for both nitrogen and hydrogen. The all-electric system considered in this work satisfies these requirements to a higher extent than the conventional synthesis gas from natural gas; this brings inherent advantages such as preventing the catalyst

being deactivated by trace sulphur compounds in the feed, and cost savings due to a smaller purge stream. This stream is necessary due to small quantities of argon in the N$_2$ stream from the air separation unit. Oxygen, a by-product of electrolysis, was reacted with small amounts of hydrogen to avoid its presence in the loop, because it is poisonous to the catalyst in the reactor (Appl, 2012).
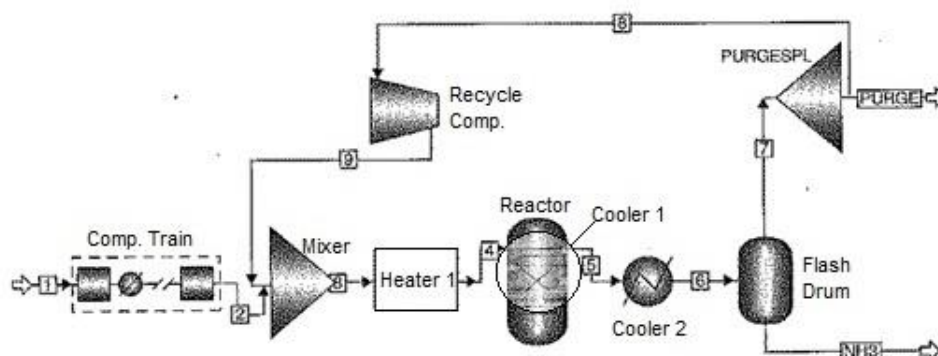
Figure 2-10: Simplified flowsheet of the conventional HB synthesis loop. Source: (Finlayson, 2012).

The thermodynamic and kinetic limitations of the reaction cause the conversion per pass in the reactor to be low; in the conventional HB synthesis loop these conversions tend to be in the range of 15-25%. This creates the need for a recycle stream, to avoid wasting expensive synthesis gas. There is a pressure drop through the loop, normally around 6% (Morgan, 2013), so a recycle compressor is employed to bring the unreacted synthesis gas to the reactor pressure. This compressor has a mass flow input four to six times higher than the compressors in the input train, but the required work will be smaller due to the minimal pressure increase it needs to raise in comparison to those in the input compression train.

There are various heat exchangers in the system; apart from the intercoolers in the compressor train we can distinguish three in Figure 2-10. Heater 1 brings the feed along with the recycle stream from the mixer to the reactor operating temperature. Cooler 2 ensures the reactor operates isothermally; Figure 2-11, taken from (Appl, 2012), shows lines of constant reaction rate for different ammonia concentrations and temperatures. The line (v=0) corresponds to the temperature concentration dependence at equilibrium. The dashed line (a) is the locus of maximum reaction rates.

In order for the reactor to follow this dotted line, thus minimising catalyst utilization, it is necessary that the reactor operates adiabatically for the first part,

followed by isothermal operation achieved by a cooler that remove the heat from the exothermic reaction. There are a number of other kinetic and thermodynamic considerations that affect the operating conditions of the synthesis loop; these are detailed in Section 3.
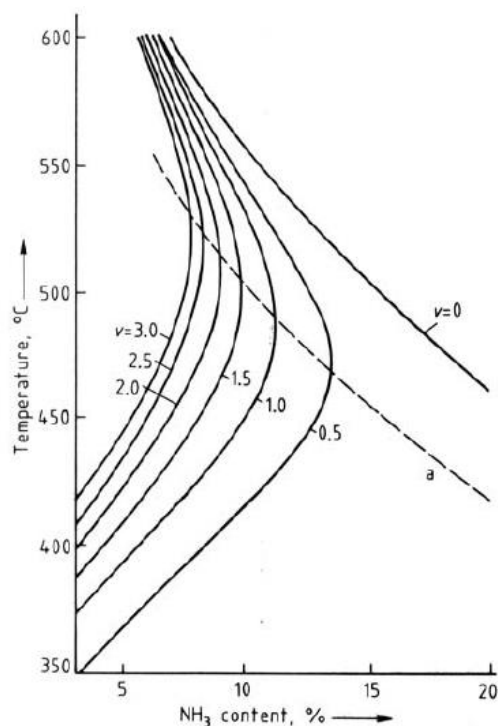
Figure 2-11: Locus of reaction rates for different temperatures and ammonia concentrations. Source: (Appl, 2012)

Cooler 3 has the task of reducing the temperature of the mixture of ammonia and unreacted synthesis gas to -33 C, the boiling point of ammonia. This will allow an easy separation of the liquid ammonia product in the flash drum.

Most ammonia plants produce 1000-1500 tons/ day (Morgan, 2013). This main features and considerations of the synthesis loop described in this section are valid for conventional Haber-Bosch flowrates, i.e. it is assumed that this design is valid for any ammonia plant sizes. In reality this is not the case; (Morgan, 2013) reports that heat transfer from the pipes and the reactor become a priority for plants with flowrates smaller than 250 tons/ day. Hughes (Hughes, 2013) states that the energy requirements vary from 0.6 kWh/kg_NH₃ (2.16 GJ/ton_NH₃) to 4.0 kWh/kg_NH₃ (14.4 GJ/ton_NH₃) when the loading varies from 100 to 10%. Hence one may expect high reductions in the efficiency of this system as it is scaled down. This will have implications in the range of scenarios to be investigated.

The load range of the synthesis loop is hard to quantify since there are various pieces of equipment in the unit. Compressors have a load range of 55 -115 %. The

conventional synthesis loop is designed to be operated at stable conditions throughout most of its lifetime, as temperature and pressure fluctuations can damage the catalyst in the reactor (Morgan, 2013). This will have implications in the logic used to dispatch the power generated by the wind farm.

2.2.3.2   Electrochemical ammonia synthesis

One of the alternatives to the conventional synthesis process involves the use of a fuel cell, similar to a proton exchange membrane (PEM) to produce ammonia either from hydrogen and nitrogen or water and nitrogen. This latter option, if implementable with reasonable cost and efficiencies, would bypass the high capital costs and energy requirements of an electrolyser route, which means in the near future it could become a competitive technology.

Ammonia can be synthesised through a number of electrochemical routes, many of them are currently in very early stages of development (Giddey et al., 2013). These are shown schematically in Figure 2-12.
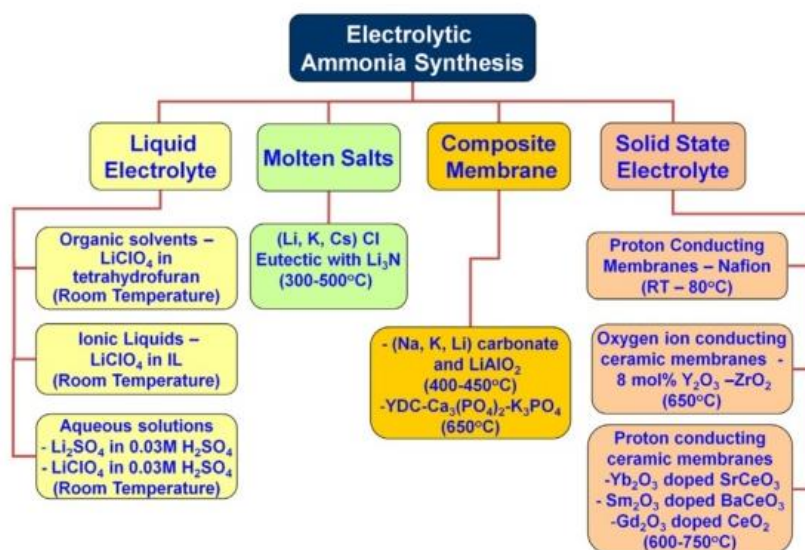
Figure 2-12: Various electrolytic options under consideration for ammonia synthesis. Source: (Giddey et al., 2013)

Referring to Figure 2-12, out of the displayed options solid state electrolyte membranes are reported to be the most promising; they allow an easy separation of the hydrogen feed from the ammonia product, giving them more versatility (Giddey et al., 2013). However, none of these technologies is ready for commercial production. There are various reasons for this:

- Higher temperatures and pressures, necessary to drive rates of reaction up, cause stringent material requirements which cannot be met at present.
- There is an inverse relationship between current density and current efficiency; low current densities imply low ammonia production rates, hence it quickly becomes uneconomical to scale up this process.
- The rates reported for all of these routes were in the range of $10^{-13} - 10^{-8}$ mol / (cm^2 s) (Giddey et al., 2013).

The potential of these devices to operate at lower temperatures and pressures than the conventional HB process could lead to future energy and material savings. Its easy integration with an all-electric process, i.e. renewable energies, makes them interesting alternatives for the future, provided higher rates of reaction can be attained without a compromise on current density.

2.2.3.3 "Mini" Haber-Bosch technologies

One of the main issues in assessing the feasibility of wind to ammonia systems is the lack of information regarding the potential of small scale systems, as sub-units in our process such as cryogenic ASU or the synthesis loop are mainly employed for large production purposes. This constrains the lower bound of wind power input our process would require without the uncertainty of a substantial reduction in efficiency.

A hypothetical islanded system satisfying a small demand would be a logical scenario in the context of a self-sustained process with the technologies reviewed; these tend to be modular, such as the electrolyser or PSA, and some of them cannot provide high production outputs cost-effectively. The disparity between the "comfortable" ranges of the technologies taken from the conventional HB process and the ones emerging as alternatives requires attention in order to assess the feasibility of small-scale systems.

In the past years some companies have developed mini ammonia systems using conventional sub-units that have been explored in this literature review. Proton Ventures is a Dutch company which claims, in a presentation ("Mini Ammonia Production Unit Presentation," 2010), they employ a process that can produce up to 1 ton_NH₃/h. Figure 2-13 shows a simplified flowsheet for the process.

This process can produce 99.9% pure anhydrous ammonia, with production capacities in the range 3 kg/hr to 1 ton/hr, an intermediate case being 3 tons/day as shown in Figure 2-13. The power requirements associated with these rates are

5 kW for 3 kg/hr, 100 kW for 1 ton/day, to 11.5 MW for 1 ton/hr. The NH₃ production plant operates at a pressure of 460 bars and a temperature of 550 C. The company claims several advantages to this process including a service lifetime of 20 years for the catalyst, no cooling water requirements and the recovery of ammonia without the need of a refrigeration system.
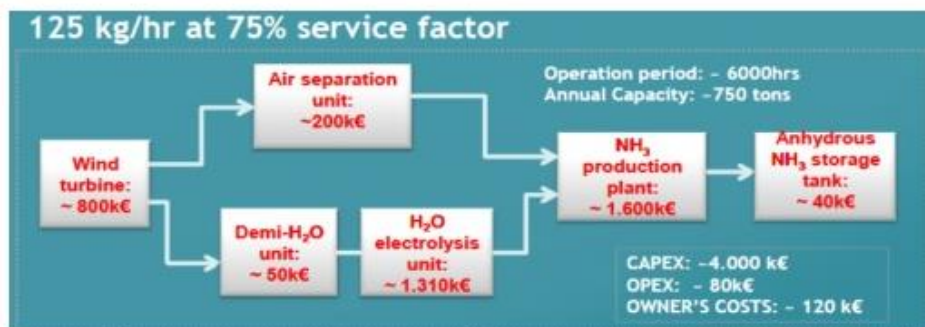
Figure 2-13: Breakdown of the proposed employed by Proton Ventures. Source: ("Mini Ammonia Production Unit Presentation," 2010).

(Morgan et al., 2014) proposes a process that uses a PSA unit for nitrogen production, a series of PEM electrolysers and synthesis loop, along with an ammonia storage system, for a production range of 0.1 – 5 tons/day. They fitted their capital cost estimation to a single curve, shown in Eqn. 2-2 (Morgan et al., 2014):

Eqn. 2-2: $$C_{NH3} = 3,322,500 * X^{0.6}$$

where X represents the capacity of the ammonia plant in tons/day. For 3 tons/day the capital cost comes down to around 6.4 million dollars, not too far away from the capital cost Proton Ventures claims for their unit, i.e. about 4.0 million euros (Figure 2-13).

These two pieces of information give a ballpark idea of the investment necessary for small scale applications; however, the lack of information in the region of 75 - 250 tons/day complicates the portrayal of scenarios for wind power outputs that could only satisfy these production rates. Extrapolation to these sizes would have to come from scaling up these mini ammonia plants or scaling down commercial units, both approaches raising questions on scalability and efficiency.

2.2.3.4 Ammonia storage

In a similar fashion to hydrogen storage technologies, ammonia storage can be achieved via cryogenic methods, at -33 C, or at medium pressures ranging from 8 – 17 bars (Morgan, 2013) and (Bartels, 2008). The disparities between these operating condition options and those stated for hydrogen earlier have large implications on the capital and operating costs necessary to successfully store these two chemicals.

Ammonia has an energy density of 13.77 MJ/L when stored at high pressures, slightly less than the value of 15.37 MJ/L when stored cryogenically (Bartels, 2008). For large scale systems low temperature storage is preferred, as pressure vessels have a maximum capacity of 270 tonnes, compared to 60,000 tonne capacities achieved by low temperature storage vessels (Bartels, 2008). The typical boil-off of this latter system is around 0.04% per day, creating the need of a recompression and flash loop to avoid the loss of valuable product (Morgan, 2013).

It seems obvious from the above figures of merit that the energetic and economic costs of an ammonia storage system will be much lower than for its hydrogen counterparts. Bartels (Bartels, 2008) establishes this comparison, adjusting the values of ammonia to hydrogen higher by a factor of 5.63, to account for the higher mass of ammonia per stored quantity of hydrogen. Thus for the same initial quantity of hydrogen, and for the same length of time of storage (182 days), the liquefaction and storage energy demands were 117.9 kJ/kg_H₂ and 650 kJ/kg_H₂ respectively, significantly less than the hydrogen storage system. This analysis included the synthesis of ammonia to make a fair comparison, but even including its energy requirements, quoted as 7,907 kJ/kg_H₂, the overall energy requirements of an ammonia storage system were 20% of the hydrogen storage system requirements, stated earlier as 42,552 KJ/kg_H₂.

2.2.3.5 Comparison of ammonia production technologies

In this section the main aspects of the synthesis loop, the framework for the analysis of the three catalytic options, are detailed, along with a discussion of current small scale ammonia production and a review of the state of the art in electrochemical ammonia synthesis. The data taken from the model is shown in Table 2-6.

As appreciated in Table 2-6, the operating conditions of the three catalysts have three main differences, the pressure of operation, the rate of reaction and the conversion. Referring back to Figure 2-10, there are various trade-offs that will influence the overall costs and power requirements:

- Low pressures of operation will reduce compression requirements; on the other hand, high pressures result in increased equilibrium conversions and rates of reactions, so there is a balance between compression and reactor costs.
- A lower conversion per pass will lead to higher recycle rates. This will increase flowrates through the recycle loop, resulting in increased costs due to larger pipes and heat exchangers, and a higher work input to the recycle reactor. This again could be balanced against higher pressures of operation with higher conversions.

	HB technology			
Main Parameters	HB_Fe	HB_Ru	HB_CoMoN	mini-HB
Power Requirements(KWh/Kg)	4	4	4	14
Load Range (%)	10-100	10-100	10-100	(*) - 100
Production range (tons_NH$_3$ /day)	250-3000	250-3000	250-3000	0.072-72
Power requirements at load range (GJ/ton)	14.4 – 2.16	14.4 – 2.16	14.4 – 2.16	(*) – 50.4
Operating Pressure (Bar)	150	100	31	-
Operating Temperature (C)	400	400	400	-
Catalyst Density (kg/m^3)	2.88	1.4	2.88**	-
Conversion at operating conditions (%)	41.4	36.6	7.5	-
Reaction rate (kg_NH$_3$/Kg/s)	4.55e-4	5.14e-4	7.08e-5	-
Catalyst price (£/kg)	13	1930	56	-

(* No data; ** Assumed density.)

Table 2-6: Parameters taken for the model for the different catalysts and the mini-HB process

The analysis of the HB synthesis loop using different catalysts will explore these trade-offs.

Referring back to Table 2-6, we can see that the mini-HB process is not competitive both in terms of power requirements and production rates, compared to the three previous options. However, there is a great variation in efficiency when the catalytic processes are ramped down to lower loads. Combined with the fact that this ramping process could severely damage the catalysts considered, it is clear that in order to successfully merge wind power and its variability with an

ammonia HB synthesis loop, this last unit should operate continuously for the lifetime of the plant. This decision would mean sometimes the power input to the synthesis loop would have to come from the combustion of previously produced ammonia. The role of mini-HB processes needs to be quantified within different application scenarios. These will be studied by using the model developed in this work.

2.2.4 Conclusions on ammonia for energy storage technologies

In this section we present a review of the current state of the art, along with an assessment of the available technology options for an alternative all-electric process that was detailed above.

There are various technical properties that are desired in the technologies reviewed for all three modules: hydrogen, nitrogen, and ammonia production. Amongst them are low energy requirements, flexible production capacities, flexibility to variations in operating loads and a low variation of efficiency with load. A table with these performance indicators is shown at the conclusion of each subsection, for the technologies that were subject of analysis.

A number of conclusions and observations can be extracted from this literature review:

- The technologies drawn from the conventional HB process for analysis and implementation in our process are designed for large scale production of ammonia, so they tend to be economical only from a certain production threshold, requiring a substantial amount of wind power to satisfy their energy requirements. Additionally, their load range tends not to be flexible, compared to other options. This is the case for the HB synthesis loop and the cryogenic air separation unit.
- The use of electrolysis as the hydrogen production route, as opposed to the steam reforming of natural gas, would be the main difference with respect to current practice in ammonia production. Electrolysis appears not to be as competitive as steam reforming of natural gas; detailed assessment of its capital and energy requirements is needed to understand its dominance on the overall cost of the process.
- Amongst the technologies reviewed, there seems to be two categories; technologies with large production capacities and technologies which are only cost effective for small scale applications. Amongst these latter ones are PEM electrolysers, PSA for air separation, and the mini-HB process. This fact will

influence both the combinations of technologies we regard as competitive and the scenarios portrayed.

- Following from this last point, there is little information on the efficiency and scalability of all technologies reviewed for the range of 70 tons/day (maximum production rate of PSA and mini-HB) to 250 tons/day (minimum production rate for the HB synthesis loop). This will create uncertainty in our results for the scenarios where production is in that range.
- In general, the emerging technologies explored tend to have flexible load ranges and an adequate dynamic response, allowing them to have a synergy with intermittent renewables, such as wind power.

The operational model parameters discussed in Section 4.2, and the technical decisions that influence the logic presented in Section 4.3, will provide a framework to analyse the technology options and configuration preferences in more detail.

3.   Critical review of catalytic ammonia systems

3.1 Catalysts for Ammonia Synthesis

3.1.1   Introduction

As stated in other sections, catalytic production of ammonia from nitrogen and hydrogen is the second-largest-volume industrial chemical manufacture in global trade; its main drivers are agricultural sectors, as fertilizers, and industrially diverse applications as an enabling chemical (Erisman et al., 2008). Thus, the main performance indicators have been mostly driven by its production volume and cost of the process. With increasing concerns for the energy consumption of the process and its environmental impacts (carbon emission and water contamination), both nationally and internationally, this catalytic process is currently subject to renewed assessments.

The high hydrogen storage capacity (17.7 wt%) and energy density content (3000 Wh/K) of ammonia have rendered it as one of the best *carbon-free chemicals* for hydrogen and energy storage (S. F. Yin et al., 2004). As we face increasing challenges in economic, energetic and environmental management, the role of catalysis to provide some of the answers to these challenges has become more important than ever. In this section, we will review the existing catalysts and associated catalytic technologies in traditional industrial ammonia Haber–Bosch synthesis (Section 3.1.3) and electrochemical synthesis (Section 3.1.4), and assess their technical aspects in a new route for the production of renewable ammonia *via* wind power as a flexible energy storage system or buffer.

3.1.2   Thermodynamic and Kinetic Aspects

To produce ammonia, hydrogen is catalytically reacted with nitrogen (derived from air) to form anhydrous liquid ammonia as

Eqn. 3-1 $N_2 + 3 H_2 \rightarrow 2 NH_3$ $(\Delta H = -92.4 \text{ kJ / mol})$
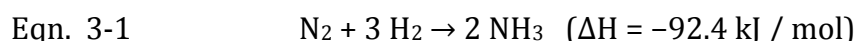
Ammonia synthesis from nitrogen and hydrogen is an exothermic reaction ($\Delta H = -92.4$ kJ / mol) which means, from a thermodynamic point of view, that its conversion will increase at a lower operational temperature. However, high

temperatures are actually required to achieve industrially acceptable rates, which overcome kinetic barriers for the rearrangement of chemical bonds in this reaction. Also, according to thermodynamics, higher operational pressures can drive this synthesis process forward due to the reduction in total number of molecules produced (see Eqn. 3-1). It is noted that the extent of this reaction is strongly limited, dependent on the unfavourable thermodynamic equilibrium at extreme conditions, as appreciated in Figure 3-1.
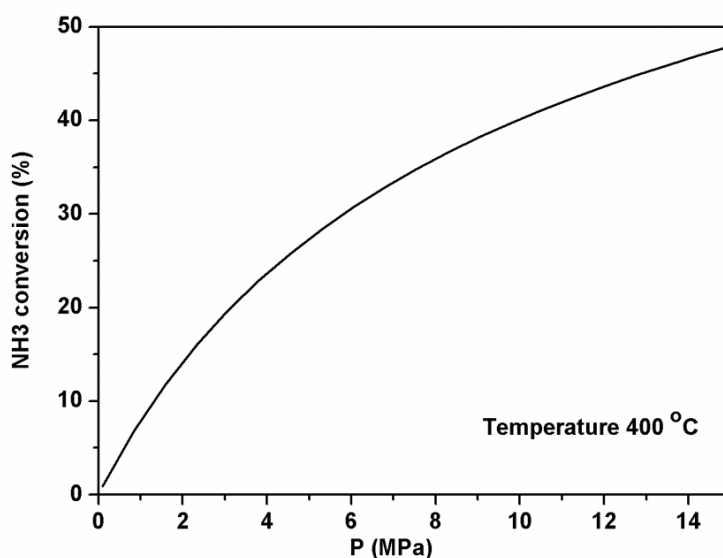
Figure 3-1: Equilibrium ammonia conversion at different pressures and 400 C.

3.1.3 Conventional Ammonia Synthesis

3.1.3.1 Iron Based Catalysts

In the traditional industrial Haber-Bosch process, production volume and cost are highly dependent on natural gas availability. Most current industrial plants were built in locations with a plentiful supply of natural gas and water (for steam reforming and water gas shift reactions). In order to obtain the optimal productivity of ammonia, the reaction conditions are usually set at a temperature regime of 400-500 C, and pressures of 15-30 MPa under a maximal flow of reactant gases. The ammonia conversion per single pass is close to equilibrium conversion (Figure 3-1), with cooling and subsequent separation in a synthesis loop. Any unreacted gases are recycled, and eventually an overall conversion of 97% is achieved. Under these conditions, catalyst selection can be less critical since

slightly less active or deactivated catalysts can reach the same conversions at smaller reactant flows. Other criteria including the cost of manufacture, sensitivity to poisons and ammonia itself, durability, mechanical strength and ease of regeneration are of more importance (Appl, 2012).

The inexpensive fused iron catalysts have been employed in industrial ammonia synthesis for nearly one hundred years. The typical fused iron catalyst precursor is composed of Fe_3O_4 or Fe_2O_3, Al_2O_3, K_2O, CaO, MgO and SiO_2. Multi-promoted fused iron catalysts have many merits such as high activity (sustained for higher reactant flow rate), low cost, robustness and so on. In particular, the service lifetime of the fused iron catalysts could be up to 14-20 years in modern single-train ammonia plants (Appl, 2012), (Kowalczyk and Jodzis, 1990). However, the activity of the fused iron catalysts is strongly related to the operation conditions, residual oxygen compounds concentration in the supply gas and the NH_3 concentration produced from the reaction. The decline in their activity is mainly caused by the growth of crystallites and rebuilding of the catalyst structure. Furthermore, the fused iron catalysts cannot not deliver sufficiently high reaction rates at around 377-572 C for thermodynamic reasons, making it necessary to work at high operating pressures, usually above ca. 14 MPa (Hagen, 2003).

Kowalczyk et al. (Kowalczyk and Jodzis, 1990) examined the activities and thermo-resistances of five industrial fused iron catalysts using a short term overheating sequence to replace the slow natural thermal deactivation. The compositions of the catalysts are listed in Table 3-1, No. 1-5. Their kinetics were assessed under 10 MPa at 520 C and the thermo-resistances were measured at 650 C for 24 h. Activities of the catalysts were characterized by the "k" constants according to the Tempkin-Pyshev equation. According to their results, the lower resistance of the catalyst could be related to the lower CaO content and high K_2O/Al_2O_3 ratio, while the high initial activity could be ascribed to high potassium content.

Liu et al. (Huazhang et al., 2003), (Guan and Liu, 2000) compared the activities of α-Fe reduced from the different iron precursors: traditional Fe_3O_4, $Fe_{1-x}O$ and their mixtures (Table 3-1, No. 6-14). It was suggested that the α-Fe reduced from $Fe_{1-x}O$ showed the best reaction activity; the order of the activity was as follows: $Fe_{1-x}O > Fe_3O_4 >$ their mixture. This is because the α-Fe produced from the reduction of $Fe_{1-x}O$ could effectively adsorb H_2, which could in turn react with N_2 to form ammonia. Furthermore, there was no strong chemisorption state of H_2 over this catalyst surface, which might interfere with N_2 adsorption. The best reaction rate was determined to be 96,500 μmol g^{-1} h^{-1} under the reaction conditions (400 C, 15 MPa, 30,000h^{-1}, H_2:N_2 = 3:1). Liu et al. (Liu et al., 1996) reported the comparative

reduction conditions of Fe$_{1-x}$O, FeCo and Fe$_3$O$_4$ catalysts. Fe$_{1-x}$O showed the lowest reduction temperature, but stronger mechanical strength. As shown in Table 3-1, No. 15–17, at the same pressure, temperature and space velocity, the Fe$_{1-x}$O gives the highest exit ammonia concentration than the other two catalysts. Additionally the cost of Fe$_{1-x}$O is generally lower than that of FeCo. Compared to Fe$_3$O$_4$ the industrial production of ammonia by Fe$_{1-x}$O can be increased from 150 tons to 180 tons per day and the operating pressure can be decreased from 30 MPa to 28 MPa. Thus, the use of Fe$_{1-x}$O catalysts could exhibit some remarkable energy saving effects in a modern Haber-Bosch or related new plant.

The synthesis of ammonia from its elements is proved to be very sensitive to the structure over the iron catalysts. Spencer et al. (Spencer, 1982) first studied the activity of ammonia synthesis over a fused iron catalyst, in which surface crystallographic structure under high pressure conditions was correlated to measured activity. Under the given conditions, the relative rates of ammonia formation were found to be 418: 25: 1 for Fe (111), Fe (100) and Fe (110) respectively (Table 3-1, No. 18-20). After the reaction all three surfaces were partially covered with nitrogen, but the surface nitrogen would not affect the performances of the single crystal catalysts and it could be removed by heating in the N$_2$/H$_2$ feed gas. Unfortunately, a small amount of water and sulphur would readily deactivate catalytic activity dramatically. Strongin et al. (Strongin, 1987) suggested that the high activity of the Fe(111) surface was related to the high amount of C$_7$ coordination sites, which were in the second and third layers and could exposed to the reactant gas. The kinetics of Fe (210) and Fe (211) surfaces were measured in addition to the previous Fe (111), Fe (100) and Fe (110) (Table 3-1, No. 21-25). They concluded that the presence of highly coordinated sites is more important than that of surface roughness in order to sustain a high catalytic activity.

Hagen et al. (Hagen, 2003) investigated barium promoted iron-cobalt alloys supported on carbon as the catalyst for ammonia synthesis (Table 3-1, No. 26-33). A barium promoter can significantly enhance the reaction rate of iron, iron-cobalt and cobalt catalysts in ammonia synthesis. Especially for cobalt catalysts, the reaction rate (22,320 µmol g^{-1} h^{-1} under 400 C, 10 bar) can be increased by more than two orders of magnitude compared to that of unpromoted cobalt catalysts. With the increased cobalt content in the catalysts, the inhibition of the ammonia synthesis rate by the product ammonia itself is also decreased; this is because the cobalt atom will not form bonds with nitrogen species as strongly as iron.

From the above it is clear that there are variations in catalytic activity when different forms and structures of iron catalysts are used. However, under the

Haber–Bosch process with a plentiful supply of natural gas and water for hydrogen production, catalysts placed in reaction conditions approaching to thermodynamic equilibrium in a recycle loop are chosen for optimal ammonia synthesis (> 240 tons/day). Thus, the choice of catalysts is not solely made based on their activity but on other factors, e.g. their cost and tolerance to impurities are also important factors. This is because the H$_2$ source of the Haber-Bosch process is natural gas. In the steam reforming processes, methane converts to carbon monoxide and H$_2$. Then, the carbon monoxide serves as reducing agent for water to yield carbon dioxide and additional H$_2$. As ammonia synthesis only needs N$_2$ and H$_2$, the residual carbon monoxide, methane, higher hydrocarbons (hydrogenation products) and a large amount carbon dioxide must be removed from the raw gas.

It has been shown that some of these oxygen-containing compounds such as H$_2$O, CO, CO$_2$, and O$_2$ are the most common poisons encountered in ammonia synthesis. These oxygen compounds may cause permanent poisoning phenomena at lower operation conditions, but may become reversible on some forms of iron catalysts at high temperatures. That is, the activity of damaged catalysts can be practically completely restored by reduction with clean synthesis gas for a finite period of time. This damage depends approximately linearly on the quantity of adsorbed water taken up by the catalyst, which is proportional to $(P_{H2O}/P_{H2})^{1/2}$ (Appl, 2012), where (P_i) represents the partial pressure of the subscript component. With respect to resistance to carbon monoxide species, Fe$_{1-x}$O catalysts have a unique advantage over the conventional Fe$_3$O$_4$ catalysts. It is seen from Figure 3-2 that when carbon monoxide is introduced into a reaction system, the attenuation of the rate of activity of Fe$_{1-x}$O catalyst is slower than that of conventional Fe$_3$O$_4$ catalyst; after it is eliminated from the reaction system the dynamic response in the activity of Fe$_{1-x}$O catalyst can be better than that of the conventional Fe$_3$O$_4$ catalyst (Liu et al., 1996).

On the other hand, the limited and non-steady supply of renewable H$_2$ produced from offshore wind may affect the choice of catalysts and subsequent reaction, transport and separation systems for renewable ammonia production. For example, H$_2$ obtained from electrolysis of water using wind power is carbon free, hence there is no need for further downstream purification, nor for using robust catalysts with high tolerance to CO and hydrocarbons (Appl, 2012).
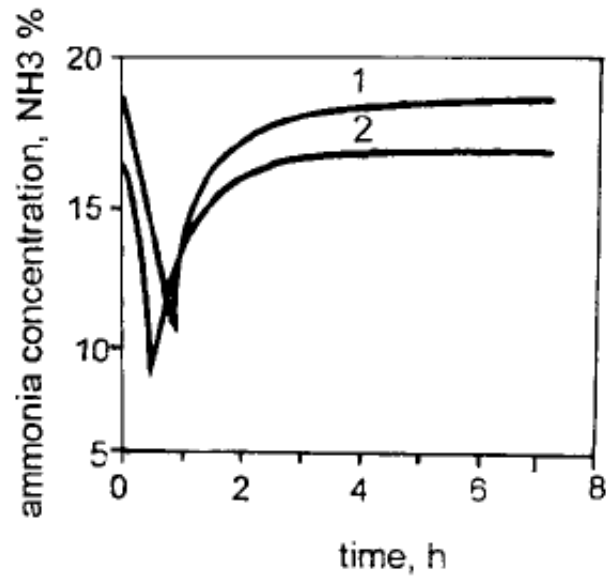
Figure 3-2: Comparison of resistance to carbon monoxide of Fe$_{1-x}$O and conventional Fe$_3$O$_4$ catalyst. Test conditions: space velocity, 30000 h^{-1} temperature; 450 C, pressure, 15 MPa; CO concentration, 500 ppm. (1) Fe$_{1-x}$O catalyst, (2) conventional Fe$_3$O$_4$ catalyst (Liu et al., 1996).

It is noted that the Haber–Bosch conditions may not be economically sustainable if the ammonia productivity falls below 240 tons/day. On the other hand, new more active type of catalysts may be well suited to these reaction conditions with different stoichiometric conditions and lower space velocities, for a smaller and more flexible production of ammonia (3-240 tons/day), under a kinetic controlled regime as local energy store/buffer or as fertilizer for isolated farms.

The reaction mechanism, involving the heterogeneous catalyst, is believed to involve the following steps:

Eqn. 3-2 $\quad\quad$ N$_2$ (g) $\rightarrow$ N$_2$ (adsorbed)

Eqn. 3-3 $\quad\quad$ N$_2$ (adsorbed) $\rightarrow$ 2 N (adsorbed)

Eqn. 3-4 $\quad\quad$ H$_2$(g) $\rightarrow$ H$_2$ (adsorbed)

Eqn. 3-5 $\quad\quad$ H$_2$ (adsorbed) $\rightarrow$ 2 H (adsorbed)

Eqn. 3-6   N (adsorbed) + 3 H(adsorbed)→ NH₃ (adsorbed)

Eqn. 3-7   NH₃ (adsorbed) → NH₃ (g)
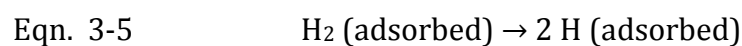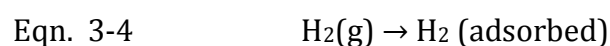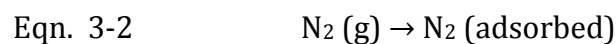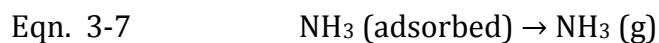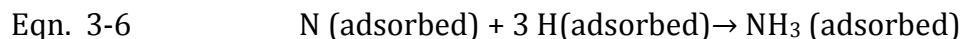
The reaction in Eqn. 3-6 occurs in three steps, forming NH, NH₂, and then NH₃. Experimental evidence points to the reaction in Eqn. 3-3 as being the slow, rate-determining step under kinetic controlled conditions.

Honkala et al. (Honkala, 2005) and Hellman et al. (Hellman et al., 2006) reported a potential energy diagram for the ammonia synthesis reaction under kinetic controlled conditions, shown in Figure 3-3. Their calculations indicated that step sites are much more reactive for N₂ dissociation. By combining the results of step sites in Figure 3-3, with harmonic transition state theory, it was shown that N₂ dissociation is the slowest step under all realistic reaction conditions. In other words, the N₂ dissociative adsorption is the rate determining step in ammonia synthesis (Hwang and Mebel, 2003). Therefore, a more efficient catalyst for ammonia synthesis should have a suitable surface potential for more favourable adsorption and dissociation of nitrogen under the kinetic controlled conditions.
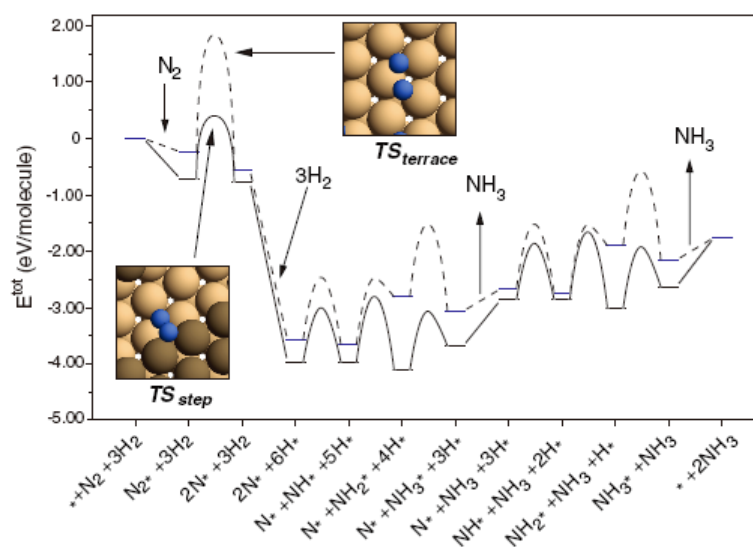
Figure 3-3: The calculated the potential energy (E^{tot}) diagram for NH₃ synthesis from N₂ and H₂ over close-packed (001) and stepped Ru surfaces. A '*' denotes an empty site and 'X*' an adsorbed species. The configuration of the transition states (TS) for N₂ dissociation over the terrace and step sites is shown in the insets (Honkala, 2005).
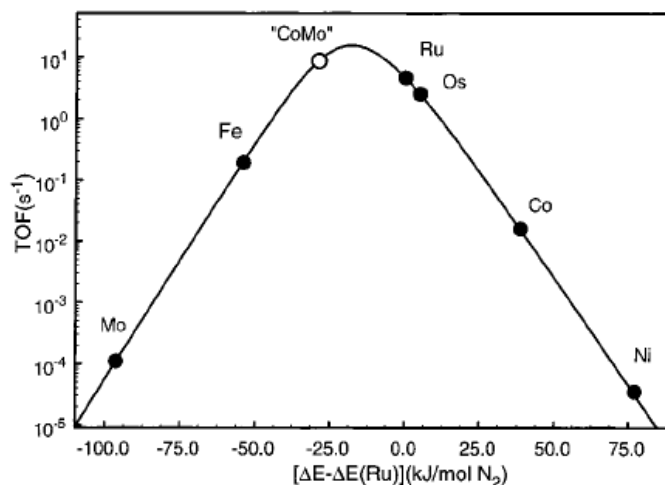
Figure 3-4: Calculated turnover frequencies for ammonia synthesis as a function of the adsorption energy of nitrogen (Jacobsen et al., 2001).

Additionally, according to the calculations from Jacobsen et al. (Jacobsen et al., 2001), the turnover frequency for ammonia synthesis is a function of the adsorption energy of nitrogen and there is an optimum energy for nitrogen adsorption, yielding a maximum ammonia production rate (Figure 3-4). The high activity reflected by this optimum energy is achieved from two contradictory conditions: small activation barrier for N_2 dissociation but at a low coverage and weakly adsorbed atomic nitrogen for hydrogenation; both are needed for the ammonia synthesis. This may require metal sites to carry out a strong dissociative adsorption followed by transfer of the N-surface species to weaker sites to reach the optimal kinetics. From theoretical and experimental data, single metal Ru or Os catalysts could provide sites to get close to this optimum value. However, these metals are also very expensive and thus become much less commercially attractive compared to the third-best catalyst, Iron.

3.1.3.2　Ru Based Catalysts

In the 1970s, a promoted Ru catalyst on graphitized carbon support was first studied by BP (Brown et al., 2014). As the second generation catalyst for ammonia synthesis, the activity of Ru-based catalyst was found to be about twenty times more active than a commercial Fe-based catalyst, and can also be operated under lower temperatures and pressures (Table 3-1, No. 34-37). Thus, the applied pressure can be reduced to less than 10 MPa, which may save substantial

operational and energy costs for a potential new renewable ammonia synthesis. Under reaction conditions of 400 C, 10 MPa, 10,000 h^{-1}, H$_2$:N$_2$ = 3:1, the ammonia synthesis rate of barium and potassium promoted ruthenium supported on active carbon catalyst was found to be 108,900 µmol g^{-1} h^{-1}, while for the Fe$_{1-x}$O catalyst this was measured to be 22,300 µmol g^{-1} h^{-1} under the same conditions (Pan et al., 2011) (Table 3-1, No. 38-41). The incorporation of active carbon and graphite was thought to facilitate the electronic transfer from promoter to Ru, which is an important factor for the superior performance of ruthenium based catalysts in ammonia synthesis (Kowalczyk et al., 1999) and (Liang et al., 2001).

Chen et al. (Chen et al., 2001) developed a novel alkali promoted ruthenium catalyst supported on multi-walled nanotubes (MWNT). Compared to C$_{60-70}$ and graphite, K and Ru could be well dispersed on the MWNT. The K-doped Ru-MWNT catalyst gave a high adsorption capacity for both hydrogen and nitrogen. This was also attributed to the electronic transfer between these promoters and Ru by the unique support. The ammonia synthesis rate of K/Ru/MWNT = 4/4/100 was found to be 2048 µmol g^{-1} h^{-1} at 400 C at atmospheric pressure, N$_2$/H$_2$ = 1:3 and at a flow rate of 1800 ml/h. Under the same conditions, the ammonia production rate of K/Fe/MWNT was only 129 µmol g^{-1} h^{-1} (Table 3-1, No. 42-46).

Hansen et al. (Hansen et al., 2002) studied the support effect over the Ba promoted ruthenium catalysts. It was found that the Ba atoms covered most of the Ru surface over the Si$_3$N$_4$ supported catalyst, which led to low ammonia production rates. But when MgAl$_2$O$_4$ and graphite were used as a support, there was no evidence for the extensive coverage of Ru surface with Ba atoms. This type of deactivation seemed to be dependent on the nature of the promoter and support used (Table 3-1, No. 47-49).

With reference to the recent density functional theory (DFT) calculations, it was suggested that the active site on the surface of Ru can be greatly influenced by the nearby promoter atom. Electrons can be transferred from the promoter to the Ru via the electronic conductive support; the high electron density of d-orbitals of Ru can donate electrons into the anti-bonding orbital of adsorbed N$_2$, hence facilitating its dissociation. Furthermore, the DFT calculations indicated the active site for ammonia synthesis is likely to be the B$_5$-type site with an exposed three-fold hollow site, at a proximity to bridge site to ensure two nitrogen atoms are not bonded to the same Ru atom (Dahl et al., 1999) and (Dahl et al., 2000). The concentration of B$_5$-type sites in Ru surfaces was found to correlate well with ammonia production activity. Jacobsen et al. (Jacobsen et al., 2000) showed the optimal Ru size of 1.8-2.5 nm which contained the maximum number of B5-type sites; this number decreased for larger particle sizes. Fernandez et al. (Fernández

et al., 2014) further investigated the average size and distribution of Ru particles on the activity of ammonia synthesis. Different amounts of Ru loaded $Ru/\gamma\text{-}Al_2O_3$ catalysts were prepared via wet impregnation, colloidal and micro-emulsion methods. In this case, the average Ru particle size of around 6 nm exhibited the best ammonia production rate of 6,300 µmol g^{-1} h^{-1} at 100 C and 0.4 MPa in a space velocity of 6,000 ml g^{-1} h^{-1} (Table 3-1, No. 50-58). However, the number of B_5-type sites was higher over the smaller Ru particles. It was believed that larger Ru particles with a board size distribution in the range 2 – 10 nm (provided sites for H_2 activation) could lead to an overall higher activity via a synergic effect with smaller Ru particles (strongly adsorbed N_2 atoms).

However, an obstacle for industrial ammonia synthesis with Ru-based catalysts was found to be their deactivation at high hydrogen pressure. The base promoted Ru surface not only reduced the activation barrier for N_2 dissociation, but also increased the competitive adsorption of H_2 which attenuated the overall activity of the Ru-based catalysts in ammonia synthesis (Kitano et al., 2012). In addition, the graphitic or active carbon support adopted was more prone to methanation (methane formation) and higher hydrocarbon formation due to the oxygen containing functional group on carbon surfaces under industrial conditions. Consequently, the carbon supported Ru catalysts would progressively deactivate under industrial conditions (Jacobsen, 2001).

To overcome the significant drawback of using an active carbon support in ammonia synthesis, many other stable supports like, MgO, Al_2O_3, CeO_2 and other porous materials were studied (Seetharamulu et al., 2007), (Xu et al., 2008), (Yang et al., 2010), (Zhang et al., 2011) and (Zheng et al., 2009). Wang et al. (Zi-qing Wang et al., 2013) reported the use of a high surface area, basic (198 m^2 g^{-1}) ZrO_2 support for Ru, which was prepared by the digestion of hydrous zirconia in mother liquor. Compared to $K\text{-}Ru/ZrO_2$, $K\text{-}Ru/MgO$, $K\text{-}Ru/Al_2O_3$ and other Ru catalysts, the catalytic activity of $Ru/ZrO_2\text{-}KOH$ catalyst gave the highest activity in ammonia synthesis (Table 3-1, No. 59-63). Wang et al. (Ziqing Wang et al., 2013) also reported the use of a perovskite type $BaZrO_2$ support, which exhibited a higher ammonia production rate than the $Ru/ZrO_2\text{-}KOH$ (Table 3-1, No. 64-67). Because the transfer of electrons was facilitated from the base support $ZrO_2\text{-}KOH$ and $BaZrO_2$ to Ru, the catalyst was also subjected to H_2 poisoning at high pressure as a trade-off.

Jacobsen et al. (Jacobsen, 2001) investigated the ruthenium on barium-boron nitride catalyst, which showed a high activity (184,972 µmol g^{-1} h^{-1}) with good stability in ammonia synthesis at 400 C and pressures of 10 MPa (Table 3-1, No. 68-70). At 100 bars and 550 C for 3500 h, there was still no deactivation of the

Ru-Ba/BN catalyst. Kitano et al. (Kitano et al., 2012) stated the Ru-zeolitic electride $[Ca_{24}Al_{28}O_{64}]^{4+}(e^-)_4$ catalyst (C12A7:e-) displayed a high electron transfer ability as well as satisfactory stability. The 1.2 wt% Ru loaded of Ru/C12A7:e- catalyst showed a superior performance in ammonia synthesis at 400 C and ambient pressure.

The above discussion clearly suggests that N_2 dissociation on Ru can be facilitated by enriching the electron density of the metal (electron back donation) via electron transfer from the promoter or the support. However, the higher electron density of Ru will also be subject to rapid H_2 activation, leading to surface competition which yields a slower ammonia production. On other hand, using supports such as boron nitride and zeolitic electride, which exhibit fast transfer of hydrogen species, the metal could display higher tolerance for H_2 poisoning on Ru (Table 3-1, No. 71-84).

3.1.3.3   Bimetallic Nitride Catalysts

According to the theoretical calculations from Jacobsen et al. (Jacobsen et al., 2001) a metal surface (containing active sites) should be tuned with desirable intermediate nitrogen adsorption energy by combining the contributions from using two metals: one with high adsorption energy and one with low adsorption energy. As indicated in Figure 3-4, a combination of Mo (which binds N strongly) with Co (which binds N weakly) was found to be close to the theoretical optimum. Because of the high affinity for nitrogen the CoMo alloy would be expected to be in form of Co_3Mo_3N during ammonia synthesis. The turnover frequency of the Co_3Mo_3N catalyst was indeed found to be higher than Fe and Ru for low NH_3 concentrations at 400 C, 5 MPa, H_2: N_2 = 3:1 (Figure 3-5). Jacobsen et al. (Jacobsen, 2000) studied three ternary nitride catalysts experimentally, namely Fe_3Mo_3N, Co_3Mo_3N and Ni_2Mo_3N. Among these three catalysts, Co_3Mo_3N showed the highest activity: 5,375 μmol g^{-1} h^{-1} at 400 C and 10 MPa. After adding a small amount of Cs, the activity of Co_3Mo_3N dramatically increased to 46,429 μmol g^{-1} h^{-1} evaluated at 400 C and 10 MPa, higher than the activity of Fe based catalyst mentioned before, stated as 33,482 μmol g^{-1} h^{-1}. Both Co_3Mo_3N and Fe based catalysts were inhibited by high concentrations of ammonia in their exit gas (Table 3-1, No. 85-92).
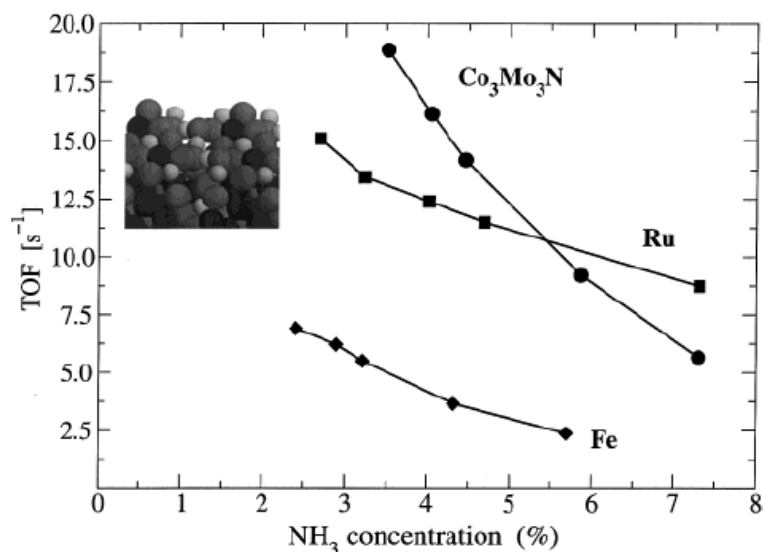
Figure 3-5: Measured turnover frequencies for promoted Ru, Co₃Mo₃N, and Fe catalysts. (Inset): Surface structure of Co₃Mo₃N showing the existence of mixed Co-Mo sites. Light gray: N; dark gray: Co; black: Mo (Jacobsen et al., 2001).

Aika et al. (Kojima and Aika, 2000) studied a Cs promoted cobalt molybdenum bimetallic nitride synthesized by nitridation of cobalt molybdate hydrate with ammonia at 973 K. This catalyst was more stable and active than the corresponding promoted iron catalysts. The reaction rate could reach 15,000 $\mu mol\ g^{-1}\ h^{-1}$ at 400 C under 3.1MPa with a flow rate 60 ml min^{-1}, H₂:N₂ = 3:1 (Table 3-1, No. 93-96). Aika et al. (Kojima and Aika, 2001a), (Kojima and Aika, 2001b) and (Kojima and Aika, 2001c) also studied hydrogen poisoning over the Cs promoted Co₃Mo₃N. They reported that the rate of Cs-Co₃Mo₃N was dramatically enhanced by increasing the applied pressure from 0.1 to 3.1 MPa. In contrast, the Ru based catalyst was not enhanced to the same extent due to hydrogen inhibition. In addition, they found that the apparent activation energies of Fe₃Mo₃N, Co₃Mo₃N and Ni₂Mo₃N were almost the same (11 – 14 kcal mol^{-1}) and were not altered much when adding a small amount of alkali promoter.

Cata No.	Catalysts	Particle size	Feed gas	Temp.	Press.	F	SV	NH3 conv. Equil.	NH3 conv.	Raction rate	Raction rate	Activity	Ref. No.
	Catalysts of ammonia synthesis												
			Reaction conditions					**Performance of catalysts**					
		(mm)	(H2:N2 (NH3 %))	(°C)	(MPa)	(ml min-1)	(h-1)	(%)	(%)	(μmol g-1 h-1)	(mol cm-2 sec-1)		
1	Fe3O4 Fe2+/Fe3+ = 0.71 (CaO/K2O/Al2O3 = 3/0.85/2.8 wt%)		3:1 (7 %)	520	10		300,000					TP: K0 = 61.3, K1 = 40.7	[4]
2	Fe3O4 Fe2+/Fe3+ = 0.73 (CaO/K2O/Al2O3 = 2.4/0.70/3.2 wt%)		3:1 (7 %)	520	10		300,000					K0 = 51.9, K1 = 33.1	[4]
3	Fe3O4 Fe2+/Fe3+ = 0.56 (CaO/K2O/Al2O3 = 3.5/0.50/3.2 wt%)	1.0 - 1.25	3:1 (7 %)	520	10		300,000					K0 = 51.5, K1 = 31.2	[4]
4	Fe3O4 Fe2+/Fe3+ = 0.73 (CaO/K2O/Al2O3 = 2/0.74/2.5 wt%)		3:1 (7 %)	520	10		300,000					K0 = 69.5, K1 = 30.9	[4]
5	Fe3O4 Fe2+/Fe3+ = 0.55 (CaO/K2O/Al2O3 = 3.1/0.62/3.0 wt%)		3:1 (7 %)	520	10		300,000					K0 = 55.8, K1 = 32.0	[4]
6	Fe3O4 Fe2+/Fe3+ = 0.31 (CaO/K2O/Al2O3/SiO2 = 1.8/0.7/2.4/0.4 wt%)		3:1 ()	400	15		30,000	48	36.5	84,970			[6]
7	Fe3O4 Fe2+/Fe3+ = 0.50 (CaO/K2O/Al2O3/SiO2 = 1.8/0.7/2.4/0.4 wt%)		3:1 ()	400	15		30,000	48	36.9	85,820			[6]
8	e3O4 FeO Fe2+/Fe3+ = 0.89 (CaO/K2O/Al2O3/SiO2 = 1.8/0.7/2.4/0.4 wt%		3:1 ()	400	15		30,000	48	32.7	76,040			[6]
9	eO Fe3O4 Fe2+/Fe3+ = 1.11 (CaO/K2O/Al2O3/SiO2 = 1.8/0.7/2.4/0.4 wt%		3:1 ()	400	15		30,000	48	33.6	78,120			[6]
10	eO Fe3O4 Fe2+/Fe3+ = 2.16 (CaO/K2O/Al2O3/SiO2 = 1.8/0.7/2.4/0.4 wt%	1.0 - 1.4	3:1 ()	400	15		30,000	48	35	81,600			[6]
11	FeO Fe2+/Fe3+ = 3.15 (CaO/K2O/Al2O3/SiO2 = 1.8/0.7/2.4/0.4 wt%)		3:1 ()	400	15		30,000	48	37.6	87,610			[6]
12	FeO Fe2+/Fe3+ = 4.62 (CaO/K2O/Al2O3/SiO2 = 1.8/0.7/2.4/0.4 wt%)		3:1 ()	400	15		30,000	48	41.4	96,500			[6]
13	FeO Fe2+/Fe3+ = 6.52 (CaO/K2O/Al2O3/SiO2 = 1.8/0.7/2.4/0.4 wt%)		3:1 ()	400	15		30,000	48	41.3	96,160			[6]
14	FeO Fe2+/Fe3+ = 7.54 (CaO/K2O/Al2O3/SiO2 = 1.8/0.7/2.4/0.4 wt%)		3:1 ()	400	15		30,000	48	41	95,280			[6]
15	A301 Fe2+/Fe3+ = 4 ~ 9	0.034 - 0.044	3:1 ()	400	15		30,000	48	26.8			relative rate: 118	[8]
16	ICI74-1 Fe-Co		3:1 ()	400	15		30,000	48	24.6			106	[8]
17	A110-2 Fe2+/Fe3+ = 0.5 ~ 0.6		3:1 ()	400	15		30,000	48	23			100	[8]
18	Fe(111)		3:1 ()	525	2						4.60E-08		[9]
19	Fe(100) order		3:1 ()	525	2						2.80E-09		[9]
20	Fe(110) order		3:1 ()	525	2						1.10E-10		[9]
21	Fe(111)		3:1 ()	400	2						1.30E-08		[10]
22	Fe(211)		3:1 ()	400	2						9.80E-09		[10]
23	Fe(100)		3:1 ()	400	2						1.90E-09		[10]
24	Fe(210)		3:1 ()	400	2						1.70E-09		[10]
25	Fe(110)		3:1 ()	400	2						none		[10]
26	Unprom. Fe/C		3:1 ()	400	1	267		8	0.63	7560			[5]
27	unprom. Co/C		3:1 ()	400	1	267		8	0.007	79.2			[5]
28	Ba0.35 - Fe/C		3:1 ()	400	1	267		8	1.2	14400			[5]
29	Ba0.35 - Fe50Co50/C		3:1 ()	400	1	267		8	1.14	13680			[5]
30	Ba0.35 - Co/C		3:1 ()	400	1	267		8	1.86	22320			[5]
31	Sr0.35 - Co/C		3:1 ()	400	1	267		8	0.42	5040			[5]
32	Cs0.5 - Co/C		3:1 ()	400	1	267		8	0.021	252			[5]
33	Fe - cat. (KMI)		3:1 ()	400	1	267		8	2.11	37800			[5]

Table 3-1: Performances of various catalysts for ammonia synthesis.

#	Catalyst	Val	Ratio	T	P					Yield	Ref
34	Haber catalyst (magnetite)		3:1 ()	380	8.6					Relative yield: 1	[15]
35	Promoted Ru/HSAG (5 % Ru asn 5 % Rb, prom. Ba and Cs)		1.5:1 ()	380	8.6					26	[15]
36	Haber catalyst (magnetite)		3:1 ()	400	13.8					3	[15]
37	Promoted Ru/HSAG (5 % Ru asn 5 % Rb, prom. Ba and Cs)		1.5:1 ()	400	13.8					55	[15]
38	Ru catalyst (Ba-Ru-K/AC)		3:1 ()	400	10	10,000	40	36.6	108,900		[16]
39	A301 catalyst (FeO)		3:1 ()	400	10	10,000	40	28.8	22,300		[16]
40	Fe - Ru catalyst (two consecutive catalytic beds)		3:1 ()	400	10	10,000	40	39.4	none		[16]
41	equilibrium		3:1 ()	400	10	10,000	40	40	none		[16]
42	K/Ru/C60-70 (2/10/100 w)		3:1 ()	400	0.1	30	637		430		[19]
43	K/Ru/Graphite (2/10/100 w)		3:1 ()	400	0.1	30	637		494		[19]
44	K/Ru/MWNT (multi-walled nanotube) (2/10/100 w)		3:1 ()	400	0.1	30	637		2,048		[19]
45	Fe-based K/Fe/MWNT (4/4/100 w)		3:1 ()	420	0.1	30	637		129		[19]
46	Ru-based K/Ru/MWNT (4/4/100 w)		3:1 ()	420	0.1	30	637		2,117		[19]
47	Ru/C (Ru 8 wt%, Ba/Ru = 0.6)	2.7	3:1 ()	400	5			exit 7%	38880		[20]
48	Ru/MgAl2O4 (Ru 8 wt%, Ba/Ru = 0.6)	1.3	3:1 ()	400	5			exit 5%	28880		[20]
49	Ru/Si3N4 (Ru 8 wt%, Ba/Ru = 0.6)	4.4	3:1 ()	400	5			exit 1.2%	10800		[20]
50	Ru7/Al-WI (Ru 7 wt%, γ-Al2O3, wet impregnaiton)	6.10E-06	3:1 ()	100	0.4	6,000		9.4	6300		[24]
51	Ru3/Al-WI (Ru 3 wt%, γ-Al2O3, wet impregnaiton)	4.40E-06	3:1 ()	100	0.4	6,000		3.6	2412		[24]
52	Ru7/Al-COLL (Ru 7 wt%, γ-Al2O3, colloidal method)	5.90E-06	3:1 ()	100	0.4	6,000		8.2	5508		[24]
53	Ru3/Al-COLL (Ru 3 wt%, γ-Al2O3, colloidal method)	4.10E-06	3:1 ()	100	0.4	6,000		5.1	3420		[24]
54	Ru2/Al-COLL (Ru 2 wt%, γ-Al2O3, colloidal method)	3.10E-06	3:1 ()	100	0.4	6,000		3.4	2268		[24]
55	Ru3/Al-MIC (Ru 3 wt%, γ-Al2O3, microemulsion method BRIJ/heptane)	2.60E-06	3:1 ()	100	0.4	6,000		1.7	1152		[24]
56	Ru3/Al-MIC (Ru 3 wt%, γ-Al2O3, microemulsion method AOT/heptane)	2.40E-06	3:1 ()	100	0.4	6,000		1.9	1260		[24]
57	Ru3/Al-MIC (Ru 3 wt%, γ-Al2O3, microemulsion method CTAB/butanol)	2.00E-06	3:1 ()	100	0.4	6,000		2.4	1620		[24]
58	u3/Al-MIC (Ru 3 wt%, γ-Al2O3, microemulsion method CTAB/cycloehenan	1.50E-06	3:1 ()	100	0.4	6,000		3.2	2124		[24]
59	Ru/ZrO2-KOH (Ru 3.80 wt%, K/Ru = 2.81 mol/mol)	2.2	3:1 ()	400	3	10,000	19	7.6	11,100		[32]
60	K-Ru/ZrO2 (Ru 3.86 wt%, K/Ru = 2.78 mol/mol)	6.4	3:1 ()	400	3	10,000	19	3.1	4,410		[32]
61	Ru/ZrO2 (Ru 3.87 wt%, K/Ru = 0.21 mol/mol)		3:1 ()	400	3	10,000	19	1	1,040		[32]
62	K-Ru/MgO (Ru 3.92 wt%, K/Ru = 2.75 mol/mol)	7.8	3:1 ()	400	3	10,000	19	2.7	8,910		[32]
63	K-Ru/Al2O3 (Ru 3.79 wt%, K/Ru = 2.84 mol/mol)	4	3:1 ()	400	3	10,000	19	0.8	2,080		[32]
64	Ru/BaZrO3 (4 wt%)		3:1 ()	400	3	10,000	19	12	15,300		[33]
65	Ru/MgO (4 wt%)		3:1 ()	400	3	10,000	19	2.5	8,380		[33]
66	Ru/CeO2 (4 wt%)		3:1 ()	400	3	10,000	19	4.7	8,430		[33]
67	Ru/ZrO2 (4 wt%)		3:1 ()	400	3	10,000	19	2.8	4,580		[33]
68	Ba-Ru/BN (Ba ca. 5.6 wt%, Ru 4.5 wt%)	2.00E-6	3:1 (4.5 %)	360	10			exit 12%	27,660		[26]
69	Ba-Ru/BN (Ba ca. 5.6 wt%, Ru 4.5 wt%)	-	3:1 (4.5 %)	400	10			exit 12%	184,972		[26]
70	Ba-Ru/BN (Ba ca. 5.6 wt%, Ru 4.5 wt%)	2.50E-6	3:1 (4.5 %)	400	5			exit 12%	95,668		[26]

71	Ru/C12A7:e- (C12A7: 12CaO·7Al2O3, 1 wt% Ru)		3:1 ()	400	0.1	60	1	0.68	2,750	[25]
72	Ru/C12A7:O2- (C12A7: 12CaO·7Al2O3, 1 wt% Ru)		3:1 ()	400	0.1	60	1	0.15	600	[25]
73	Ru/AC (1 wt% Ru)		3:1 ()	400	0.1	60	1	0.1	400	[25]
74	Ru-Cs/MgO (1 wt% Ru)		3:1 ()	400	0.1	60	1	0.57	2,300	[25]
75	Ru-Ba/AC (1 wt% Ru)		3:1 ()	400	0.1	60	1	0.05	200	[25]
76	Ru/CaO (1 wt% Ru)		3:1 ()	400	0.1	60	1	0.05	200	[25]
77	Ru/γ-Al2O3 (1 wt% Ru)		3:1 ()	400	0.1	60	1		none	[25]
78	Ru-Ba/AC (9.1 wt% Ru)	9.30E-06	3:1 ()	400	1	60	8.3	2.05	8,285	[25]
79	Ru-Cs/MgO (6.0 wt% Ru)	7.20E-06	3:1 ()	400	1	60	8.3	3	12,117	[25]
80	Ru/C12A7:O2- (C12A7: 12CaO·7Al2O3, 1.2 wt% Ru)	3.92E-05	3:1 ()	400	1	60	8.3	0.22	888	[25]
81	Ru/C12A7:e- (C12A7: 12CaO·7Al2O3, 0.1 wt% Ru)	8.50E-06	3:1 ()	400	1	60	8.3	0.25	994	[25]
82	Ru/C12A7:e- (C12A7: 12CaO·7Al2O3, 0.3 wt% Ru)	3.29E-05	3:1 ()	400	1	60	8.3	0.91	3,686	[25]
83	Ru/C12A7:e- (C12A7: 12CaO·7Al2O3, 1.2 wt% Ru)	4.13E-05	3:1 ()	400	1	60	8.3	2.04	8,245	[25]
84	Ru/C12A7:e- (C12A7: 12CaO·7Al2O3, 4.0 wt% Ru)	6.85E-05	3:1 ()	400	1	60	8.3	1.5	6,089	[25]
85	γ-Mo2N		3:1 (4.5%)	400	10			exit 12%	1,339	[34]
86	Fe3Mo3N		3:1 (4.5%)	400	10			exit 12%	4,018	[34]
87	Co3Mo3N		3:1 (4.5%)	400	10			exit 12%	5,357	[34]
88	Ni3Mo3N		3:1 (4.5%)	400	10			exit 12%	3,571	[34]
89	5 wt% Cs/Fe3Mo3N		3:1 (4.5%)	400	10			exit 12%	19,643	[34]
90	5 wt% Cs/Co3Mo3N		3:1 (4.5%)	400	10			exit 12%	46,429	[34]
91	5 wt% Cs/Ni3Mo3N		3:1 (4.5%)	400	10			exit 12%	23,661	[34]
92	KMI (commercial multi-promoted iron catalyst)		3:1 (4.5%)	410	10			exit 12%	33,482	[34]
93	Co3Mo3N (from CoMoO4·nH2O)		3:1 ()	400	3.1	60	20	2.25	ca. 4,500	[35]
94	2% Cs promoted Co3Mo3N (from CoMoO4·nH2O)		3:1 ()	400	3.1	60	20	7.5	ca.15,000	[35]
95	10% Cs promoted Co3Mo3N (from CoMoO4·nH2O)		3:1 ()	400	3.1	60	20	2.5	ca.5,000	[35]
96	Fe-K2O-Al2O3		3:1 ()	400	3.1	60	20	2	ca.4,000	[35]

The above review on the catalysts suggests that Fe-based catalysts are the preferred option for the Haber-Bosch process; they deliver under the process conditions an ammonia conversion that is close to the thermodynamic equilibrium value, with a recycle loop to ensure near complete conversion to ammonia.

More active catalysts for ammonia production could be considered. Other elements, such as Os and Ru, promise better performance both theoretically and experimentally. The high cost of these catalysts, as compared to Fe, could be an issue in their future development.

The sensitivity of the working catalysts to CO_x and hydrocarbon impurities is also an important issue in the Haber-Bosch process. Changes to the reaction conditions of the Haber-Bosch process could make the use of more active catalysts commercially favourable. Among the options are smaller scale for ammonia production, more dilute H_2 concentrations, and non-steady and smaller flow.

The impurities in the reaction stream could also differ from the conventional Haber-Bosch process. Electrolytic production of hydrogen would eliminate any carbonaceous source.

Ru catalysts are more active than Fe catalysts but they progressively suffer deactivation at higher hydrogen pressures. Intuitively and also based on consideration of the reaction stoichiometry, it would seem obvious to operate the reaction over Ru catalysts at a $H_2:N_2$ ratio of 3:1. However the kinetic characteristics of ruthenium and iron catalysts are very different. Whilst the traditional iron catalysts give an optimum performance at 3:1 H_2/N_2 ratio, the ruthenium catalysts show a continuous increase in rate with increasing nitrogen partial pressure. However, the processes for producing the hydrogen/nitrogen mixture and other commercial factors dictate the synthesis loop is operated at around 2.2-3/1 hydrogen to nitrogen ratios, making the Ru catalysts operate differently under these conditions (Brown et al., 2014). There are new Ru catalyst formulations which show promising results in laboratory testing, but this issue needs to be resolved at larger scale synthesis. Clearly, the reported promoted bimetallic catalysts such as $CoMoN_x$ and $FeMoN_x$ show impressive ammonia production rates that should be considered for any renewable ammonia synthesis processes. However, one key issue is that these active catalysts could also suffer from a strong competitive adsorption of produced ammonia under reaction conditions and thus the rate would be much slower at a high exit ammonia concentration. This issue may need to be properly addressed if high rates and high concentrations of ammonia are simultaneously required. Their comparison under specified reaction conditions is shown in Table 3-1.

3.1.4   Non-conventional Ammonia Synthesis (Electrochemical)

As it is accepted that the Haber-Bosch process is an energy demanding, thermodynamic constrained and environmentally polluting process, an alternative development for ammonia synthesis processes should be considered. Electrochemical activation of nitrogen to ammonia in water or hydrogen may have the potential to overcome these limitations. Whilst ammonia conversion by Haber-Bosch synthesis is clearly restricted by thermodynamic equilibrium, high pressure may not be required using solid state electrochemical ammonia synthesis (Marnellos et al., 1999), (Marnellos et al., 1997) and (Panagos et al., 1996). The solid state electrochemical device consists of a porous anode electrode, a porous cathode electrode and a dense solid electrolyte which allows ion transport and serves as a barrier to gas diffusion (Malavasi et al., 2010) and (Amar et al., 2011).
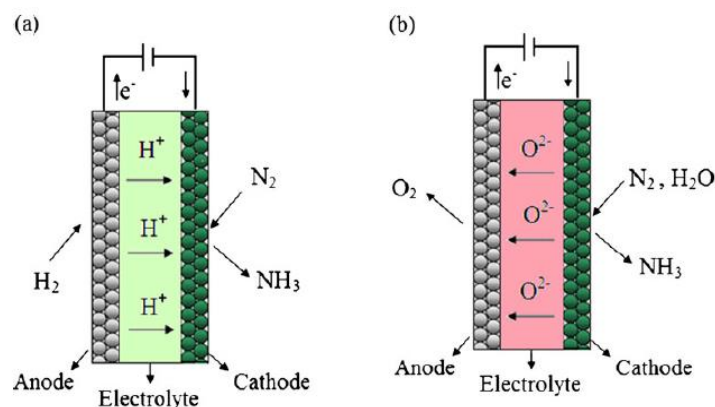
Figure 3-6: Schematic illustration of solid state electrochemical ammonia synthesis device: (a) proton conducting electrolyte and (b) oxide ion electrolyte (Amar et al., 2011).

3.1.4.1   Proton Conducting Electrolytes

Panagos et al. (Panagos et al., 1996) and Marnellos et al. (Marnellos, 1998) studied a new route to synthesize ammonia from H$_2$ and N$_2$ at atmospheric pressure by using a solid state proton conductor electrolyte where electromotive force provided the energy to overcome the elementary activation barriers. The principle can be explained in Figure 3-6 (a); in the electrolytic cell, two metal electrodes are placed on the two sides of the proton conductor electrolyte. H$_2$ gas is passed over the anode and is converted to H$^+$ under an oxidation step. The proton will then migrate across the conductor to the cathode. At the cathode, the

flowing N$_2$ is then reacted with the H$^+$ to form ammonia under a reduction step. It was reported that 78% of the supplied protons were converted to ammonia with a rate of 4.5e-9 mols^{-1}cm^{-2} at 570 C when SrCe$_{0.95}$Yb$_{0.05}$O$_3$ and Pd were used as the electrolyte and electrode, respectively.

Li et al. (Z. Li et al., 2007) investigated the use of BaCe$_{0.9}$Sm$_{0.1}$O$_{3-\delta}$ and BaCe$_{0.8}$Gd$_{0.1}$Sm$_{0.1}$O$_{3-\delta}$ as electrolytes and Ag-Pd as the electrode. At ambient pressure and 620 C, the measured rates were 5.23e-9 and 5.82e-9 mols^{-1}cm^{-2}, respectively. Chen et al. (Chen and Ma, 2009) reported the use of BaCe$_{0.85}$Gd$_{0.15}$O$_{3-\delta}$ as electrolyte, Ni-BaCe$_{0.85}$Gd$_{0.15}$O$_{3-\delta}$ as anode and Ag-Pd as cathode; the ammonia production rate was found to be 4.63 mol s^{-1} cm^{-2} at 480 C. Liu et al. (Liu et al., 2006) employed Ce$_{0.8}$Sm$_{0.2}$O$_{2-\delta}$ as electrolyte and Ag-Pd as the electrode, and stated the ammonia synthesis rate to be 8.2e-9 mols^{-1}cm^{-2} at 650 C. By using Nafion as electrolyte, NiO-Ce$_{0.8}$Sm$_{0.2}$O$_{2-\delta}$ as anode and Sm$_{1.5}$Sr$_{0.5}$NiO$_4$ as cathode, Xu et al. (Xu and Liu, 2009) claimed that the ammonia production rate reached 1.05e-8 mols^{-1}cm^{-2} at 80 C. Wang et al. (Wang et al., 2006) reported a new route to synthesize ammonia from natural gas and N$_2$. They used Ce$_{0.8}$Y$_{0.2}$O$_{1.9}$-(Ca$_3$(PO$_4$)$_2$)-K$_3$PO$_4$ as the electrolyte and Ag-Pd as electrode materials. The ammonia production rate was found to be 6.59e-9 mols^{-1}cm^{-2} at 650 C.

The layout for this electrochemical reaction is shown in Figure 3-7.
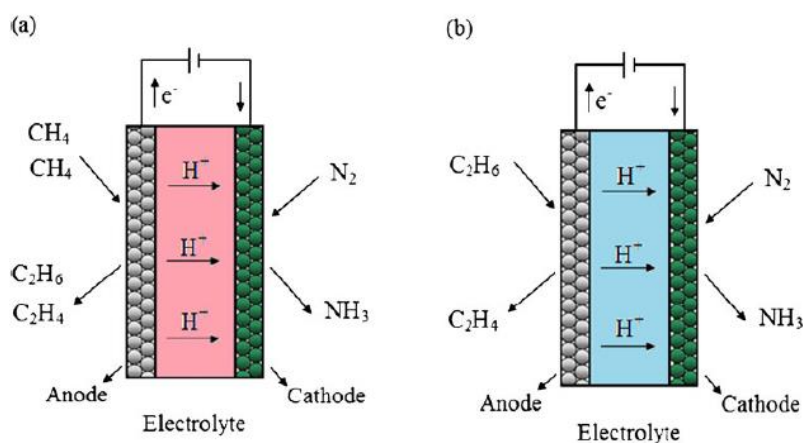
Figure 3-7: Ammonia synthesis from natural gases and N$_2$ (Amar et al., 2011).

3.1.4.2   Oxygen Ion Conducting Electrolytes

Stoukides et al. (Skodra and Stoukides, 2009) reported the synthesis of ammonia for the first time from nitrogen and steam rather than using molecular hydrogen. It is worthy to note that using steam instead of hydrogen can be in principle advantageous (Figure 3-6(b)). First, the costs for hydrogen production and its further purification would be bypassed. Steam is electrolyzed at the cathode where it reacts with the adsorbed nitrogen to produce ammonia and O^{2-} is transported through the solid electrolyte to the anode. This means that only nitrogen needs purification and synthetically useful oxygen can be produced at a minimal cost. The ammonia was thus made successfully in their electrolytic cells at 450-700 C using yttria stabilised zirconia (YSZ)-based oxides, a Ru-based catalyst, and Pd as a solid electrolyte, cathode and anode, respectively. Although promising, current reported rates are extremely low, because of the poor electrical conductivity of the materials used.

3.1.5   Conclusions for ammonia synthesis

In conclusion, fused iron catalysts still appear to be the most appropriate catalysts in the industrial Haber-Bosch process. By changing the iron sources and tuning the pre-treatments and operating conditions, more effective fused iron catalysts could be obtained. While Ru catalysts are associated with a higher intrinsic activity than Fe, they cannot be used in the industrial practice unless problems relating to H$_2$ poisoning and degradation of the support are solved. For the new generation of the more active Co$_3$Mo$_3$N catalysts, the conversion may still be too low at the evaluated temperatures and pressures of operation, and published data at higher temperatures and pressures is unfortunately unavailable for a proper comparison. As far as the calculations suggest, further improvement in the activity for this type of Co$_3$Mo$_3$N catalysts would render the new renewable process economically more viable.

Regarding the electrochemical approach to synthesize ammonia, there are a number of potential candidates which have recently been demonstrated to be active for this reaction. The potential elimination of the separation and purification steps for H$_2$ when H$_2$O is used as the reductant for N$_2$, along with the input of electrochemical energy at milder conditions, is very attractive. However, the reported rates are unfortunately very far away from those of industrial practices using heterogeneous catalysis approaches. It would be difficult to see their contribution to a new and large industrial process but it is equally difficult to rule out some small but niche applications in this area.

3.2 Catalysts for Ammonia Decomposition

3.2.1 Introduction

Ammonia is relatively easy to store and deliver, as stated previously, so there is an increasing interest in using ammonia as an indirect hydrogen storage material. By using ammonia as a hydrogen provider, it can produce COx free hydrogen for fuel uses. Using an efficient adsorbent a large amount of unconverted gaseous ammonia can be reduced in a gas stream to less than 200 ppb (Chellappa et al., 2002). In this reversed process, NH$_3$ decomposition to its elements is an endothermic reaction. N$_2$ recombination on catalyst surface is expected to be the rate determining step in the catalytic ammonia decomposition.
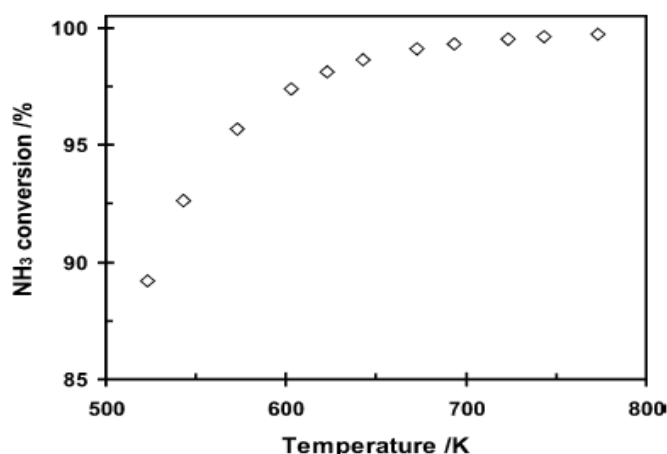
Figure 3-8: Equilibrium conversions of ammonia at different temperatures at 1 atmosphere (S. F. Yin et al., 2004).

The equilibrium conversions shown in Figure 3-8 are a function of applied temperatures, i.e. the equilibrium conversions are 99.31% at 693 K and 99.53% at 723 K. However, the conversion shows diminishing returns for temperatures above 673 K. For fuel cell applications, a stream of ammonia at high concentrations, employing atmospheric pressures, is needed to produce pure hydrogen without much residual ammonia (conversion > 99.5%). Therefore, higher operation temperatures may be required. For instance, some trials using inexpensive supported Ni catalysts, widely used in the catalysis industry, were attempted. They were able to decompose ammonia at this demand level but 1000 C was required (S. F. Yin et al., 2004). Apparently, a more efficient catalyst at low cost is urgently needed for this reaction.

			catalysts of ammonia decomposition						
						performance of catalyst			
Cata No.	catalyst promoted and support	ammount of cata.	Feed gas	Temp.	Press.	SV	NH3 conv.	rate (H2)	Ref. No.
		(g)	(NH3)	(°C)	atm	(ml g-1 h-1)	(%)	(mmol g-1 min-1)	
1	Ru/CNT (ca. 4.75e-4 mol gcat-1)	0.1	pure	500	1	30,000	84.65	28.35	[52]
2	Rh/CNT (ca. 4.75e-4 mol gcat-1)	0.1	pure	500	1	30,000	ca. 12	4.19	[52]
3	Pt/CNT (ca. 4.75e-4 mol gcat-1)	0.1	pure	500	1	30,000	none	1.41	[52]
4	Pd/CNT (ca. 4.75e-4 mol gcat-1)	0.1	pure	500	1	30,000	ca. 4	1.43	[52]
5	Ni/CNT (ca. 4.75e-4 mol gcat-1)	0.1	pure	500	1	30,000	ca. 9	2.9	[52]
6	Fe/CNT (ca. 4.75e-4 mol gcat-1)	0.1	pure	500	1	30,000	ca. 1	0.65	[52]
7	Ru/CNTs (5 wt% Ru)	0.1	pure	450	1	60,000	43.7	14.6	[54]
		0.1	pure	550	1	60,000	100	33.5	[54]
8	Ru/MgO (5 wt% Ru)	0.1	pure	450	1	60,000	30.9	10.4	[54]
		0.1	pure	550	1	60,000	91.8	30.7	[54]
9	Ru/Ac (5 wt% Ru)	0.1	pure	450	1	60,000	28.7	9.6	[54]
		0.1	pure	550	1	60,000	78.9	26.4	[54]
10	Ru/ZrO2 (5 wt% Ru)	0.1	pure	450	1	60,000	24.8	8.3	[54]
		0.1	pure	550	1	60,000	77	25.8	[54]
11	Ru/Al2O3 (5 wt% Ru)	0.1	pure	450	1	60,000	23.4	7.8	[54]
		0.1	pure	550	1	60,000	73.7	23.5	[54]
12	K-Ru/CNTs (5 wt% Ru, Ru/K (mol) = 1)	0.1	pure	400	1	60,000	59.8	20	[54]
		0.1	pure	450	1	60,000	97.3	32.6	[54]
13	10% Ru/SiO2	0.1	pure	450	1	30,000	36.4	11.4	[55]
14	5% Ru/CNTs	0.2	pure	550	1	30,000	84.7	26	[56]
15	5% Ru/GC	0.2	pure	550	1	30,000	95	29.1	[56]
16	MoNx/α-Al2O3	0.7	pure	700	1	3600 h-1	99.7		[59]
17	NiMoNy/α-Al2O3	0.7	pure	700	1	3600 h-1	99.8		[59]
18	commercial NiO/MgO (6 wt%)	0.7	pure	750	1	3600 h-1	96.8		[59]
19	commercial NiO/MgO (6 wt%)	0.7	pure	750	1	1800 h-1	99.9		[59]
20	Cr-CTAB-160-600 (160: Cr decomp. T)	0.2	pure	600	1	60,000	43.3	13.3	[60]
21	10%Ni/SiO2-600	0.2	pure	600	1	60,000	36.4	11.4	[60]
22	5%Ru/SiO2-550	0.2	pure	550	1	60,000	96.5	32.3	[60]
23	C-Fe-2.33-400 (C: carbon) active	0.025	pure	600	1	7500	100		[61]
24	S-Fe-2.33-400 (C: carbon, S: silicon) stabl	0.025	pure	675	1	7500	100		[61]
25	NiO/Al2O3	0.025	pure	600	1	7500	76		[61]
26	α-Fe2O3-50@pSiO2	0.25	pure	650	1	15,000	100		[62]
27	α-Fe2O3-50@pSiO2	0.25	pure	750	1	120,000	80		[62]
28	nano-Fe	0.1	pure	650	1	50 ml min-1	68.1	22.8	[63]
29	nano-Fe@micro-SiO2	0.1	pure	650	1	50 ml min-1	97	32.48	[63]
30	nano-Fe@meso-SiO2	0.1	pure	650	1	50 ml min-1	100	33.48	[63]
31	10% Ni/SiO2	0.1	pure	650	1	50 ml min-1	70	21.1	[63]
32	Ni/MCM-41(TIE)	0.1	pure	650	1	50 ml min-1	91.5	30.6	[63]

Table 3-2: Performances of various catalysts for ammonia decomposition.

3.2.2 Ammonia Decomposition

Yin et al. (S.-F. Yin et al., 2004) investigated the use of more expensive elements including Ru, Rh, Pt, Pd as the active component in ammonia decomposition. It was shown that Ru supported on CNTs exhibited the highest ammonia conversion (84.65%) with the H_2 formation rate to be 28.35 mmolg^{-1}min^{-1}. This was evaluated under ambient pressure at a space velocity of 30,000 ml g$_{cat}$$^{-1}$h^{-1}, at 500 C (Table 3-2, No. 1-6). After CNTs were modified with KOH, the ammonia conversion was promoted to 99.74% and the H_2 formation rate reached to 47.88 mmol g^{-1} min^{-1}. Consequently, the strong basic support was apparently essential for the high catalytic performance.

Zheng et al. (Zheng et al., 2007) stated supported Ru clusters, with mean sizes ranging from 1.9-4.6 nm, can display a high activity for the ammonia decomposition reaction. Yin et al. (Yin, 2004) investigated the ammonia decomposition reaction over Ru, using different supports. After testing the same amount of Ru on various supports, the order of activities was ranked as Ru/CNTs > Ru/MgO > Ru/AC > Ru/ZrO$_2$ ≈ Ru/Al$_2$O$_3$, evaluated at 450-550 C. The H_2 formation rate was found to be 33.5 mmol g^{-1} min^{-1} for Ru/CNTs under ambient pressure, with a space velocity of 60,000 ml g$_{cat}$$^{-1}$ h^{-1} at 550 C (Table 3-2, No. 7-12). Moreover, Ru/CNTs exhibited a superior activity than the 10% Ru/SiO$_2$ at 450 C (Table 3-2, No. 13) (Choudhary et al., 2001). Li et al. (L. Li et al., 2007) found graphitic carbon was an excellent support for Ru catalyst. The ammonia conversion was found to be 95% over the Ru/GC catalyst and 84.7% over the Ru/CNTs at 550°C (Table 3-2, No. 14, 15). They suggested the graphitic structure of carbon is more important than the surface area provided for the superior catalytic activity.

So far, from the systematic screening of a large amount of catalysts, Ru and Ir have demonstrated to be the most active metals for ammonia decomposition under mild conditions (Choudhary et al., 2001), (Bradford, 1997), (Mary et al., 1999). However, they are rarely used in commercial processes, because of their high costs. Liang et al. (Liang et al., 2000) reported their studies on MoNx/α-Al$_2$O$_3$ and NiMoNx/α-Al$_2$O$_3$ catalysts, which showed higher ammonia conversions than that of commercial NiO/MgO catalyst. The stated conversions were 99.7% and 99.8% respectively at 700 C (Table 3-2, No. 16-19). Their high activity was attributed to the intrinsic active nitride phase present in these catalysts. Li et al. (Li et al., 2009) reported the use of a mesoporous Cr$_2$O$_3$ catalyst for the ammonia decomposition. It was suggested that the N atom is inserted into Cr$_2$O$_3$ during the reaction, which could enhance the activity of this catalyst (Table 3-2, No. 20-22).

Lu et al. (Lu et al., 2010) used the high mesoporosity of CMK-5 carbons and C/SBA-15 composites as supports for the ammonia decomposition reaction. γ-Fe$_2$O$_3$ was found to disperse uniformly on these supports with an average diameter of 6 nm. The γ-Fe$_2$O$_3$/CMK-5 catalyst showed a higher activity than that of a commercial NiO/Al$_2$O$_3$ catalyst; the ammonia conversion was found to be nearly 100% at 600 C. In addition, the C/SBA-15 phase as the support was found to be more stable than CMK-5 but was less active (Table 3-2, No. 23-25). Feyen et al. (Feyen et al., 2011) also reported a new high temperature but stable α-Fe$_2$O$_3$ nanoparticle core and porous silica shell catalyst. The α-Fe$_2$O$_3$ was reduced to Fe during the reaction with the appearance of some FeNx species. With an average size of 50 nm, the α-Fe$_2$O$_3$-50@pSiO$_2$ cracked the ammonia completely at 650 C

under the space velocity of 15,000 ml g_{cat}^{-1} h^{-1}. Even at 750 C under the space velocity of 120,000 ml g_{cat}^{-1} h^{-1}, the conversion was maintained at around 80% (Table 3-2, No.26, 27). Li et al. (Li et al., 2010) also tested the nano-Fe@meso-SiO$_2$ catalyst for the ammonia decomposition, which gave 100% ammonia conversion in the temperature range of 650 -670 C. The nano-Fe@meso-SiO$_2$ catalyst was more active and stable than the supported Ni catalyst under the same conditions (Table 3-2, No. 28-32). It was believed that the silica shell can prevent the aggregation of Fe nanoparticles in this solid system.

Itoh et al. (Itoh et al., 2002) investigated a series of Fe-MOx catalysts where M represented different metal components. It was found that the activity of ammonia decomposition over the Fe-(Ce, Zr)O$_2$ catalysts was the highest, because of the electron donation to the iron metal from Ce^{3+} due to the reduction of CeO$_2$ through the reaction for low ammonia flow rates. David et al. (David et al., 2014) reported an interesting new class of catalysts for ammonia decomposition, which was not based on the common usages of transition metals or noble metals. Instead, sodium amide and sodium metal were used as catalysts via their in-situ stoichiometric decomposition and regeneration. The reported ammonia conversion was 99.2% at 530 C under their flow rate of 60 ml min^{-1}.

3.2.3   Conclusions for ammonia decomposition

The review identified many catalysts that have been screened for the ammonia decomposition reaction. Among all these catalysts reported, potassium promoted CNTs supported ruthenium catalysts appear to be the most promising candidates due to their high ammonia conversion rates at lower temperatures. Considering the high costs of noble metals and their preparations, a low cost but highly active catalyst is needed for the practical conversion of ammonia under industrial conditions. For example, the core-shell approach may reduce the usage of any expensive metal component in the working catalysts, and the stability of them against metal sintering may also be improved. The sodium amide based catalysts represent a new type of catalysts for ammonia decomposition at mild conditions but further studies on their stability and recyclability are required.

3.3 Conclusions

This section provided a critical review of catalytic options concerning two very important processes in the system: (a) the Haber-Bosch synthesis loop, and (b) the ammonia to power module.

Regarding the former, the maturity of the conventional Haber-Bosch process means that a qualitative improvement of this technology is likely to come through the development of new catalysts. The review provides a platform for further analysis of a synthesis loop driven by catalysts other than Fe, specifically Ru and CoMoN. This analysis is detailed in Section 5. Electrochemical synthesis of ammonia is also explored, but the rates of reaction associated with this route are still too low for a practical implementation of this system at present.

Regarding the latter, the efficiency and power output of a catalytic ammonia decomposition system will be critical parameters for the overall feasibility of the process; the review concludes a catalytic route for this process is still in the development stage, hindered by the price of noble metals and their stability under the process conditions.

4. Description of the model

4.1 Introduction

The purpose of developing a computer model was to investigate the influence of different variables on the size and cost of the modules in the process. There are trade-offs to be found when varying the design parameters; in most cases the use of a mathematical model is the only way to determine where the sensitivities in our system lie. For example, we know that operating the Haber-Bosch ammonia synthesis loop at lower pressures will result in fewer, smaller and cheaper compressors in the compressor train, but would also decrease the conversion to ammonia and thus increase the recycle flowrate (with the consequent increase in size and cost of the equipment in the loop).

A model to investigate the key parameters and their trade-offs has been developed in Matlab[1]. The model integrates the generation of alternatives, their sizing and costing, and the plotting of results. Other implementation options that were considered initially (e.g. Excel and Aspen Plus) would have resulted in less efficient or incomplete results.
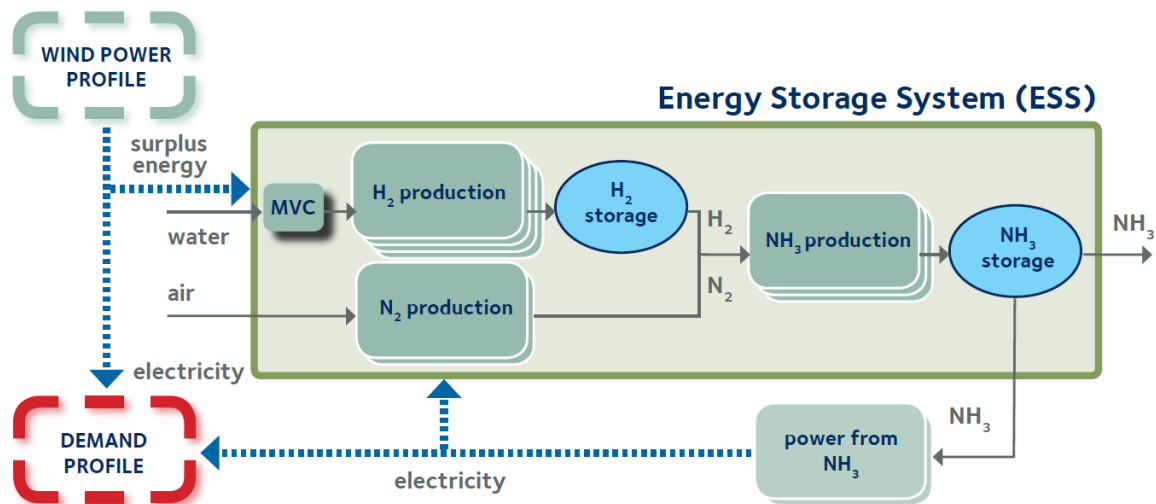
Figure 4-1: Modular representation of the energy system (ES) including the energy storage system (EES) sub-system.

Figure 4-1 illustrates the system driven by an intermittent power input from a wind farm which is used to satisfy a given electricity demand (*Demand profile*). Surplus power from the wind farm is used to operate an *Energy Storage System (ESS)* consisting of *H₂, N₂ and NH₃ production* modules. Power deficits are overcome by converting NH_3 from *NH₃ storage* via the *Power from NH₃* module back to electricity. This ensures that (a) the *Demand profile* is satisfied, and (b) a minimum level of operation of the *ESS* is maintained.

---

[1] http://www.mathworks.co.uk/products/matlab/

Storage of H_2 and NH_3 is considered to ensure that (a) the minimum operation loads of the ESS components are met, and (b) the NH_3 production process operates with minimal load variations –to maximise the lifetime of the catalyst. A condition for a feasible system is that no cumulative deficits in any of the intermediate products (H_2, N_2 and NH_3) occur and that the *Demand profile* is satisfied.

This section briefly describes the model inputs and outputs (Section 4.2); its structure and functionality (Section 4.3); the methods used to size and cost the modules and some selected individual components (Section 4.4); and lists the assumptions made in constructing the model, its limitations and design parameters (Section 4.5).

4.2 Model Inputs and Outputs

A schematic of the Inputs and Outputs of the model is shown in Figure 4-2.

1. Wind and Demand profiles

2. Properties of technologies

3. System parameters

Model
- MVC
- Electrolyser
- ASU
- HB
- NH3 to power

Plots of wind and demand profiles

H2, N2, NH3 surplus/deficits (storage)

Number, size and cost of modules

Levelised costs of energy & NH3
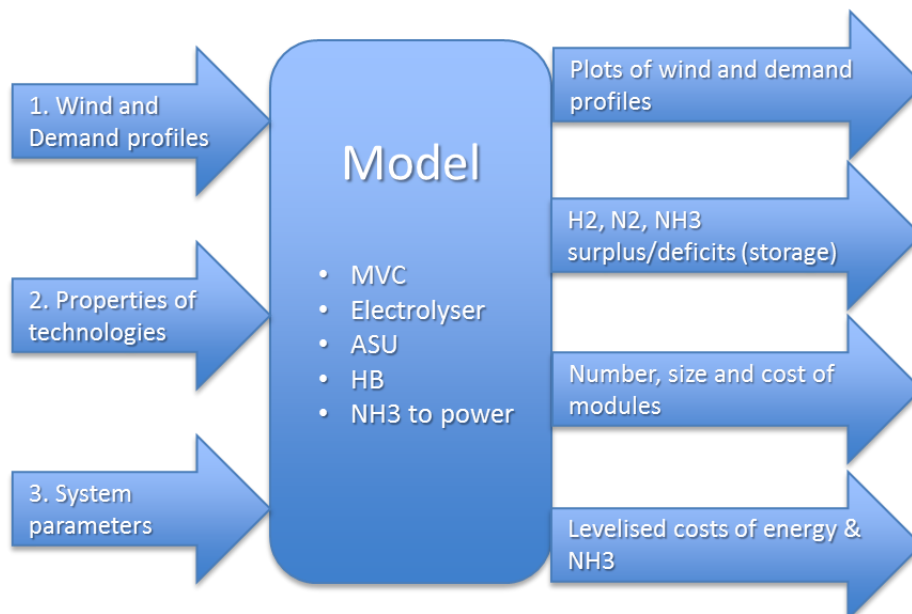
Figure 4-2: Inputs and Outputs of the model

4.2.1   Model inputs

The system has three types of inputs, see Figure 4-2:

1. Input data in the form of a wind power profile and a demand profile (see Figure 5-3 for a plot of both profiles).

   - The wind power profile is a 5-minute time series over one year with empirical wind generation output in MW.

We have not been able to obtain wind power generation data for the UK; for this reason we are using data from a wind farm in Australia from where there are instantaneous readings for the last few years reported every 5 minutes[2]. We have selected the Portland wind farm in the state of Victoria because it has a nominal power generation of 102 MW.

- A daily demand profile is read from a text file containing two columns: a time of day (in hours) and a percentage of the total demand to be satisfied at that time (in %). The maximum and minimum demand values were set at 19 and 5.7 MW respectively.

  A daily demand profile was adapted from (Hildmann and Saffre, 2011). We assume that the daily demand is identical for the whole period of the simulation (one year).

2. Types and characteristics of the technologies to be considered in the simulation.

   For each of the three modules in the process a number of technologies are considered and modelled in terms of a set of parameters.

   Based on the review in Section 2, the technology options considered are (see Table 4-1):

   - Hydrogen production:
     Atmospheric Alkaline Electrolysis; (2) High-Pressure Alkaline Electrolysis; and (3) PEM.

   - Nitrogen production:
     Cryogenic ASU; and (2) PSA.

   - Ammonia production:
     Fe-based catalyst HB; (2) Ru-based catalyst HB; (3) CoMoN-based catalyst HB; and (4) mini-HB.

Each one of these technologies is described in terms of the following characteristics (their values are taken from those shown in Table 2-4, Table 2-5 and Table 2-6):

- Product (H_2, N_2 or NH_3).
- Energy requirement (at a given operating range) in [GJ / ton_product].
- Capacity range, min/max in [tons_product / day].
- Operation load range, min/max in [fraction], e.g. 0.8 to 1.0.

---

[2] The data can be downloaded from http://windfarmperformance.info . We used the year 2011.

The Haber-Bosch processes have the following additional characteristics (their corresponding values are reported in Table 2-6):

- Pressure of operation, in [bar].
- Temperature of operation, in [C].
- Catalyst, type of catalyst used (Fe-, Ru- or CoMoN-based).
- Conversion, in [fraction].
- Reaction rate, in [kg_NH$_3$ / kg_cat / s].
- Catalyst density, in [kg_cat / lt].
- Catalyst price, in [£ / kg].

3. Model parameters.

By setting the values of these parameters the user can adapt the model to specific cases.

- Ammonia plant size, in [ton_NH$_3$ / day].
- Purge ratio in the ammonia synthesis loop, in [fraction].
- Overproduction of hydrogen, a scaling factor.
- Maximum demand (in [MW]). Since the demand profile is defined in terms of percentage, this allows an easy scaling of the required electricity demand.

4.2.2   Model outputs

The system has several outputs, see Figure 4-2 and the results in Section 5, which allow the visualisation of the relation between the wind power and demand inputs and the required H$_2$ and NH$_3$ storage over time. The system also reports the size and cost of all the modules in the process.

A more detailed list of the outputs is:

- Plots of wind power generation and satisfied demand profiles.
- Plots of H$_2$, N$_2$ and NH$_3$ production - surplus and deficits.
- Plots of the sensitivity analyses, e.g. Cost of the NH$_3$ synthesis loop vs. Purge Ratio.
- Tables of the number of units required for each module in the system for a given case, e.g. 62 electrolysers, 2 PSA units and one HB plant.
- Sizes, energy efficiencies and annualised costs of the modules and, in some cases, of the individual items of equipment (compressors, heat exchangers, pressure vessels)
- H$_2$ and NH$_3$ storage requirements.

4.3 Structure and functionality

4.3.1 Structure of the model

The model generates all the possible configurations of modules. There are alternative technologies for each of the modules in the model, see Table 4-1.

key	i H₂ production technology	j N₂ production technology	k NH₃ production technology
1	Atmospheric Alkalyne Electrolysis	Cryogenic ASU	Fe-based HB (commercial system)
2	High-Pressure Alkalyne Electrolysis	PSA	Ru-based HB
3	PEM		CoMoN-based HB
4			mini-HB

Table 4-1: Technologies considered in each of the three main modules of the model.

The combination of technologies allows for 24 configurations, $(i)(j)(k) = (3)(2)(4) = 24$.

So, for example,
- Configuration [1, 1, 1] stands for Atmospheric Alkalyne Electrolysis for H_2 production, Cryogenic ASU for N_2 production, and Fe-based HB for NH_3 synthesis, and
- Configuration [3, 2, 3] stands for PEM for H_2 production, PSA for N_2 production, and CoMoN-based HB for NH_3 synthesis.

The following results are calculated by the model for each of the configurations:
- Number of plants required.
- H_2, N_2 and NH_3 storage required, in [ton].
- Instantaneous and cumulative deficit/surplus, of H_2, N_2 and NH_3 at the end of the time period, in [ton].
- Annualised capital cost for each of the modules in Table 4-1and for the MVC and the NH_3-to-power modules, in [USD / yr].
- Annualised total cost for the configuration.

Additionally, in the case of the NH_3 synthesis loop
- For each stream in the loop: flowrate, composition, temperature, and pressure.
- For the compressor train: number of stages and intercoolers, and pressure ratio per stage (maintaining it below a value of 3.5).
- For each compressor: power and electrical drive power, in [kW], and annualised cost, in [USD]; the model selects whether to use a centrifugal (if the power is greater than 950 kW) or a rotary compressor
- For each heat exchanger: heat transferred in [kW], area, in [m²] and annualised cost, in [USD].

- For the reactor and the flash vessels: diameter in [m], volume in [m^3], and annualised cost, in [USD].
- Amount in [kg_catalyst] and cost of required catalyst in [USD].
- H_2, N_2 and NH_3 flowrates in the purge, in [kg / s].

Note that a separate module for NH_3 synthesis loop allows the investigation of catalyst variation; Fe-, Ru- and CoMoN-based catalysts determine the pressure and temperature of operation of the reactor and the loop, as well as the conversion and reaction rate, which in turn have a large effect on the flowrate (size) in the loop.

4.3.2 Strategy for wind power dispatch

The priority in the system is to satisfy the required power demand expressed in the demand profile, either directly from wind power generation or, if there is not enough wind power at a given point in time, from a combination of wind power and NH_3 being transformed into power.

There are several scenarios that must be taken into account when deciding how to dispatch the wind power being generated by the wind farm:

a. Wind power exceeds combined demand and Energy Storage System (ESS) capacity.

   In this case the demand is satisfied and the ESS is operated at maximum load to produce NH_3 as energy storage. Surplus wind is curtailed.

b. Wind power exceeds demand but ESS can operate only at partial loads.

   The demand is satisfied and the ESS is operated at a partial load.
   There are, however, several sub-cases:
   - if there is enough energy for all the ESS components to work above their minimum operating load, they all operate at a load that will maintain the stoichiometric relation of H_2 and N_2 to produce NH_3,
   - otherwise, some of them operate at minimum load, else
   - the H_2, N_2 and NH_3 production processes are maintained at minimum load.

   The two additional constraints related to NH_3 production derive from the fact that HB catalysts deactivate with operating condition variations.

c. Wind power matches demand.

   The demand is satisfied and the NH_3 production process is kept at minimum operating load by using stored NH_3 to provide its power. The production of NH_3 is never stopped to avoid catalyst deactivation and start-up dead times.

d. Demand exceeds wind power.

All the wind power is used to (partially) satisfy the demand. Power from stored NH_3 is used to satisfy the rest of the demand and to keep the NH_3 production process at a minimum operating load.

The decision of which case to apply is done for every time interval (5 minutes in the case of the current wind power input).

4.4 Sizing and costing methods

Sizing and costing of alternatives is done to compare configurations and operating conditions in terms of economic criteria.

The ESS sizing methods are explained in Section 4.4.1. Section 4.4.2, establishes three costing methods for different parts of the system (depending on the available information). The first method (Module Factor, Section 4.4.2.1) estimates the cost based on the estimated sizes. When this is not possible, sizing and costing are done, in effect, in one single step (Sections 4.4.2.2 and 4.4.2.3).

4.4.1 Sizing

Sizing is performed for compressors and their drivers, the heat exchangers (heaters and coolers) and the pressurised vessels (the reactor and the flash unit in the synthesis loop).

4.4.1.1 Compressors

Compressors (and their associated drivers) are used in the synthesis loop feed stream compressor train, and in the recycle stream within the synthesis loop.

Eqn. 4-1 calculates the output temperature from an adiabatic compressor, T_{out} in [K], given its input temperature and pressure, T_{in} [K] and P_{in} [bar], its output pressure P_{out} [bar], the number of stages, N, and the adiabatic exponent, n.

Eqn. 4-1:
$$T_{out} = T_{in} \left[\left(\frac{P_{out}}{P_{in}} \right)^{\frac{1}{N}} \right]^{\left(\frac{n-1}{n} \right)}$$

The fluid power, $\dot{W}$ in [kW], is calculated using Eqn. 4-2,

Eqn. 4-2:
$$\dot{W} = T_{in} \cdot N \cdot \frac{n}{(n-1)} \cdot R_{spec} \cdot \dot{m} \cdot \left[\left(\frac{P_{out}}{P_{in}} \right)^{\left(\frac{n-1}{n} \right)} - 1 \right]$$

where R_{spec} is the specific gas constant in [kJ / (kg K)] and $\dot{m}$ the mass flowrate in [kg / s].

The shaft power, W_{shaft}, and driver power, W_{drive}, can be estimated through Eqn. 4-3 and Eqn. 4-4, after accounting for the adiabatic and the driver efficiencies, η_i and η_{drive} respectively.

Eqn. 4-3:
$$\dot{W}_{shaft} = \frac{\dot{W}}{\eta_i}$$

Eqn. 4-4:
$$\dot{W}_{drive} = \frac{\dot{W}_{shaft}}{\eta_{drive}}$$

4.4.1.2   Heat Exchangers

We can calculate the amount of heat exchanged, $\dot{Q}$ in [kW], with Eqn. 4-5. Cp_{mix} is the specific heat of the mixture in [kJ / (kg K)]. Eqn. 4-6 can then be used to estimate the area of the heat exchanger, A in [m^2]; where U is the in [W / (m^2 K)] and ΔT_{LM} the log-mean temperature difference in [K].

Eqn. 4-5:
$$\dot{Q} = \dot{m} \cdot Cp_{mix} \cdot \left(T_{out} - T_{in} \right)$$

Eqn. 4-6:
$$A = \frac{\dot{Q}}{U \cdot \Delta T_{LM}}$$

4.4.1.3   Reactor and Flash vessels

The volume of the reactor, V in [m^3], is obtained through Eqn. 4-7, where ρ_{cat} is the packing catalyst density in [kg_cat / lt] and r the reaction rate in [kg_NH$_3$ / (kg_cat s)].

Eqn. 4-7:
$$V = \frac{\dot{m}}{1000 \cdot \rho_{cat} \cdot r}$$

4.4.2   Capital cost estimations

The estimated capital cost includes equipment purchase and installation, and it is then adjusted to 2014 costs using the CEPCI indexes (Chemical Engineer's Plant Cost Index). These estimations do not account for working capital nor for a discount or capital return factor (time value of money). The reported capital costs are annualised assuming a project lifetime of 20 years.

There are three different methods used in this work to cost the modules and components of the process.

1. The Module factor approach (Section 4.4.2.1).
2. A "modular" approach (Section 4.4.2.2).
3. Correlations using scaling components (Section 4.4.2.3).

4.4.2.1   Module Factor method

The module factor method was developed by Guthrie (Guthrie, 1974) and modified by Ulrich (Ulrich, 1984). We based our calculations in the description given in Appendix A of (Turton et al., 2008).

In this method the purchasing cost of the equipment listed in Table 4-2, and operating at atmospheric pressure, is estimated using Eqn. 4-8.

Eqn. 4-8:
$$\log_{10} C_p^o = K_1 + K_2 \log_{10}(A) + K_3 \left(\log_{10}(A)\right)^2$$

where C_p^o is the purchased equipment cost (in [USD]), A is the capacity parameter for the equipment, and K_1, K_2 and K_3 are constants for a given type of equipment, retrievable from Table A.1 of (Turton et al., 2008).

The Bare Module cost, C_{BM}, which takes into account the material of construction, the pressure of operation and the installation costs through the factors F_M and F_B respectively, is calculated using Eqn. 4-9.

Eqn. 4-9:
$$C_{BM} = C_p^o \left(B_1 + B_2 F_M F_P\right)$$

where B_1 and B_2 are constants found in Table A.4 of (Turton et al., 2008).

The items of equipment costed using the Module Factor method are shown in Table 4-2.

Equipment in the process	Type of equipment	Description of equipment	Capacity, A, in [units]	Min / Max size
Compressors in the compressor train and the recycle stream	Compressor	Centrifugal, axial and reciprocating	Fluid power [kW]	450 / 3000
Compressors in the compressor train, the recycle stream and the MVC modules	Compressor	Rotary	Fluid power [kW]	18 / 950
Compressor Drives	Drives	Electric, totally enclosed	Shaft power [kW]	75 / 2600
Coolers and heaters in the HB process	Heat Exchangers	Floating head	Area [m^2]	10 / 1000
Reactor and Flash in HB synloop	Process vessels	Vertical	Volume [m^3]	0.3 / 520
NH_3 storage	Tank	API - Fixed roof	Volume [m^3]	90 / 30000

Table 4-2: Types of equipment that were costed using the Module Factor method.

4.4.2.2 "Modular" method

For the electrolyser (H_2), PSA (N_2) and mini-HB (NH_3) modules, appropriate costing data for the Module Factor method was not available at the time of writing. We therefore drew on manufacturer information and quotations obtained for different capacities, as shown in Table 4-3.

The model selects the least cost option based on the capacity requirements. Units are selected in integer quantities, which can lead to oversizing in some cases.

Equipment in the process	Unit capacity [units]	Cost per unit	Source
High-pressure alkaline electrolyser*	0.001451 [kg_H₂/s] (279 kW)	558,000 [€]	Manufacturer: Norsk Hydro. Figure 5-19 (Jensen et al., 2008)
PEM	0.9 [ton_H₂ / day]	2'750,000 [USD]	Proton OnSite quotation (11/08/2014)
PSA**	50 [Nm³ / h]	52,000 [USD]	Hangzhou Kelin Aier Qiyuan Equipment Co., Ltd quotation (29/08/2014)
PSA**	1000 [Nm³ / h]	196,000 [USD]	Beijing Feda Geron Air Separating Technique Ltd Co. quotation (29/08/2014)
PSA**	2000 [Nm³ / h]	382,000 [USD]	Same as above
PSA**	3000 [Nm³ / h]	565,000 [USD]	Same as above
mini-HB	3 [ton_NH₃ / day]	3'200,000 [£]	Proton Ventures (NFuel) quotation (15/08/2014)
H₂ storage		37 [€/m³] at 20 bar	(Hughes, 2013)

(*for 16 bar electrolyser maximum capacity is 279 kW; ** 99.99% pure N₂)

Table 4-3: Types of equipment costed using the "modular" method

4.4.2.3   Correlations using scaling exponents method

Four modules were costed using a correlation in terms of the required capacity:

1. Mechanical Vapour Compression (MVC) module.

   A correlation taken from Figure 53 of (Morgan, 2013) was used to estimate the cost of the MVC module in [USD]:

   Eqn. 4-10 $$C_{MVC} = \left[\frac{3}{200} \dot{m}_{water} + 4.5 \right] \cdot 1 \times 10^6$$

   where $\dot{m}_{water}$ is the water flowrate in [ton/day]. Figure 53 plots the grassroot costs of the MVC, so that cost is then adjusted to account only for installation assuming a grassroot factor of 2.0 and and installation factor of 1.725.

2. Atmospheric alkaline electrolyser for the production of H_2.

The correlation used, Eqn. 4-11, is based on Eqn 92 of (Morgan, 2013) and estimates the cost in [USD]:

Eqn. 4-11:

$$C_{AAE} = \frac{1'291,536}{1.66} \cdot \left[0.32X + 0.06X^{0.5} + 0.29X^{0.7} + 0.15X^{0.75} + 0.18X^{0.8} \right]$$

where X is the number of electrolysers, which is calculated by dividing the required H_2 flowrate by the maximum capacity of a single electrolyser (1.205 [kg_H_2/s]). The cost of a single electrolyser is 11'620,000 [Norwegian kroner, 2002], i.e. 1'291,536 [£] in 2014. This data is taken from Table 38, (Morgan, 2013) and corresponds to a Norsk Hydro electrolyser.

This correlation aims to get economies of scale out of a stack of electrolysers, otherwise the option would not be cost effective.

3. Cryogenic ASU for the production of N_2.

The correlation used, Eqn. 4-12,was taken from (Morgan, 2013), p. 356, and estimates the cost in [USD]:

Eqn. 4-12:

$$C_{CryoASU} = 0.46 \cdot \left[\begin{array}{l} 5.0E6 + 53319\,(0.8224 \cdot A) - 68.725\,(0.8224 \cdot A)^2 \\ + 0.0593\,(0.8224 \cdot A)^3 \end{array} \right]$$

where A is the amount of NH_3 to be produced, in [tons_NH_3 / day].

3. Ammonia to power to satisfy demand and run the ESS when the wind power input is not enough.

This cost is approximated to the cost of a conventional turbine that would generate power from the combustion of NH_3. The reference cost is 973 USD/kW for a turbine with nominal capacity of 85 MW (Energy Information Administration (EIA), 2013) and assuming a combustion efficiency of 50%. The cost was scaled according to the capacity power law (Turton et al., 2008):

Eqn. 4-13
$$Cost_{Cap2} = Cost_{Cap1} \cdot \left[\frac{Cap_2}{Cap_1} \right]^{0.7}$$

where Cap_i is the capacity of the turbine at condition i (in [MW]).

4.4.3   Operating costs

As a first-pass estimation of the operating costs, only the energy consumption was taken into account, i.e. costs related to labour, maintenance and depreciation were disregarded.

All the energy in the system comes from the wind farm, and the levelised cost of energy (LCOE) value from wind varies widely according to whether the windfarm is onshore or offshore, geographical location (49 to 136 USD/MWh, (Salvatore, 2013)), and time (a 3-6% reduction in cost per annum is expected (Hughes, 2013)). The value used in this work is the same as in (Hughes, 2013): 50.8 USD/MWh, which accounts for price reductions by the time the ESS would be operational, and assumes that the location of the plant is Europe.

4.5 Assumptions, limitations and main design parameters

4.5.1   Assumptions

The following basic assumptions were made:

- Costing methods cannot be regarded as accurate, but they should be good enough to compare alternatives and to estimate trends when a design variable is changed, i.e. for conceptual design, option selection and sensitivity analyses.

- Capital costs include the purchase and installation of equipment but disregard other costs such as auxiliary facilities, contingencies, etc.

- Operation costs only include those associated to energy consumption but disregard other factors such as labour costs, maintenance, etc.

- Operation is assumed to be at steady state or with instantaneous changes, i.e. controllers are 'perfect' and thus there are no fluctuations in the temperature and pressure of operation. This also implies that no ramping constraints are taken into account.

- The size of all Haber-Bosch technologies is chosen so that they operate at maximum capacity almost always. This is to ensure that there are few or no variations in load so as to maximise the lifetime of the catalyst.

    It is also assumed that the mini-HB technology always operates at 100% capacity.

- The ammonia reaction is exothermic and the reactor is cooled during operation; for costing purposes this is modelled as a separate heat exchanger (rather than a cooling jacket).

- There are two thermodynamic parameters used in the sensitivity analyses that are estimated by interpolation from external data:

- o K values at different pressures for the vapour-liquid equilibrium calculations in the flash vessel.

- o Equilibrium conversion of ammonia at a given P and T; this requires a double interpolation from data in Table 2 of (Appl, 2012).

- We assumed that data for the CoMoN-based catalyst (conversion and reaction rate) from the literature at laboratory conditions can be scaled up to industrial conditions, i.e. reaction rate is improved through an increase in temperature, and conversion through an increase in pressure and an 80% approach to equilibrium conversion[3].

- Capital costs include only equipment purchase and installation, but do not account for working capital nor for a discount or capital return factor. Operating costs include only the energy consumption of the ESS, i.e. costs related to labour, maintenance and depreciation were disregarded.

4.5.2 Limitations

The most important limitations of the model are briefly listed:

- Future analysis should consider the sensitivity to alternative wind and demand profiles, in particular the scale of aggregated demand. Day-to-day variations and seasonal changes in demand are expected to affect the findings presented in this report.

- The models of the individual modules in the ESS (H_2, N_2 and NH_3 production) are not detailed. This was a modelling decision based on the objective of the models being to compare options rather than to estimate costs accurately.

- There was enough and reliable costing data and correlations for industrial size Haber-Bosch processes (> 250 ton_NH_3/day) and for one particular configuration of an ammonia-based ESS (atmospheric alkaline electrolysis + PSA + mini-HB technologies; 3 ton_NH_3/day; from a Proton Ventures quotation of 15/08/2014). However, there was no reliable data for the intermediate range of sizes (between 3 and 250 ton_NH_3/day) and extrapolation had to be used in these cases.

- A set of messages has been put in place to warn the user when a calculation is outside the minimum/maximum range of applicability. In most cases these warnings are related to the costing correlations.

- Related to the previous item, only one mini-HB configuration could be costed through an industrial quotation, but the rest of mini-HB configurations (all of those including

---

[3] Data from the literature indicate that the approach to conversion is 87% for Fe-based catalysts, 91.5% for Ru-based catalysts and 37.5% for CoMoN-based catalysts, the last one at laboratory conditions.

high-pressure alkaline electrolysis, PEM or cryogenic ASU) could not be reliably costed, because the costs of their components was unknown or unreliable.

- The required amounts of heating and cooling in the ESS were calculated, but no heat integration calculations were performed.

4.5.3 Main design parameters

Design Variable	Value	Comments
Project lifetime	20 years	Implications for catalyst lifetime
Installation costs	72.5% of equipment costs	Average value from Chapter 6 (Peters et al., 2003); applied when the "correlations" method is used (Section 4.4.2.3)
CRF	0.08	(Hughes, 2013)
Days per year	330	
Levelised cost of wind power	50.8 USD/MWh	(Hughes, 2013)
Density of CoMoN catalyst	2.88 kg_cat/lt	Same as for Fe catalyst
Approach to equilibrium conversion for CoMoN catalyst	80%	
NH$_3$ to power	18.646 MJ/kg_NH$_3$	LHV of ammonia
NH$_3$ to power efficiency	50%	
H$_2$:N$_2$ feed ratio	3:1	Stoichiometric (even though Ru works best at 2.0-2.25 : 1)
Argon mole fraction at the synloop feed	0.0012 (0.12% Ar)	
Pressure drop in HB synloop	6%	(Morgan, 2013), p. 140
Maximum pressure ratio for single compression stage	3.5	
Compressors efficiencies	75% (adiabatic) 95% (driver)	
Cooling water	T_{in}/T_{out} = 280/290 K U = 60 W/m^2/K	Used in compressor train intercoolers and reactor cooling jacket
Heating utility	873 K U = 200 W/m^2/K	Pre-heating of reactor feed with, e.g. Dowtherm
Refrigeration	240 K U = 865 W/m^2/K	In flash separation, ammonia as refrigerant

Table 4-4: Main process design parameters

5. Techno-economic assessment

5.1 Efficiency analysis

Based on the output of the model corresponding to different technical options, efficiencies at the component and system levels are analysed for two systems boundaries:

a) Wind power to NH_3, and

b) Wind power to NH_3-generated power.

More specifically, efficiencies are measured by three different quantities, namely power consumption, exergy loss, and exergy efficiency.

The exergy of a material or energy stream represents its "effective" energy content in terms of the maximum ability to do work in a conceived process of reaching physical and chemical equilibrium with its surrounding environment. As such, it offers a unified quantity for characterising the energy content of diverse streams of material, heat and power. For a material stream, its exergy (Ex_{total}), can be calculated by the sum of its physical exergy (Ex_{ph}) and chemical exergy (Ex_{ch}):

Eqn. 5-1
$$Ex_{total} = Ex_{ph} + Ex_{ch}$$

The physical exergy component is then given by

Eqn. 5-2
$$Ex_{ph} = (H - H_0) - T_0 (S - S_0)$$

where *H* and *S* are enthalpy and entropy of the stream, respectively; H_0 and S_0 are the values of *H* and *S* at environmental temperature (T_0) and pressure (P_0). The chemical exergy of a stream can be calculated by:

Eqn. 5-3
$$Ex_{ch} = \sum_i x_i Ex_{ch_i} + RT_0 \sum_i x_i \ln x_i$$

where x_i and Ex_{ch_i} are molar fraction and molar chemical exergy (kJ/kmol), respectively, of chemical component *i* in the mixture, and R is the universal gas constant.

For a heat stream with an amount of heat Q at temperature T, its exergy is evaluated by

Eqn. 5-4
$$Ex_Q = Q(1 - \frac{T_0}{T}),$$

while a power or work stream has an exergy content equal to its energy content.

For a processing step or unit with a set of input and output streams, its exergy efficiency (η_{Ex}) can be calculated by

Eqn. 5-5 $$\eta_{Ex} = \sum_k Ex_{out,k} \, / \sum_j Ex_{in,j}$$

where $Ex_{out,k}$ and $Ex_{in,j}$ are the exergy content of the kth <u>useful</u> outlet and that of the jth inlet, respectively. Exergy loss (Ex_{loss}) of this unit is the difference between the two terms:

Eqn. 5-6 $$Ex_{loss} = \sum_j Ex_{in,j} - \sum_k Ex_{out,k}$$

5.1.1 Assumptions

In this current analysis, the environmental conditions have been defined as 25 C and 1 bar. Enthalpies and entropies for calculating physical exergy were obtained from Aspen Plus. Chemical exergy of pure chemical compounds was based on (Dincer and Rosen, 2007). Minor impurities present in streams such as the H_2 product from electrolysis, the N_2 product from ASU, and NH_3 from the synthesis loop were ignored in exergy calculation.

In the synthesis loop, only one purge ratio (0.03) was adopted for each option considered, which represents a good balance between compression work cost and material loss. The NH_3 products from different catalysts are of different pressures. Although the specific pressure was applied to each corresponding product when calculating exergy, it was noticed that the difference in pressure does not cause any significant variation in the exergy content in the (liquid) NH_3 products. Furthermore, heat integration in the synthesis loop was treated simplistically, assuming the pre-heating of the feed is satisfied by heat recovery from the reactor effluent, and ignoring the power generation which is possible by recovering the heat of reaction. Also, the reactants (H_2 and N_2) present in the purge stream were assumed to be lost. Note that only conventional HB NH_3 processes were considered in the efficiency analysis; mini-HB processes were not included due to the lack of data.

On NH_3-based power generation, two options were considered. In the case of (direct) combustion, a 50% LHV to power efficiency was assumed, as in (Hughes, 2013). Another option is the combined use of SOFC and gas turbine; a 70% exergy efficiency was assumed according to (Patel et al., 2012).

5.1.2 Results and discussion

Table 5-1 summarises the results. The options are represented by:

- AtA: atmospheric alkaline electrolysis
- HPA: high pressure (16 bar) alkaline electrolysis
- PEM: PEM-based electrolysis
- CRY: Cryogenic distillation based ASU
- PSA: PSA-based ASU
- Fe, Ru, and CoMoN: HB NH_3 synthesis with Fe, Ru, or CoMon as the catalyst

Option	Electrolysis			ASU			NH₃ synthesis			Power to NH₃			Power to power eff.	
	Power	Ex. loss	Ex. eff.	Power	Ex. loss	Ex. eff.	Power	Ex. loss	Ex. Eff.	Power	Ex. loss	Ex. eff.	Comb-ustion	SOFC
AtA-CRY-Fe	37.81	16.93	0.55	0.35	0.18	0.49	1.86	2.65	0.8845	40.02	19.76	0.5063	0.23	0.35
AtA-CRY-Ru	37.85	16.93	0.55	0.35	0.18	0.49	1.70	2.53	0.8890	39.91	19.64	0.5079	0.23	0.36
AtA-CRY-CoMoN	39.18	16.93	0.55	0.37	0.18	0.49	1.41	2.98	0.8715	40.95	20.10	0.5093	0.23	0.36
AtA-PSA-Fe	37.81	16.93	0.55	0.33	0.31	0.06	2.33	2.96	0.8724	40.46	20.20	0.5007	0.23	0.35
AtA-PSA-Ru	37.85	16.93	0.55	0.33	0.31	0.06	2.18	2.85	0.8766	40.36	20.09	0.5023	0.23	0.35
AtA-PSA-CoMoN	39.18	16.93	0.55	0.34	0.31	0.06	1.89	3.32	0.8592	41.41	20.55	0.5037	0.23	0.35
HPA-CRY-Fe	37.81	16.31	0.57	0.35	0.18	0.49	1.11	2.52	0.8894	39.27	19.01	0.5159	0.24	0.36
HPA-CRY-Ru	37.85	16.33	0.57	0.35	0.18	0.49	0.92	2.36	0.8956	39.13	18.87	0.5176	0.24	0.36
HPA-CRY-CoMoN	39.18	16.91	0.57	0.37	0.18	0.49	0.64	2.85	0.8764	40.19	19.94	0.5037	0.23	0.35
HPA-PSA-Fe	37.81	16.31	0.57	0.33	0.31	0.06	1.15	2.40	0.8941	39.28	19.02	0.5158	0.24	0.36
HPA-PSA-Ru	37.85	16.33	0.57	0.33	0.31	0.06	0.99	2.27	0.8991	39.16	18.91	0.5171	0.24	0.36
HPA-PSA-CoMoN	39.18	16.91	0.57	0.34	0.31	0.06	0.68	2.74	0.8808	40.20	19.95	0.5037	0.23	0.35
PEM-CRY-Fe	33.28	11.64	0.65	0.35	0.18	0.49	0.82	2.37	0.8951	34.45	14.19	0.5881	0.27	0.41
PEM-CRY-Ru	33.31	11.65	0.65	0.35	0.18	0.49	0.64	2.23	0.9009	34.31	14.06	0.5902	0.27	0.41
PEM-CRY-CoMoN	34.48	12.06	0.65	0.37	0.18	0.49	0.35	2.72	0.8815	35.20	14.96	0.5750	0.26	0.40
PEM-PSA-Fe	33.28	11.64	0.65	0.33	0.31	0.06	0.86	2.26	0.8998	34.46	14.20	0.5879	0.27	0.41
PEM-PSA-Ru	33.31	11.65	0.65	0.33	0.31	0.06	0.67	2.11	0.9057	34.32	14.07	0.5901	0.27	0.41
PEM-PSA-CoMoN	34.48	12.06	0.65	0.34	0.31	0.06	0.38	2.59	0.8863	35.21	14.96	0.5751	0.26	0.40

Table 5-1: Power consumption (GJ/tonne_NH₃), exergy loss (GJ/tonne_NH₃) and exergy efficiency (-)

The following key observations can be made:

1. Individual conversion steps.

   In electrolysis, the PEM option gives the highest efficiency due to a highest outlet H_2 pressure (31 bar) obtained with an assumed level of electricity consumption 10% lower than that of the alkaline electrolysers. Between the two alkaline electrolysers, the HP option is apparently more efficient due to its elevated hydrogen product pressure (16 bar) obtained at no additional energy cost than the atmospheric option. In ASU, the cryogenic option, producing N_2 at 8 bar, apparently outperforms the PSA option which produces N_2 at 1 bar while consuming a comparable amount of energy to the former. It should be noted that although both the electrolysis and the air separation steps can produce oxygen-rich streams as a by-product, the exergy efficiency analysis showed that including these by-product streams as valuable products would not affect the exergy efficiency to any significant level. In NH_3 synthesis, the Ru option is generally more efficient than the other two options; it

appears that this option strikes a best balance between compression work reduction (compared to the Fe option, due to a lower operating pressure) and avoidance of excessive loss of reactants (compared to the CoMoN option, due to a lower purge loss). The Fe option is narrowly behind the Ru option, both noticeably better than the CoMoN option. The efficiency of the NH_3 synthesis step is also affected by the inlet conditions (particularly pressure) of H_2 and N_2, which are determined externally and hence meaningful only when considered within the context of the whole wind power to NH_3 system, as discussed below.

2. Whole system: power to ammonia.

   Overall, options with PEM electrolysis and Ru or Fe based NH_3 synthesis appear to be more efficient than the other options, which is in-line with the observations at the individual steps level. These options give rise to a nearly 60% efficiency and around 34.3 GJ/tonne NH_3 power consumption; in comparison, the "base" case, i.e. one using atmospheric alkaline electrolysis, cryogenic ASU and Fe-based NH_3 synthesis, has an efficiency of ~50% and around 40 GJ/tonne NH_3 power consumption. Note that the two options for ASU do not seem to significantly affect the overall efficiency particularly within the "best" systems, due to the very small share of ASU in the total energy consumption.

3. Whole system: Power to power.

   It can be seen from Figure 5-1 (with options giving a "base" case for NH_3 production) and Figure 5-2 (with options of one of the best cases for NH_3 production) that, across all the options, electrolysis always represents the greatest and dominating power consumption, followed subsequently by NH_3 to power conversion, NH_3 synthesis loop, and ASU. In terms of exergy loss, which gives an indication on where the focus of future improvement should be placed, the above sequence of the individual conversion steps also applies, although the relative size of the NH_3 synthesis sub-system increases. This is because the loss at the NH_3 synthesis step includes not only imperfect use of energy at this step alone, but also loss of materials (due to purge) produced at the energy cost at previous steps. Improvement to the synthesis loop thus should address both aspects.

4. NH_3-based energy storage.

   The above "power to power" analysis shows the highest cycle efficiencies that can be achieved with direct combustion and SOFC (integrated with GT) as the final conversion step are 27% and 41%, respectively. These levels are within the range of the general performance of fuel cells based systems. This is significantly lower than mechanical, electrical, and battery-based chemical storage options which generally have an efficiency over 60% (with the exception of over-ground compressed air based system, which is ~50%) (Evans et al., 2012). Therefore, before the efficiency of the key conversion steps, i.e. electrolysis and NH_3 to power conversion, is significantly improved, NH_3 as a medium for electrical energy storage needs to consider other factors than efficiency to strengthen the case. Furthermore, while the SOFC+GT option leads to a significantly higher efficiency than direction combustion, a

preliminary economic cost analysis (not included in this report), based on a unit cost of 8000 USD/kW quoted in (Adams II et al., 2013) for a 210kW installation, shows a prohibitive level of capital cost.

5. Factors causing efficiency variations.

The above overall system efficiencies are naturally results of the efficiencies assumed for individual units. For example, if DC power consumption by PEM based electrolysis drops from the assumed 47 kWh/kg H_2 to 64.5 kWh/kg H_2 as specified by Proton to their Onsite HOGEN C30 system (Proton OnSite, n.d.), the efficiency of the electrolysis step and hence that of the whole system will drop significantly. On the more positive side, inclusion of purged gas recovery and power recovery in the NH_3 synthesis step, neither considered in the current analysis, will very likely lead to an improvement of the efficiency of this step and hence of the whole system.
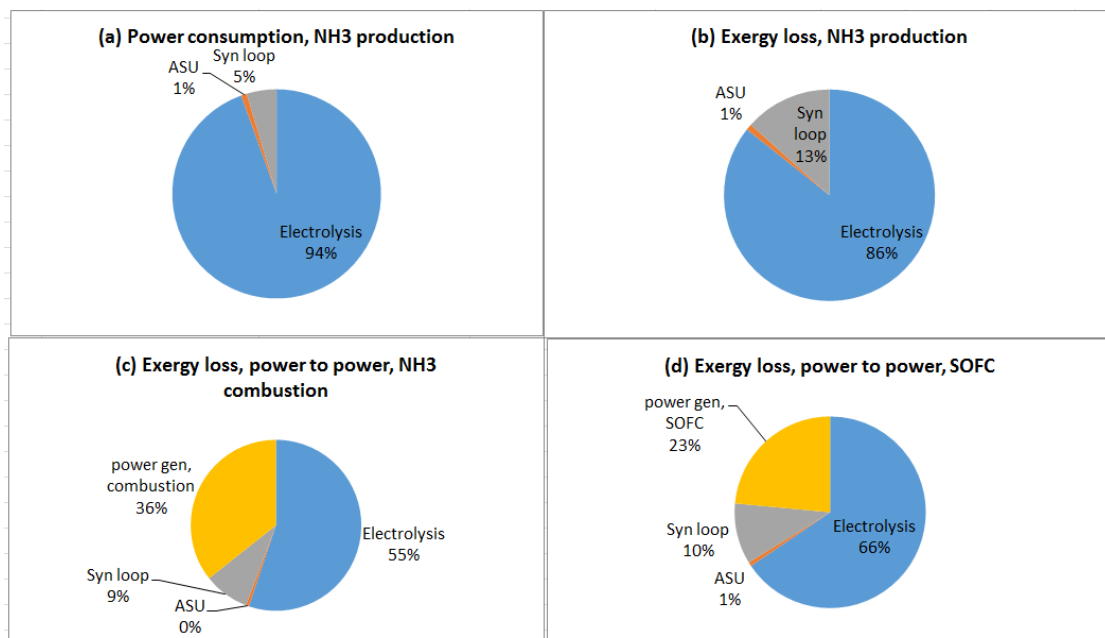
Figure 5-1: Contributions of individual conversion steps to power consumption and exergy loss. The base case (AtA-CRY-Fe).
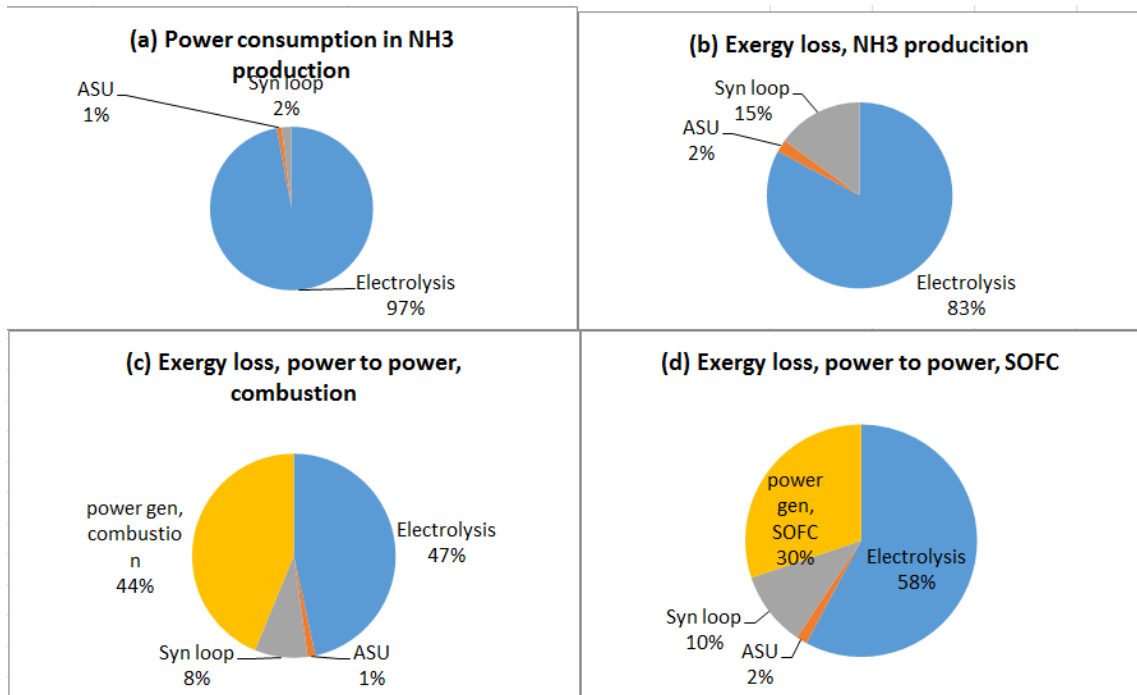
Figure 5-2: Contributions of individual conversion steps to power consumption and exergy loss. A superior case (PEM-CRY-Ru).

5.2 Wind Power and Demand profiles

Four power profiles for the four quarters of the year are shown in Figure 5-3:

- The input wind power (black lines, with a peak of 100 MW and average of 36.43 MW) which was taken from historical records of the Portland wind farm in Australia and, as expected, it is highly variable throughout the year with periods of high wind (e.g. the first part of July) and virtually no wind (in this case the end of May).

- The demand profile (magenta lines, with a peak of 20 MW and average of 11.11 MW), which is synthetic and is repeated on a daily basis throughout the year.

- The wind power diverted to the ESS (blue lines, with a peak of 36.75 MW and average of 18.33 MW); from which it is possible to see that when there is enough wind the surplus power is directed towards NH_3 production, but otherwise the wind farm power to the ESS is cut.

- The power deficit (red lines, with a peak of about -25 MW and average of -5.13 MW) exposes the rationale for energy storage for intermittent energy sources: the ESS stores surplus energy as ammonia, and transforms the stored ammonia into power in order to make up for the deficits and thus satisfy the demand.
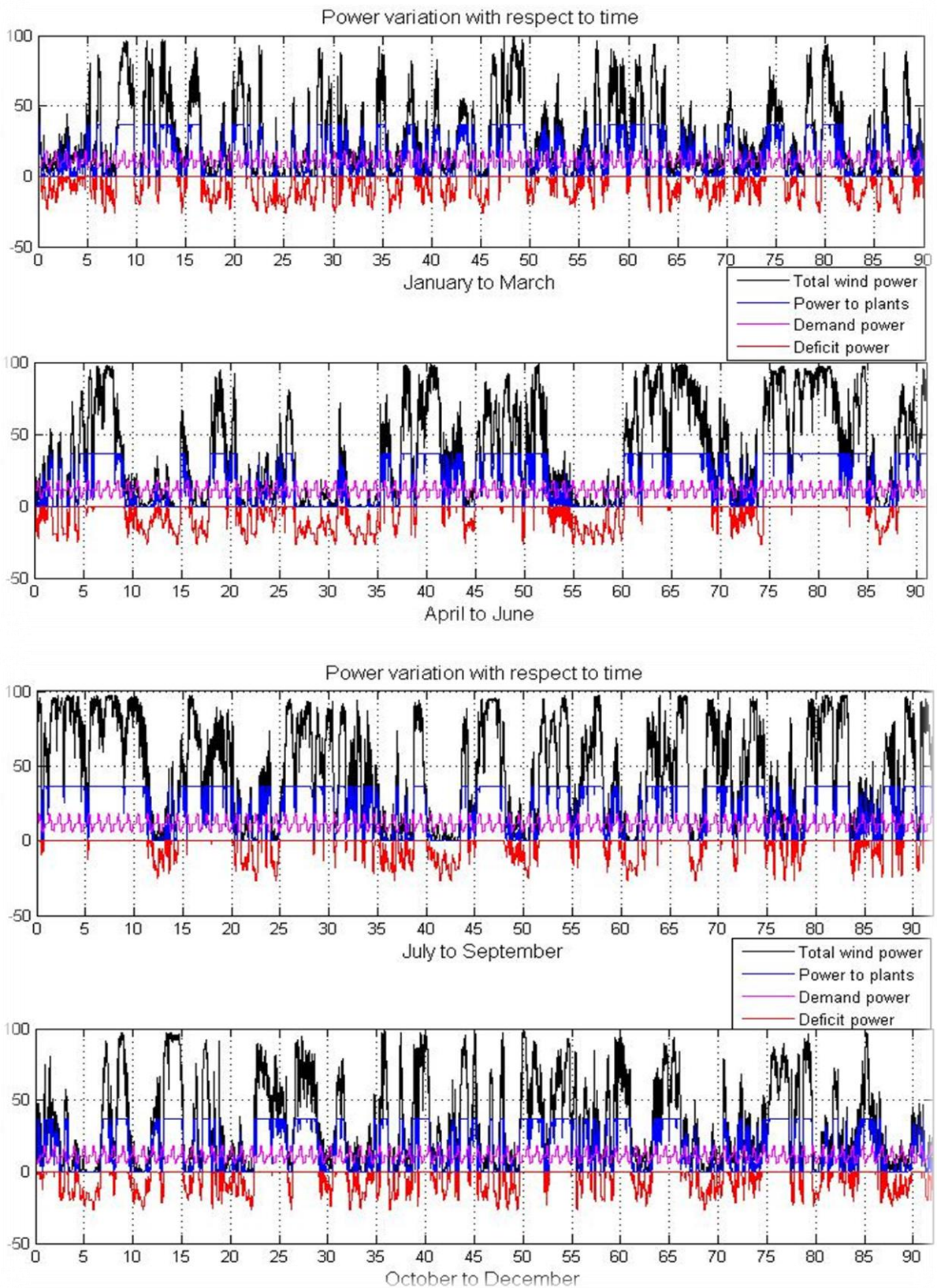
Figure 5-3: Wind power and demand profiles – (a) January to March, (b) April to June, (c) July to September, and (d) October to December 2011. Configuration: Atmospheric alkaline electrolysis / PSA / HB CoMoN catalyst (48 ton_NH$_3$/day, 31 bar, 400 C).

5.3 Cumulative H₂, N₂ and NH₃

Another illustrative plot is the one of the cumulative amounts of H_2, N_2 and NH_3 shown in Figure 5-4. It is, in effect, the surplus and deficit of each one of the chemicals involved in the ESS throughout the year.

There are several useful insights that can be gleaned out from Figure 5-4:

a) The first thing to note is that, for the operation to be feasible, the cumulative amount at the end of the period must be zero or positive, otherwise it would be necessary to import the deficit chemical.

b) The amount of storage for a given chemical can be estimated as the difference between the maximum and the minimum values in the time period. N_2 is a flat line because the model matches the production of nitrogen to that of ammonia, eliminating the need for N_2 storage.

c) The profiles also give us an indication of the ideal time to start the operation of the ESS. In the case of Figure 5-4, if the operation were to start in the month of January, a very large deficit of ammonia (and a smaller one of hydrogen) would be generated by the end of April, when a general incremental trend starts. Thus, the operation should be started at the time corresponding to the overall minimum in the profile (end of April) because no cumulative deficits would be generated in that case.
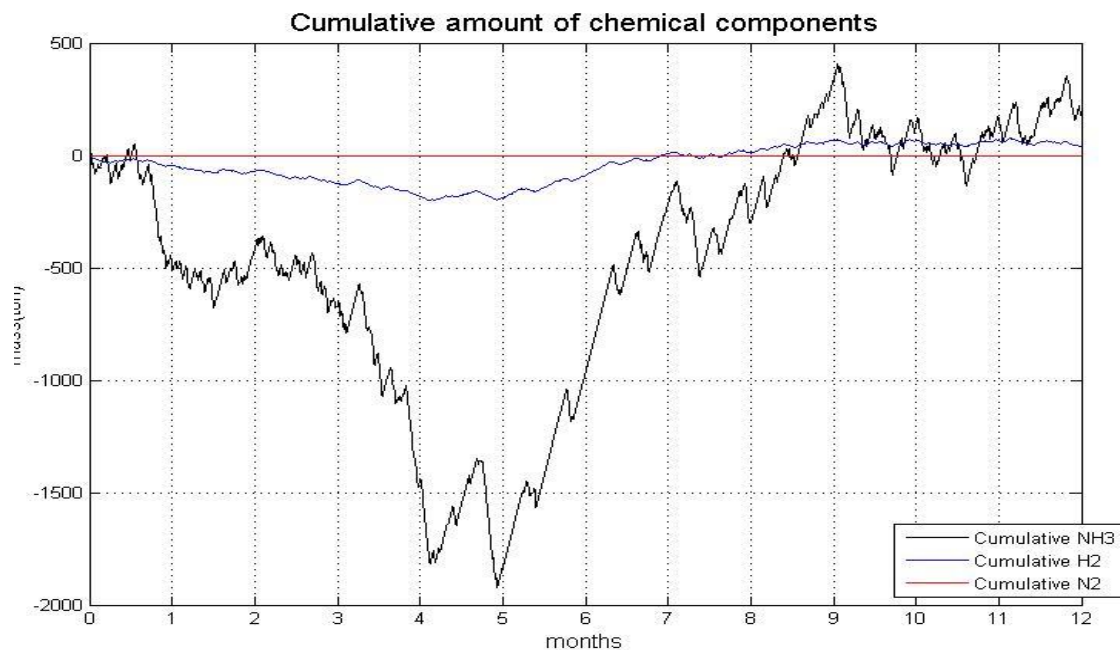
Figure 5-4: Cumulative amount of H_2, N_2 and NH_3 during the time period. Configuration: Atmospheric alkaline electrolysis / PSA / HB CoMoN catalyst (48 ton_NH3/day, 31 bar, 400 C).

The above discussion exposes an important characteristic of the design procedure; given that the wind and demand profiles are fixed, there are constraints on the configuration, size and operation conditions of the ESS. These constraints are:

- If the ESS is too large it will consume too much energy resulting in a deficit of energy.
- If it is too small it will not be able to produce enough of the NH_3 required during periods of low wind power.
- There is a range of sizes and operation conditions that can make each ESS configuration feasible, but they will differ on their economic performance.

Table 5-2 exemplifies the manual search for a feasible set of conditions for one ESS configuration { Electrolysis: atmospheric alkaline + ASU: PSA + HB: CoMoN-based catalyst }. The feasible set of conditions is highlighted in green at the bottom of the table: for the original wind power input (*Wind factor* = 1), an overproduction of 75% of hydrogen (*H_2 overprod factor* = 1.75), and a purge fraction of 0.3% in the HB synthesis loop (*Purge fraction* = 0.003), the size of the ammonia process would be 48 ton_NH_3/day (*NH_3 plant size*), and at the end of the time period 770 ton_NH_3 and 2 ton_H_2 remain in storage.

Configuration: NH3_Fe, Atm_Alka, Cryo						
CONDITIONS					END LEFT	
Wind factor	NH3 plant size (tons/day)	H2 overprod factor	Purge fraction	Max demand power (MW)	Ammonia (ton)	Hydrogen (ton)
NH3 size factor =			0.5			
1	120	2.0	0.003	18	3493	-2217
1	120	2.1	0.003	18	1739	-2132
1	120	2.2	0.003	18	-42	-2046
1	120	2.3	0.003	18	-1847	-1958
NH3 size factor =			0.4			
1	96	2.1	0.003	20	1472	-912
1	96	2.2	0.003	20	153	-830
1	96	2.3	0.003	20	-1184	-759
1	96	2.4	0.003	20	-2536	-693
NH3 size factor =			0.3			
1	72	2	0.003	20	1458	-164
1	72	2.1	0.003	20	563	-30
1	72	2.2	0.003	20	-344	96
1	72	2.3	0.003	20	-1262	214
NH3 size factor =			0.2			
1	48	1.6	0.003	20	1538	-204
1	48	1.7	0.003	20	1027	-66
1	48	1.8	0.003	20	510	68
1	48	1.9	0.003	20	-12	199
NH3 size factor =			0.2			
1	48	1.73	0.003	20	873	-25
1	48	1.74	0.003	20	821	-12
1	48	1.75	0.003	20	770	2
1	48	1.76	0.003	20	718	15

Table 5-2: Excerpt of the search for the conditions for feasible ESS operation. Configuration: Atmospheric alkaline electrolysis / PSA / HB Fe-based catalyst (150 bar, 400 C).

5.4 Comparison of configurations

Table 5-3and Table 5-4 display in tabular form the comparison of different technology configurations in terms of their costs.

Table 5-3 shows that all of the configurations are evaluated for 48 ton_NH$_3$/day production (*NH$_3$ size* = 0.2, i.e. 20% of 240 ton_NH$_3$/day), a purge fraction of 0.003 (*Purge*) and a project life of 20 years (*Project life*). To ensure feasibility only 90% of the demand could be covered (*Demand* = 0.9). Also, because of feasibility reasons, the overdesign factor of the electrolysis module ranges from 1.75 to 2.25 (*OverH$_2$*).

As the last option (*Mini_HB*) in the table is skid-based, its entry reports the number of purchased modules (23) and their annual operating and capital costs.

The required number of modules for each of the three constituent technologies (*# of plants [NH$_3$ H$_2$ N$_2$]*) is reported. Only the electrolysers require more than one module, ranging from 15-16 units in the case of Atmospheric Alkaline electrolysers, 21-22 for PEM or 119-127 for High-Pressure Alkaline electrolysers.

The storage requirements and cost for ammonia and hydrogen (*Storage of [NH$_3$ H$_2$]* and *Storage Cost [NH$_3$ H$_2$]*), the amount of leftover chemicals (*End-left of [NH$_3$ H$_2$]*) are also reported in Table 5-3.

Table 5-4 tabulates the annualised capital and operating costs for each configuration in USD. The capital cost is broken down into the CAPEX of each module: ammonia production (*HB*), hydrogen production (*H$_2$*), nitrogen production (*N$_2$*), water pre-treatment (*MVC*) and ammonia-to-power generation (*Generator*). As expected, the cost of the electrolysers dominates, but it is closely followed by that of the internal ESS power generator. The high cost of the generator is mainly due to a worst-case scenario assumption (a period with no wind power) during which the Generator will need to satisfy the entire demand (90% of up to 20 MW) and the operation of the ESS at minimum load.

The annual operating cost is based on the power consumption of the constituent ESS modules and assumes a levelised cost of wind power of 50.8 USD/MWh (Hughes, 2013), as discussed in Section 4.4.3. The annual operating costs dominate and are two to three times higher than the annual capital costs.

Finally, the last column of Table 5-4 lists the levelised cost of the energy supplied by the ESS in [USD/MWh]. The levelised cost of ammonia that could be produced by a system analogous to the ESS is discussed in Section 5.6.

	Options		[NH3, Demand, OverH2, Purge] factor				Project life (y)	# of plants [NH3, H2, N2]			Storage of [NH3 H2](tons)		End-left of [NH3 H2](tons)		Storage annual capital cost [NH3 H2] ($)
HB-Fe	Atm_Alka	Distillation	0.2	0.9	1.75	0.003	20	1	15	1	2552.3	237.9	769.5	1.8	323,099
		PSA	0.2	0.9	1.75	0.003	20	1	15	1	2561.5	238.1	789.5	2.3	323,388
	HP_Alka	Distillation	0.2	0.9	1.75	0.003	20	1	119	1	2552.3	237.9	769.5	1.8	323,099
		PSA	0.2	0.9	1.75	0.003	20	1	119	1	2561.5	238.1	789.5	2.3	323,388
	PEM	Distillation	0.2	0.9	2.25	0.003	20	1	22	1	8745.1	513.0	8741.4	255.5	696,603
		PSA	0.2	0.9	2.25	0.003	20	1	22	1	8760.1	513.5	8756.4	256.5	697,322
HB-Ru	Atm_Alka	Distillation	0.2	0.9	1.75	0.003	20	1	15	1	2547.3	237.9	758.6	0.9	323,027
		PSA	0.2	0.9	1.75	0.003	20	1	15	1	2556.5	238.1	778.7	1.5	323,317
	HP_Alka	Distillation	0.2	0.9	1.75	0.003	20	1	120	1	2547.3	237.9	758.6	0.9	323,027
		PSA	0.2	0.9	1.75	0.003	20	1	120	1	2556.5	238.1	778.7	1.5	323,317
	PEM	Distillation	0.2	0.9	2.25	0.003	20	1	22	1	8744.9	512.8	8741.1	254.5	696,430
		PSA	0.2	0.9	2.25	0.003	20	1	22	1	8759.9	513.4	8756.2	255.5	697,151
HB-CoMoN	Atm_Alka	Distillation	0.2	0.9	1.8	0.003	20	1	16	1	2327.8	277.5	159.5	42.1	376,816
		PSA	0.2	0.9	1.8	0.003	20	1	16	1	2332.4	277.8	180.6	42.7	377,266
	HP_Alka	Distillation	0.2	0.9	1.8	0.003	20	1	127	1	2327.8	277.5	159.5	42.1	376,816
		PSA	0.2	0.9	1.8	0.003	20	1	127	1	2332.4	277.8	180.6	42.7	377,266
	PEM	Distillation	0.2	0.9	2.05	0.003	20	1	21	1	8737.8	354.2	8734.0	15.0	481,048
		PSA	0.2	0.9	2.05	0.003	20	1	21	1	8753.4	354.6	8749.7	16.0	481,534
Mini_HB	Atm_Alka	PSA	0	0	0	0	20	23	23	23	0	0	0	0	0

Table 5-3: Economic comparison of ESS configurations.

	Options		Capital annual cost [NH3, H2, N2, MVC, Generator]($)					Total annual capital cost ($)	Total annual operating cost ($)	Total annual cost ($)	Levelised cost of energy ($/MWh)
HB-Fe	Atm_Alka	Distillation	769,156	1,789,435	161,031	283,935	1,769,693	5,129,714	16,008,456	21,138,170	251.38
		PSA	1,040,030	1,789,435	19,100	283,935	1,768,994	5,258,382	16,005,335	21,263,717	253.49
	HP_Alka	Distillation	371,667	4,329,678	161,031	283,935	1,769,693	7,272,468	16,008,456	23,280,925	286.97
		PSA	477,004	4,329,678	19,100	283,935	1,768,994	7,235,599	16,005,335	23,240,934	286.33
	PEM	Distillation	315,385	3,025,000	161,031	309,006	1,440,326	6,039,913	14,742,489	20,782,403	253.36
		PSA	322,402	3,025,000	19,100	309,006	1,439,561	5,905,112	14,739,652	20,644,764	251.09
HB-Ru	Atm_Alka	Distillation	1,247,542	1,789,435	161,031	284,037	1,770,073	5,608,428	16,010,621	21,619,049	259.36
		PSA	1,492,954	1,789,435	19,100	284,037	1,769,373	5,711,634	16,007,496	21,719,130	261.04
	HP_Alka	Distillation	981,475	4,366,062	161,031	284,037	1,770,073	7,918,988	16,010,621	23,929,609	297.73
		PSA	994,247	4,366,062	19,100	284,037	1,769,373	7,789,553	16,007,496	23,797,049	295.55
	PEM	Distillation	922,645	3,025,000	161,031	309,138	1,440,338	6,647,162	14,743,360	21,390,522	263.45
		PSA	930,033	3,025,000	19,100	309,138	1,439,573	6,512,731	14,740,519	21,253,251	261.19
HB-CoMoN	Atm_Alka	Distillation	1,186,663	1,892,390	161,031	289,722	1,790,804	5,720,146	16,054,548	21,774,693	261.67
		PSA	1,396,812	1,892,390	19,100	289,722	1,790,082	5,788,124	16,051,256	21,839,380	262.76
	HP_Alka	Distillation	961,398	4,620,749	161,031	289,722	1,790,804	8,223,239	16,054,548	24,277,787	303.24
		PSA	983,905	4,620,749	19,100	289,722	1,790,082	8,103,576	16,051,256	24,154,832	301.22
	PEM	Distillation	900,914	2,887,500	161,031	302,713	1,440,697	6,292,405	14,947,850	21,240,255	259.68
		PSA	904,508	2,887,500	19,100	302,713	1,439,905	6,153,956	14,944,943	21,098,899	257.35
Mini_HB	Atm_Alka	PSA	0	0	0	0	0	3,384,000	16,111,347	19,495,347	

Table 5-4: Economic comparison of ESS configurations.

The percentage cost breakdown for the configurations is very similar. As an example the cost breakdown for the { MVC + Electrolyser: PEM + ASU: PSA + HB: Fe-based + NH$_3$ to power: conventional turbine } option is shown in Figure 5-5.

Costs	USD/year	%
Operating	14,739,652	71.4
Storage NH3	177,012	0.9
Storage H2	613,030	3.0
Synloop	322,402	1.6
Electroliser	3,025,000	14.7
ASU	19,100	0.1
MVC	309,006	1.5
NH3 turbine	1,439,561	7.0
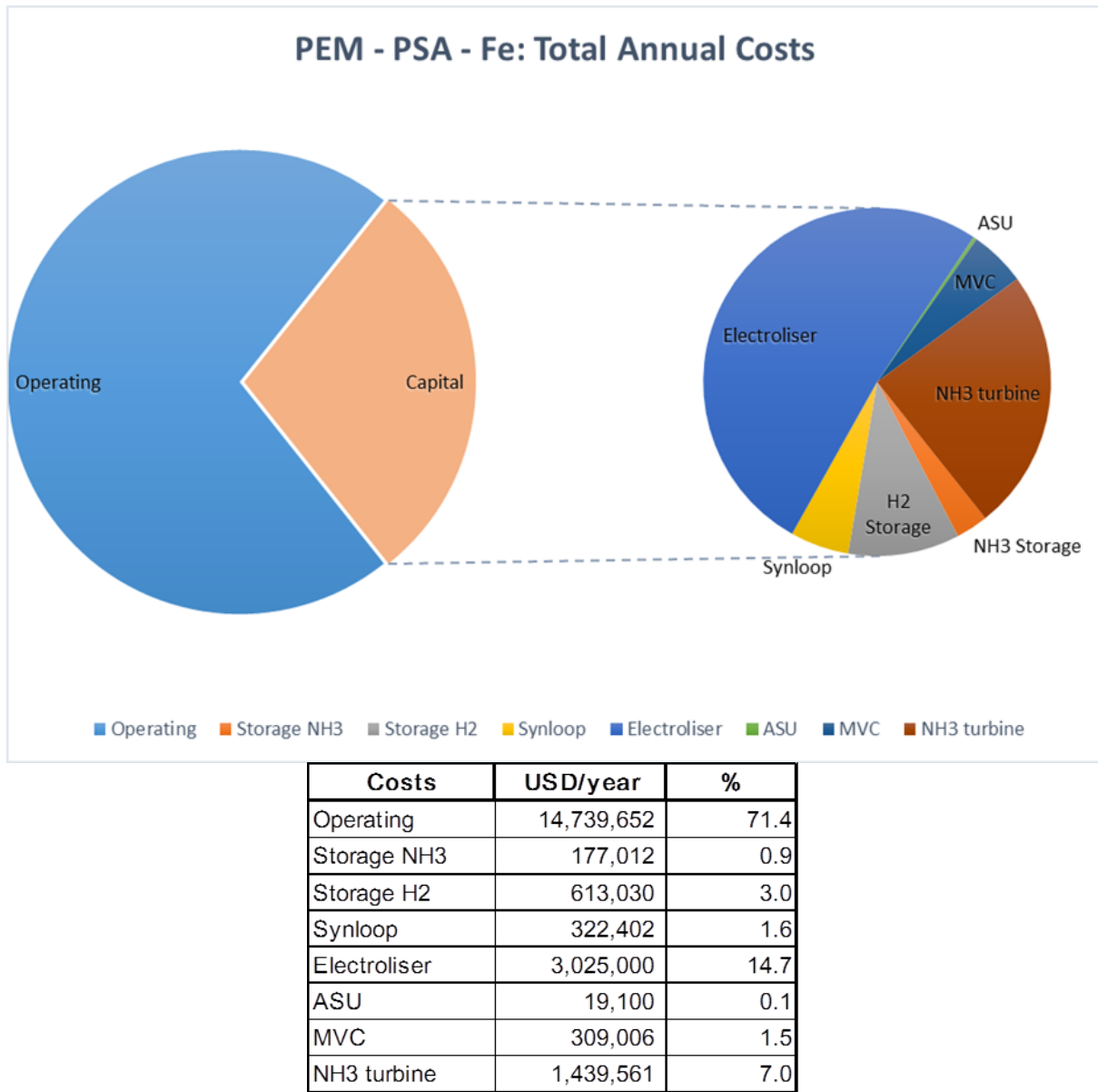
Figure 5-5: Cost breakdown for PEM/PSA/Fe configuration, costs from Figure 5-6.

5.5 Sensitivity analyses

A number of sensitivity analyses were set up to investigate the effect of several variables on the performance and annualised cost of the ESS. Section 5.5.1 examines the effect of purge fraction on capital costs of the HB synloop for the three catalysts of interest (Fe-, Ru- and CoMoN-based catalysts). Section 5.5.2 explores the effect of pressure and temperature on the overall cost of the ESS configuration { MVC + Electrolyser:

Atmospheric Alkaline + ASU: PSA + HB: CoMoN-based + NH$_3$ to power: conventional turbine }.

5.5.1   Sensitivity analysis of catalyst options

Since the conversion of ammonia per single pass over a catalyst bed is limited by low equilibrium values, industrial Haber-Bosch NH$_3$ production requires a gas recycle loop, as shown in Figure 5-6. For a given NH$_3$ production rate, the cost of the HB recycle is directly proportional to its size, which in turn is inversely proportional to conversion and reaction rate. In turn, conversion is directly proportional to the pressure of operation and reaction rate is directly proportional to the temperature of operation. The variation of pressure offers an interesting trade-off effect in costs: an increase in pressure improves the conversion and thus decreases the size of the equipment in the recycle, except that of compressors, which tend to dominate the overall recycle costs.
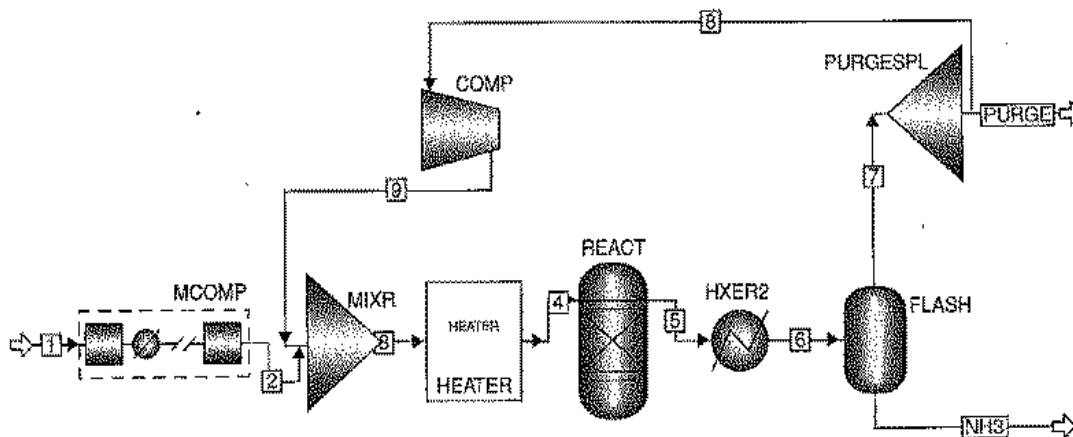
Figure 5-6: Haber-Bosch recycle loop. Source: (Finlayson, 2012).

The total annual capital costs for ammonia processes over selected Fe-, Ru- and Co$_3$Mo$_3$N-based catalysts were estimated based on the installed costs of equipment and the cost of the catalyst. Comparisons were based for an ammonia productivity of 48 ton_NH$_3$/day in a typical Haber-Bosch synthesis loop. Figure 5-7, Figure 5-8 and Figure 5-9 show the variation of capital cost vs. purge fraction for each of the catalyst options. While this analysis focuses on the cost of the synthesis loop, it should be noted that the purge fraction will affect consumption of H$_2$ and N$_2$, which needs to be taken into account when assessing the overall economics.
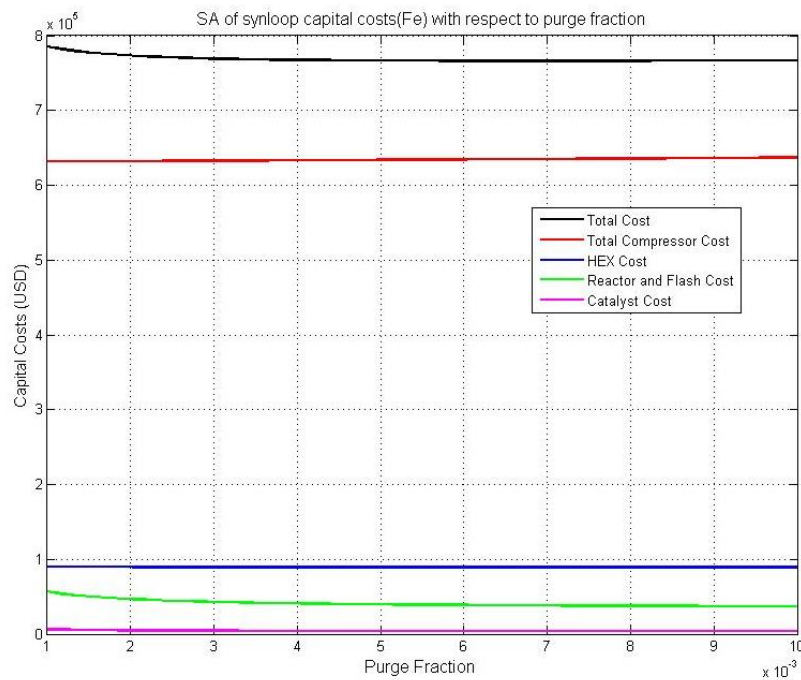
Figure 5-7: Fe-based catalyst, ammonia synthesis condition: 48 ton_NH$_3$/day, T = 400 C, P = 150 bar, conversion = 41.4%, r = 4.56E-4 kg$_{NH3}$ kg$_{cat}^{-1}$ s^{-1}, catalyst price = 13 £ kg^{-1}
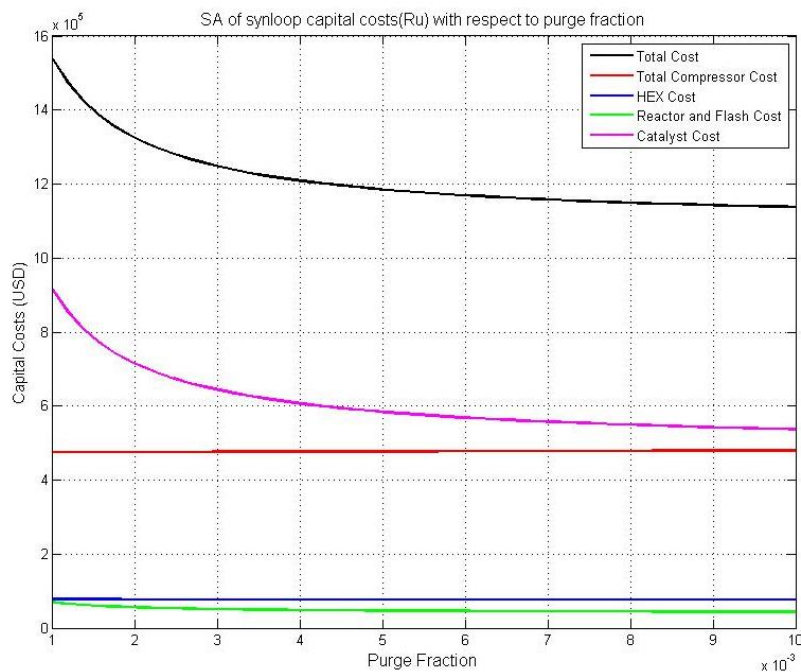
Figure 5-8: Ru-based catalyst, ammonia synthesis condition: 48 ton_NH$_3$/day, T = 400 C, P = 100 bar, conversion = 36.6%, r = 5.14E-4 kg$_{NH3}$ kg$_{cat}^{-1}$ s^{-1}, catalyst price = 1930 £ kg^{-1}
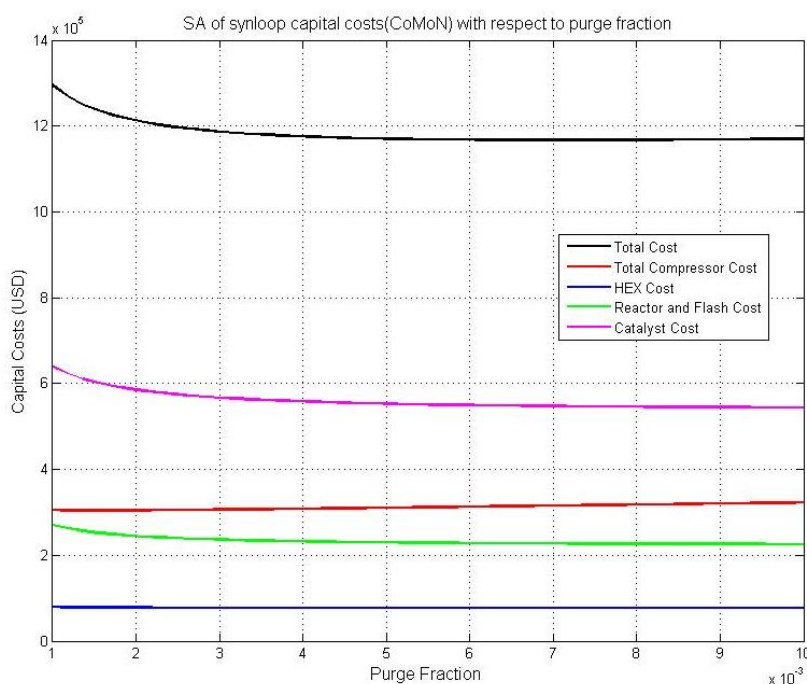
Figure 5-9: Co$_3$Mo$_3$N-based catalyst, ammonia synthesis condition: 48 ton_NH$_3$/day, T = 400 C, P = 31 bar, conversion = 7.5%, r = 7.08E-5 kg$_{NH3}$ kg$_{cat}^{-1}$ s^{-1}, catalyst price = 56 £ kg^{-1}

Cost (USD)	Catalysts		
	Fe	Ru	Co$_3$Mo$_3$N
Compressors	637.0	480.0	323.0
HEXs	89.4	77.0	77.7
Reactor and Flash	36.9	43.8	226.0
Catalyst	3.6	537.0	544.0
Total cost	766.9	1,137.8	1,170.7

Table 5-5: Costs (in thousands USD) of the ammonia synthesis processes with a purge fraction of 0.01

According to Figure 5-7, Figure 5-8, Figure 5-9 and Table 5-5, the Fe-based catalyst option is dominated by the compressors cost. In this case the reaction conditions were 150 bar and 400 C, at which the equilibrium conversion is 48%; the per-pass conversion was 41.4% (see Table 3-1).

Because of the intrinsic higher activity of Ru as compared to that of Fe catalyst, a lower pressure of operation was proposed (100 bar), but keeping the same temperature of operation, 400 C. Under these conditions, the equilibrium conversion is 40%; and the per-pass conversion is 36.6% (see Table 3-1). The lower conversion of Ru catalyst implies a larger reactor and recycle loop, but this is balanced by a lower pressure of operation (and thus lower compressor costs). In this second case the main costs were found to be the catalyst and the compressors. The significant proportion of catalyst cost to the total estimated costs, despite the drop in operational pressure by 33%, clearly reflects the expensive nature of the Ru catalyst (1930 £/kg_Ru vs. 13 £/kg_Fe).

Lastly, we evaluated a Co_3Mo_3N catalyst, and due to its highest intrinsic reaction rate, a lower pressure of operation was proposed (31 bar), again, at the same temperature of operation (400 C). Owing to its low conversion of 7.5% (Table 3-1) under this low pressure (equilibrium conversion was 20%), the main costs come from the Co_3Mo_3N catalyst, the compressors and the reactor and flash vessels.

Table 5-5 shows that the total cost for the Co_3Mo_3N-based option operating at lower pressures (31 bar) is 50% more expensive than that of the Fe-based option operating at 150 bar. It is thus economically not attractive to replace Fe catalyst with a more active Co_3Mo_3N catalyst at lower pressure. This evaluation was carried out on a conventional Haber-Bosch synthesis loop with an ammonia production rate of 48 tons/day, thus the actual costs of a mini-Haber-Bosch process with low ammonia production rate could be very different. One interesting point to note from this comparison is that the costs of compressors decrease substantially when lower pressures are employed at similar conversions (Fe vs. Ru case), but the decrease is more modest between the Ru and Co_3Mo_3N cases because the decrease in conversion results in much larger recycle flows. If the practical conversion of the Co_3Mo_3N catalyst can be enhanced to approach more closely the equilibrium conversion (e.g. to 80% of X_{eq}), the total cost for the Co_3Mo_3N–based option would be reduced to 0.95 million USD, which comes close to the current cost of Haber-Bosch synthesis using iron catalysts. In fact, preliminary calculations indicate that the cost could be reduced to around 6 million USD at higher temperatures and pressures. As a result, further research in new catalyst formulation to increase catalytic activity to cope with lower reactant flow and lower pressure is the key step for any future renewable ammonia process.

5.5.2   Sensitivity analysis with respect to T and P

It was observed that the conditions in the Haber-Bosch reactor affect every part of the ESS. Some of these effects are direct (e.g. higher pressures result in more compression work; higher temperatures in larger heat exchangers), but some are more complex (e.g. higher pressures increase conversion, which in turn reduces the flowrate in the recycle; higher temperatures increase the reaction rate thus reducing the reactor volume but also decreasing conversion). As a result, a change in temperature and/or pressure has often various opposing effects in the overall cost of the ESS, and thus it is very difficult to predict qualitatively which one will dominate.

For this reason, a sensitivity analysis of the ESS annualised costs with respect to temperature and pressure was performed. The chosen configuration was { MVC + Electrolyser: Atmospheric Alkaline + ASU: PSA + HB: CoMoN-based + NH_3 to power: conventional turbine }. Since one of the goals of this analysis was to explore the potential of CoMoN-based catalysts, it was assumed that an 80% approach to the equilibrium conversion X_{eq} is achieved; this assumption is in line with the X_{eq} of Fe and Ru found in the literature (87% and 91.5% respectively). Data for X_{eq} was retrieved from Table 2 of Chapter 2 in (Appl, 2012).

Only one data point was found for the reaction rate of CoMoN at 400 C, 31 bar (7.08333×10^{-5} kg_NH_3/kg/s (Kojima and Aika, 2001b)), but with the value of the activation energy (13.5 kcal/mol, ibid) it was possible to approximate the variation of reaction rate with respect to temperature; for lack of information it was assumed that reaction rate was independent of pressure.

The variation of conversion and recycle flow with respect to T and P are shown in Figure 5-10 (a) and (b). The best possible conditions to operate the system would be at maximum conversion and minimum recycle flow which correspond to 250 bar and 400 C (red corner for conversion and dark blue corner for recycle flowrate).
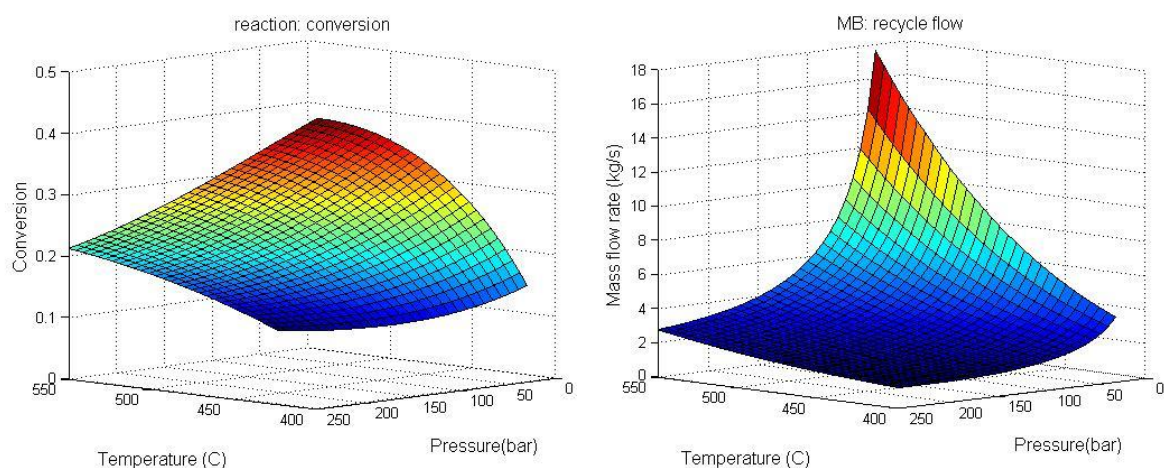
Figure 5-10: Effect of HB pressure and temperature on (a) reaction conversion, and (b) recycle flowrate.

The trends shown in Figure 5-10 help to understand the variation of annualised costs with respect to T and P changes. Figure 5-11 plots such a dependency, several features are apparent:

- The variation of total annualised cost is small over the ranges of temperatures and pressures (about 4% variation).

- The best operation conditions are at the maximum pressure and temperature; however, at a pressure of 250 bar there is little variation with respect to temperature.

- There are two steps in the cost surface corresponding to an increase in the number of electrolyser units.
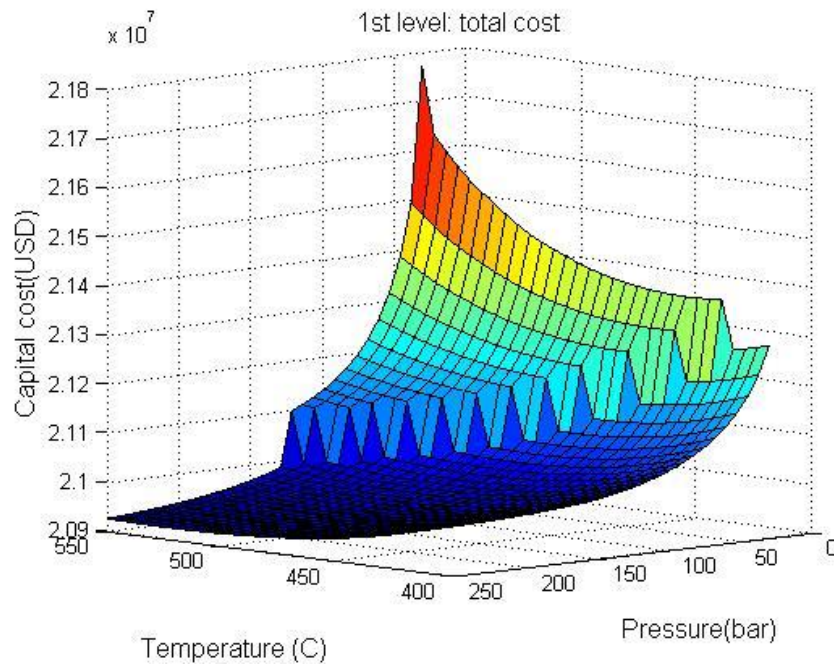
Figure 5-11: Total annualised cost of the ESS as a function of HB pressure and temperature.

The capital and operating costs are displayed in
Figure 5-12. The operating costs are about three times larger than the capital costs. The sensitivity to the operating conditions is not very large, about 16% for the capital costs and 1% for the operating costs.
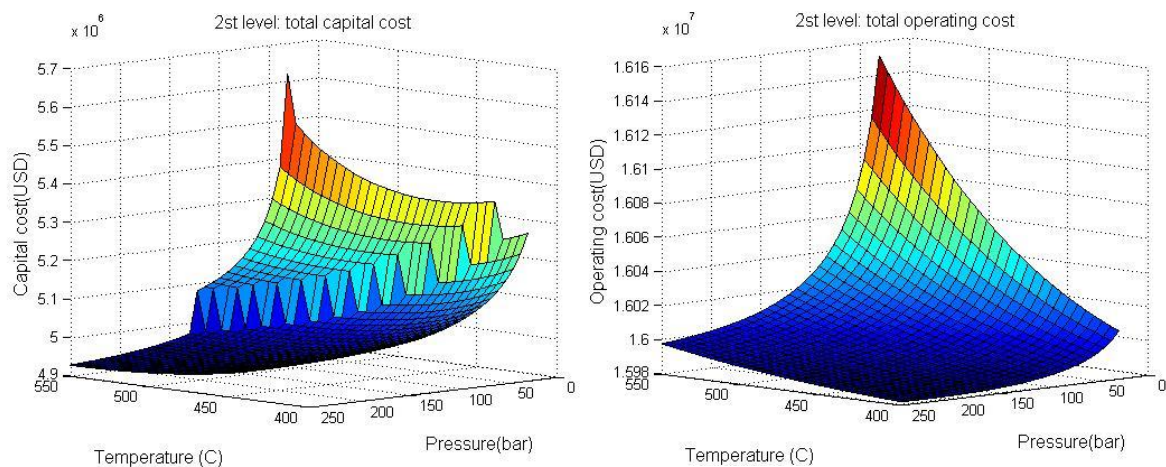
Figure 5-12: Annualised (a) capital and (b) operating costs of the ESS as a function of HB pressure and temperature.

The next figure, Figure 5-13, shows the capital cost of two of the modules in the ESS. The electrolysers, which dominate the capital costs, and the Haber-Bosch synthesis loop. The electrolyser surface clearly shows the two steps corresponding to an increment in the number of units, with an increment of up to 12% of the costs as the operating conditions are varied.

It is interesting to note that the HB synthesis loop surface shows a very strong variation with the operating conditions; it almost doubles. While this effect is of little importance in the overall cost of the ESS, it is indicative of the type of improvements that could be achieved by changing the catalyst and operating conditions of the Haber-Bosch process.
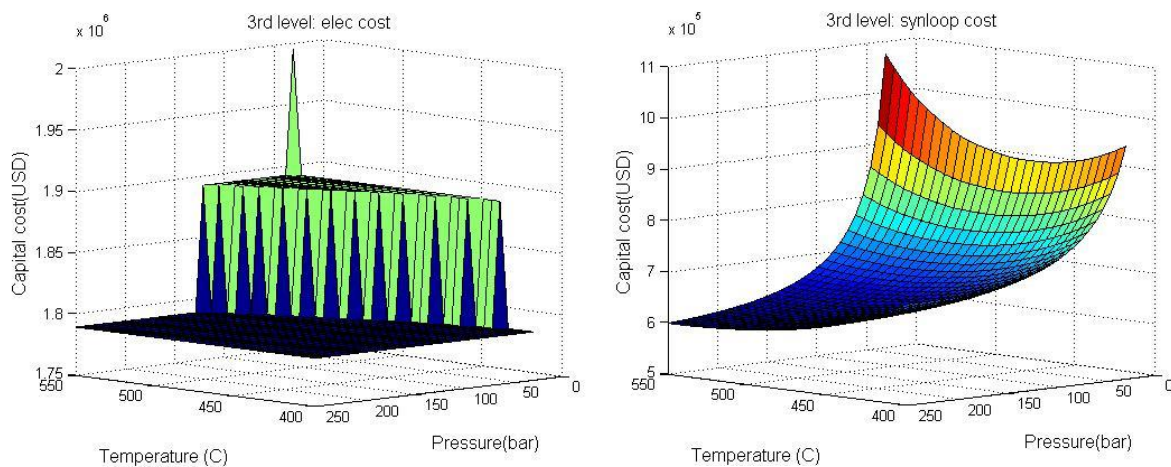
Figure 5-13: Annualised capital cost of (a) the electrolysers, and (b) the HB synthesis loop as a function of HB pressure and temperature.

Several other plots for this sensitivity analysis are available but not included in this report (costs of MVC, ASU, Generator, NH_3 and H_2 storage, and the compressor, heat exchangers, reactor and flash vessels and catalysts in the HB synthesis loop).

5.6 Levelised costs

The levelised cost of ammonia, *LCOA*, was estimated using the method described in (Hughes, 2013), Eqn. 5-7.

Eqn. 5-7:
$$LCOA = \frac{[CAPEX \times CRF] + OPEX}{NH3_{production}}$$

where *CAPEX* is the capital cost, *OPEX* the operating cost and *CRF* the capital return factor, this last parameter with a value of 0.08. This calculation returned a LCOA value of 655 USD/ton_NH_3.

In a similar manner the levelised electricity cost of the islanded system, LCOE, was estimated as the total annualised (operating and capital) cost of the islanded system, divided by the total annual kWh provided by the ESS to meet the demand (direct wind power + power from NH_3). This value was estimated as 251 USD/MWh.

6.   Market analysis

6.1 Market Overview

6.1.1   Global Production

About 140 million tonnes of ammonia are produced each year. It is the second-largest-volume industrial chemical in global trade, and is used in a diversified set of industrial sectors but primarily in agriculture as a fertiliser. Ammonia is easy to store in either low pressure or atmospheric tanks and can be transported with trucks, barges, rail, and/or pipelines. In fact, there are 3,000 miles of carbon steel ammonia pipeline operating in the U.S.
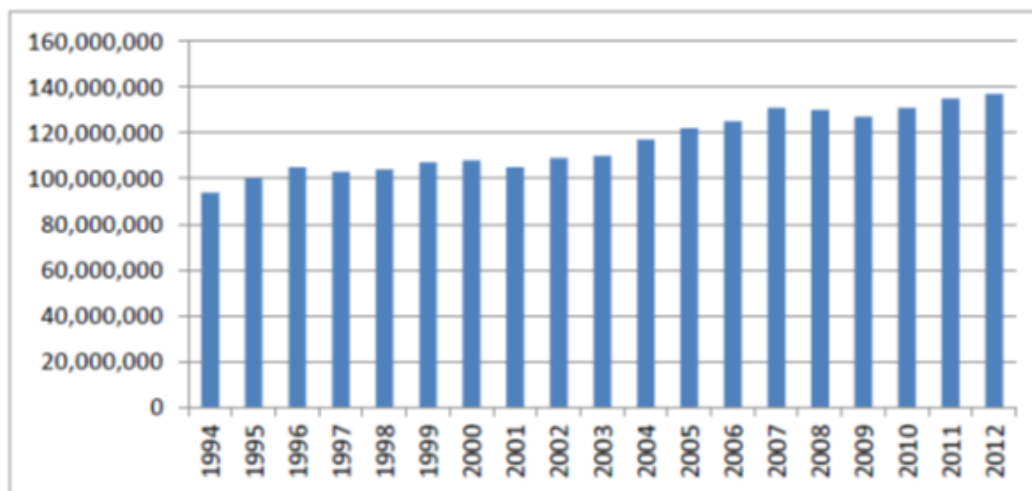
Figure 6-1: Global ammonia production (tonnes). Source: Center for European Policy Studies (2014)

At current prices, the production, transport, and consumption of ammonia generate annual worldwide revenues of US$100bn. Approximately 90% of this ammonia is produced via the Haber-Bosch process with fossil fuels providing the source of hydrogen, of which about 70% is made with natural gas and the remainder from gasifying coal (principally in China).

The two main drivers of ammonia consumption are demand in the agricultural sector and the development of applications for industrial purposes. Both of these factors have determined the increase in the consumption of ammonia in the last decade. However, as shown in Figure 6-2, the modest drop in consumption observed during the recent global economic downturn (2008-09) was primarily triggered by a decline in the demand for industrial applications, whereas agricultural demand remained strong.
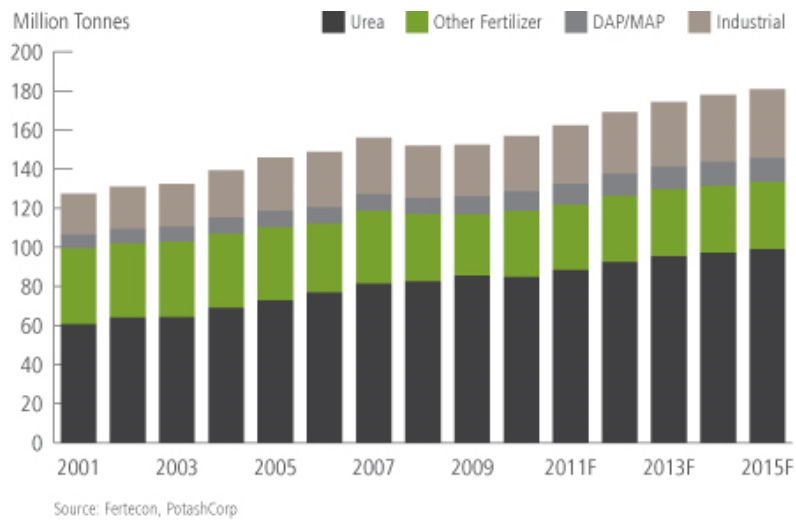
Figure 6-2: Global Ammonia consumption (mln tonnes). Source: Potashcorp (2013).
Note: Years 2011+ are forecasts, DAP/MAP – Diammonium/Monoammonium
Phosphate

Historically, global ammonia demand has grown on average by 2% per year, and can be expected to do so for the foreseeable future. The global production of ammonia is dominated by China which was responsible for 32% of the total global production in 2012; the other major producers are India (9%), US (7%) and Russia (7%); see Figure 6-3. The US is the largest ammonia importer and typically accounts for approximately 35-40 percent of world trade. Europe, a higher-cost producer, accounts for roughly 25 percent of trade. The majority of growth in imports is expected in Asian countries. The former Soviet Union, Latin America, the Middle East and North Africa are the primary ammonia-exporting regions due to their lower-cost natural gas and limited domestic consumption. Trinidad, the largest exporting country, accounts for almost 25 percent of global trade.
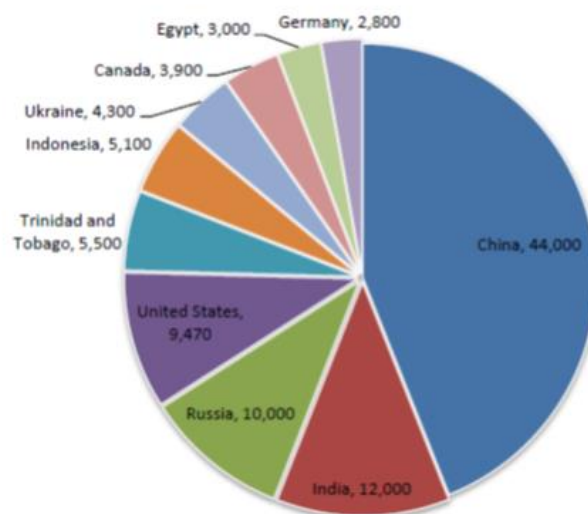
Figure 6-3: Top Ten Global Ammonia Producers 2012 (ktn). Source: Center for
European Policy Studies (2014)

6.1.2 Fossil-fuel-based Ammonia Production

6.1.2.1 Costs

Total investment and production costs of ammonia are normally around 150-300 €/ton when using conventional natural gas as feedstock, and 1.2 and 1.7 times higher when using heavy oil and coal, respectively. As a result, natural gas is generally favoured over other feedstocks. As of 2007, roughly 80% of ammonia was produced with natural gas and the remaining 20% with coal (Worrell et al., 2007).

	Natural Gas	Heavy Oil	Coal
Energy Consumption	1	1.3	1.7
Investment Cost	1	1.4	2.4
Production Cost	1	1.2	1.7

Table 6-1: Ammonia Feedstock Cost Comparison. Source: Center for European Policy Studies, 2014

Approximately 2/3 of consumed natural gas is used as a feedstock, while the remaining 1/3 is used to power the Haber-Bosch and other production processes. Natural gas is the key cost driver for the ammonia industry as, depending on its price, it makes up approximately 70-85% of ammonia total costs. We can see the primacy of natural gas in the breakdown of ammonia production costs in Figure 6-4.
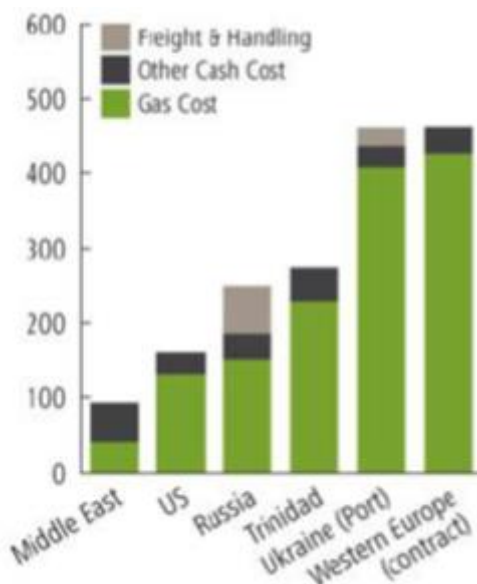
Figure 6-4: Natural Gas-based Ammonia Cost Breakdown US$/Tonne. Source: Potashcorp (2013)

Figure 6-4 also shows that Western Europe has among the highest ammonia production costs in the world. The key challenge Europe faces relative to other locations is the cost and availability of its natural gas.

6.1.2.2   Carbon Dioxide Emissions

With natural gas, about 1.8 metric tons of CO_2 are vented to the atmosphere for every metric ton of ammonia manufactured. With coal, this ratio is worse. Ammonia can also be produced without CO_2 via electrolysis, air separation, and Haber-Bosch synthesis. However, energy consumption has historically been about 12 MWh per metric ton of ammonia. Thus the fuel cost alone would be US$ 600 at 5 cents per KWh, substantially higher than even the most expensive *total* cost of ammonia production (see Figure 6-4 above). This substantial cost differential has prevented hydrolytic ammonia from competing directly with fossil fuel-based ammonia.

6.1.3   The EU Ammonia Market

In the EU virtually all ammonia is produced by using natural gas as a feedstock source of hydrogen. The EU-27 has a total capacity for the industrial production of ammonia of about 21 million tonnes (15% of global output). Production is spread over 17 different EU member states and a total of 42 production plants (see Table 6-2).

COUNTRIES	CAPACITY (k tonnes)	NUMBER OF PLANTS PER COUNTRY	% EU-27
GERMANY	3,438	5	17%
POLAND	3,210	5	16%
NETHERLANDS	2,717	2	13%
ROMANIA	2,176	6	11%
FRANCE	1,495	4	7%
LITHUANIA	1,118	1	5%
BULGARIA	1,118	3	5%
UK	1,100	3	5%
BELGIUM	1,020	2	5%
SPAIN	609	3	3%
ITALY	600	1	3%
AUSTRIA	485	1	2%
SLOVAKIA	429	1	2%
HUNGARY	383	2	2%
CZECH REP.	350	1	2%
ESTONIA	200	1	1%
GREECE	165	1	1%
TOTAL EU-27	20,613	42	100.00%

Table 6-2: EU-27 capacity and number of plants per country 2013 (Center for European Policy Studies, 2014). Source: Center for European Policy Studies, 2014.

Due to significant opportunities to exploit economies of *scale* and *scope*, the ammonia value chain is highly vertically integrated, with producers of ammonia-derived products generally producing their ammonia on-site (Center for European Policy Studies, 2014). An average scale ammonia plant produces 500-1,000 metric tonnes of ammonia per day.

Average	1,342
Median	1,110
Maximum	4,658
Minimum	25
Standard Deviation	893

Table 6-3: EU-27 Plant Annual Capacity Statistics (metric tonnes/day). Source: Adapted from Center for European Policy Studies (2014).

6.1.4 Ammonia Prices

Due to the ease of shipping, the price of ammonia varies only slightly according to geographic location. In recent decades ammonia has traded for around US$ 300/tn. This was the case until 2008, when prices briefly rose to US$ 900/tn, until falling quickly to previous levels, and then gradually climbing to the present level of around US$600/tn. This new higher level of ammonia prices appears to be stable, in line with other increases in commodity prices observed worldwide over the same period. Because the major cost of producing ammonia is closely associated with the price of natural gas, the price of ammonia is very volatile and tends to follow the natural gas price. When energy prices rise, so too does the price of ammonia, making it difficult for farmers to budget returns for their farms unless they are sophisticated enough to hedge their costs with financial derivatives.
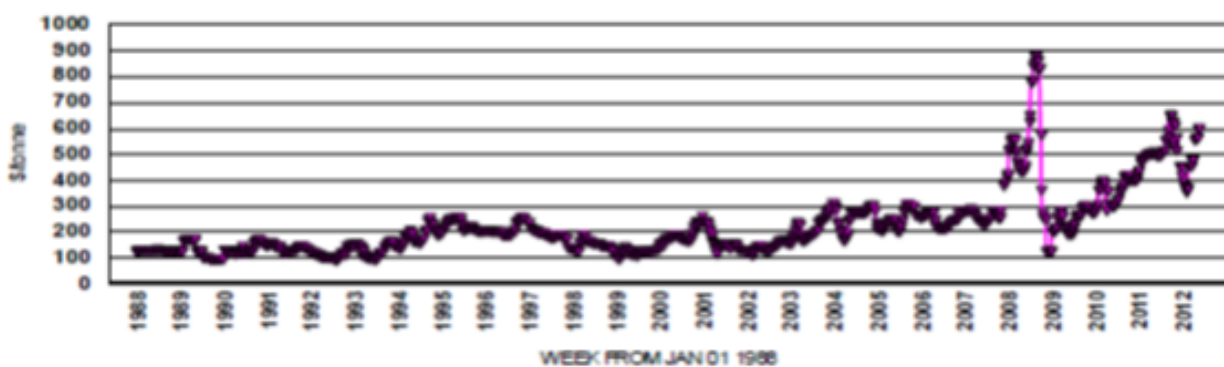
Figure 6-5: Ammonia Price Trends 1988-2012. Source: Duncan Seddon & Associates
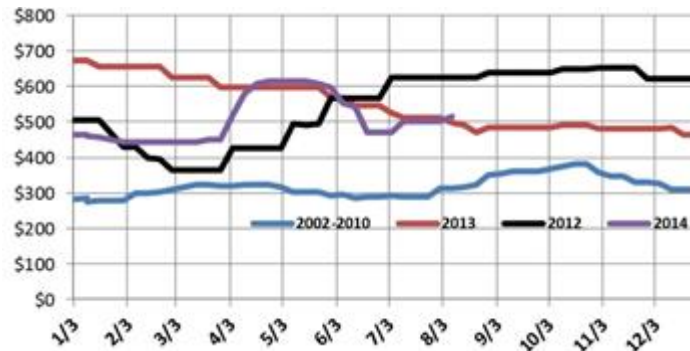
Figure 6-6: Tampa Ammonia Prices 2002-10, 2012, 2013, 2014. Source: Knorr, (2014)
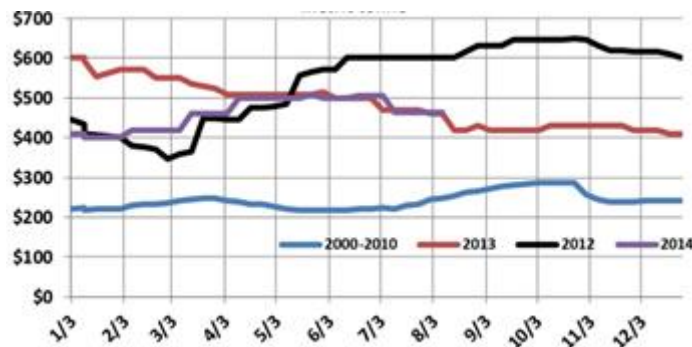
Figure 6-7: Black Sea Ammonia Prices 2000-10, 2012-14. Source: Knorr, (2014)

6.1.5   Ammonia Fertiliser

Roughly 80% of the global ammonia production is consumed by the fertiliser industry; of which only 4% is directly used as fertiliser in the form of anhydrous ammonia (AA). Other forms of ammonia-based fertiliser such as urea and ammonium nitrate require further processing.
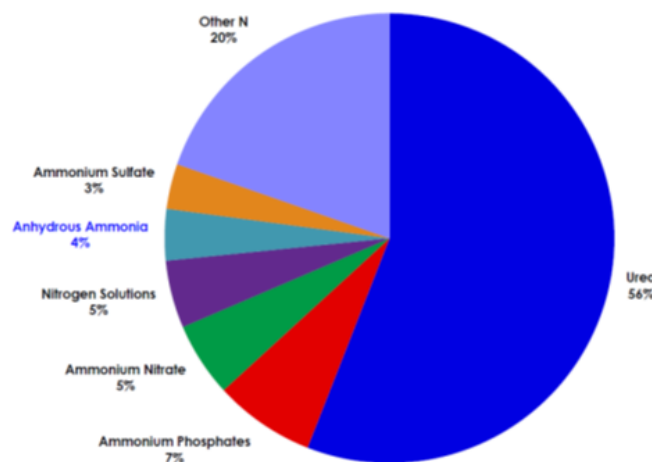
Figure 6-8: World Nitrogen Fertiliser Use 2011 (107.9 million metric tonnes N). Source: The Fertilizer Institute, 2013

Anhydrous ammonia has been used as a fertiliser for over 50 years. It has the highest nitrogen content (82% by weight) of any fertiliser and is the cheapest source of a given weight of nitrogen. The amount of nitrogen is the key metric for the nutrient content of nitrogenous fertilisers. The same weight in nitrogen regardless of fertiliser source will achieve a similar productivity response in crops.

Fertiliser	Percent Nitrogen by Weight
Anhydrous Ammonia	82%
Urea	46%
Ammonium Sulphate	21%
Ammonium Nitrate	34%

Table 6-4: Nitrogenous Fertiliser Nitrogen Content

Increased nitrogen content by weight also reduces transportation and handling costs for a given level of fertilisation. Therefore, in spite of the slightly higher price of AA per tonne relative to other nitrogenous fertilisers, AA is by far the most economical source of nitrogen.
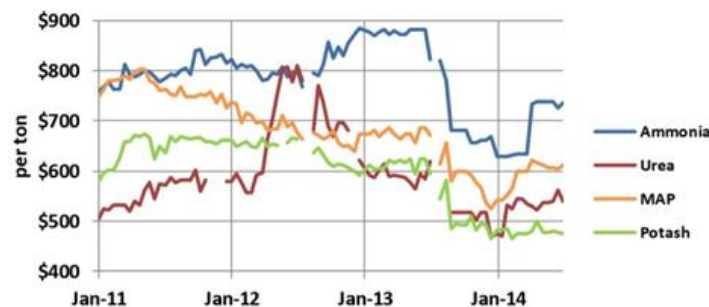
Figure 6-9: Iowa Fertiliser Prices. Source: USDA
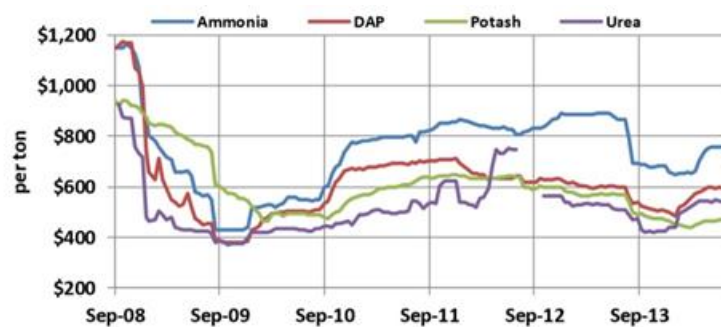
Figure 6-10: Illinois Fertiliser Prices. Source: USDA

112

Compared to the rest of the world AA is particularly popular in the US, and is associated primarily with the production corn. While AA use is 4% of total nitrogen fertiliser use globally, in the US it comprises a substantially larger 27%.
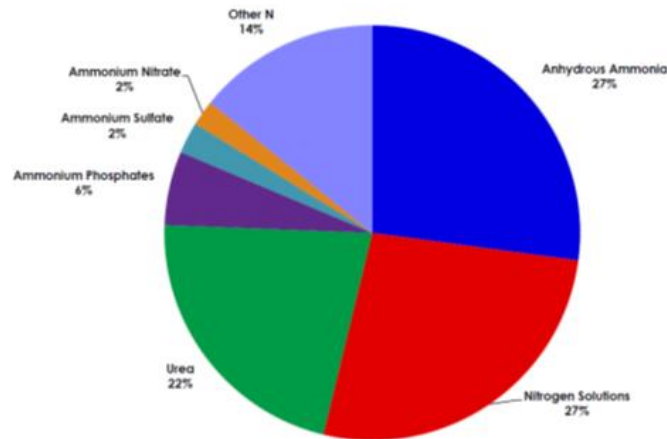
Figure 6-11: US Nitrogen Fertiliser Use, Fiscal Year 2010-11 (12.84 million tons N).
Source: The Fertilizer Institute, 2013

In fact, the demand for AA and corn are so closely related in the US that corn and ammonia prices there co-move to a high degree as can be seen in Figure 6-12 below.
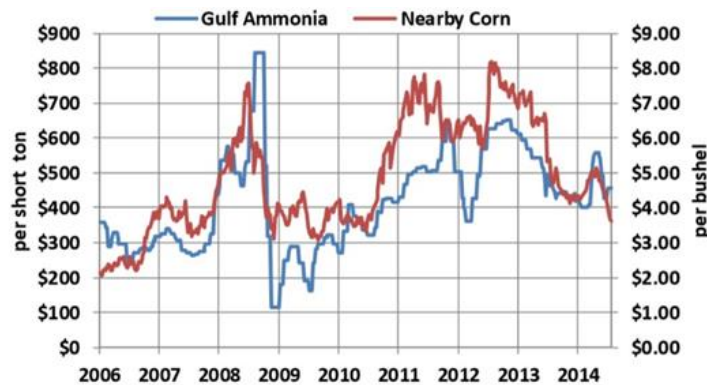
Figure 6-12: Ammonia and Corn Price Comparison. Source: Knorr, (2014)

However, in spite of its cost advantages AA is not as widely used in agriculture as other nitrogen fertilisers due to a number of intrinsic drawbacks. To begin with, AA is a hazardous gas that requires special equipment to store and apply to fields. It is caustic and corrosive on contact with flesh, and if levels in the air exceed 300 ppm it can cause fatal damage to lung tissue. Furthermore, conditions must be favourable in order to apply AA to fields. In particular, the soil must not be too dry or up to 12% of the AA will simply blow off into the atmosphere, and it must not be too warm (generally < 5 C) or much of the ammonia will be converted by microbes to less desirable nitrate. Therefore growers

often either apply AA to fields in the fall, or in both the fall and the spring just before planting.

6.2 Environmental and Social Impacts of Renewables-based Ammonia Systems

6.2.1 Environmental impact analysis

6.2.1.1 Noise

Large PSA plants required in the production of ammonia increased blower sizes and/or speeds. Increasing the blower size, however, also increases radiated noise and pulsations levels in the plant. For example, the sound pressure level at the exit of a typical large size vacuum blower can reach levels up to 170-180 dB. For safety, environmental and/or regulatory concerns, however, the sound pressure level needs to be reduced to about 90-98 dBA. This is typically done with the use of a silencer.
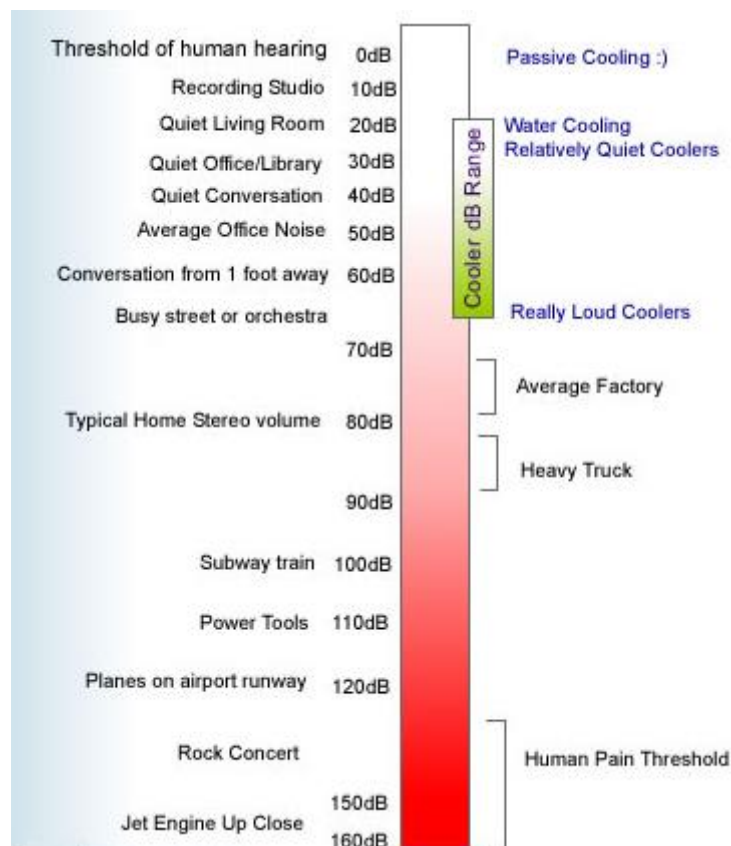
Figure 6-13: Decibel (dB) Range Chart. Source: www.neoseeker.com

6.2.1.2   Water Use

Pure fresh water will be required in order to generate hydrogen through hydrolysis. For every metric tonne of ammonia produced, 1.5 metric tonnes of water are required. On the whole this amount of fresh water would not be a significant source of demand compared to other water hungry industries such as agriculture. However, for areas which are already under water stress this could be an issue, but most of Europe would not fall under this category.
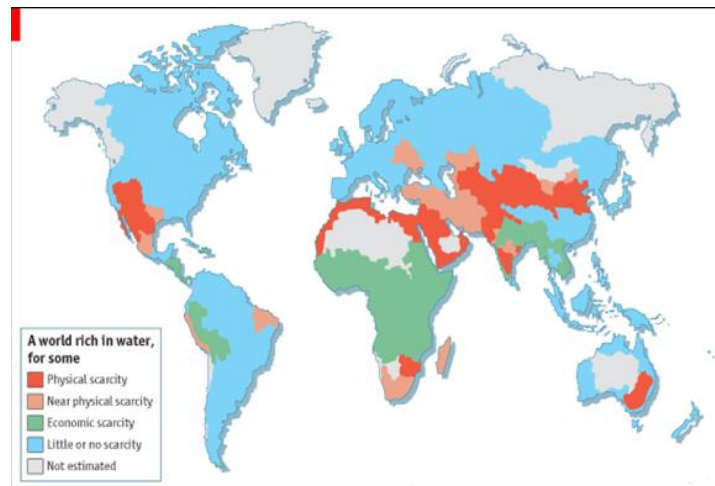
Figure 6-14: Global Water. Scarcity Source: Comprehensive Assessment of Water Management in Agriculture, 2007

6.2.1.3   Waste

Where freshwater is unavailable but seawater is, freshwater can be produced via desalination thus eliminating problems of water scarcity. However, where seawater is converted to freshwater, a waste product of this process is either concentrated brine and/or heated water. A 48 ton NH_3/day plant would require 360 tons of water, or 360,000 litres. Depending on the water purification technology, we can roughly expect a product/waste water ratio of 1:4, or in the 48 ton_NH_3/day case, 288 m^3 of waste water per day. This is not a significant amount of waste. If this water is pumped out to the surrounding environment the potential for this to cause problems for local wildlife is limited, unless the effluent pipe is located in shallow poorly circulating lagoons or very small rivers.

6.2.1.4   Safety

As previously mentioned, ammonia will cause chemical burns to exposed skin and can be life-threatening when inhaled in relatively small concentrations (300 ppm). Although gaseous ammonia is lighter than air, leaking vapours are also said to initially hug the ground upon release and therefore stay dangerous to humans at some distance. It is

recommended that protective gear be worn when pumping ammonia or handling ammonia containers.

Since 1921 17 fatal explosions involving ammonia-related compounds have been recorded, including the most deadly industrial accident in US history[4]. However, these explosions were all due to ammonium nitrate rather than to pure ammonia. Unlike its highly explosive derivatives, anhydrous ammonia is technically non-flammable in liquid form, and as a gas it does not burn readily except under extremely high temperatures (630 C) and within a narrow fuel-air mixture ratio (15-25% air). Ammonia leaks, however, have caused fatalities: as recently as last year, 15 people were killed and 26 injured when a refrigeration unit in Shanghai failed. Leaking storage facilities would therefore pose the greatest danger to human health. Still overall ammonia has a good safety record and if proper precautions are followed it is a safe industrial chemical.

6.2.2   Societal impact analysis

6.2.2.1   Visual impact

Obtaining construction permission for large renewable energy plants may be a formidable obstacle in the wider adoption of renewable energy storage. Our estimates of required storage tank volumes for the 48 ton/day plant are: 147,384 m^3 for H$_2$ at 20 bar (238 tonnes), and 3,743 m^3 for liquid NH$_3$ (2,552 tonnes). This level of storage would necessitate visually imposing containers much in line with similar permitting obstacles facing large industrial plants. This could be particularly problematic in areas which also receive tourist income from natural beauty. Many such areas are also locations which have or could have stranded renewables. These storage containers would also require substantial land-use. Although in and of itself this should not pose an issue, in many municipalities (particularly in the US) industrial ammonia storage tanks are not allowed within city limits. Therefore, for certain land-constrained locations with high population densities, it may not be possible to build ammonia plants at all. Nevertheless, it may still be easier to procure development permission for ammonia storage and generation facilities than it is to gain permission for a high-voltage electricity transmission line.

At the micro-grid level, permitting concerns for the ammonia and storage plant would not be a material issue, however the erection of wind turbines to power these facilities may still be problematic. Although views are mixed, a considerable proportion of the population find wind turbines unsightly. A recent YouGov poll in of 1001 residents in Scotland for instance found that 23% of respondents agreed strongly with the statement that wind farms, "are, or would be, ugly and a blot on the landscape" (2010). Furthermore, residents near wind farms have report health effects related to visual disturbance and noise (eg. Bakker et al., 2012; and Farbouda et al., 2013). Recent research by Gibbons (2014) has shown that these problems translate directly to lower residential land prices. According to this research, visible wind turbines reduce residential land values 5-6% on average for turbines within 2 km and 2% at 2-4 km, and that larger turbines reduce land

---

[4] A 1947 cargo ship explosion in the port of Texas City, Texas which killed at least 550 people and injured 3,500.

values even more. As a result of these effects, we can expect local opposition to onshore wind farm construction to remain a formidable obstacle to widespread deployment of localised wind-powered ammonia production.

6.2.2.2   Employment

Ammonia-based energy storage will require little in the way of operational costs including labour, with at most 10-20 trained technicians and support staff for even the largest plants. Indirect employment could rise for both the manufacture of renewables infrastructure (e.g. wind turbines) and Haber-Bosch related storage and reaction vessels. However, this indirect employment may rise primarily for foreign countries due to trade. By the same token, conventional power plants may be shut-down and employees may be let go as a result of the change. Net changes in domestic employment will depend primarily on whether components for renewables and conventional energy generation are manufactured in domestic or foreign markets. Regardless, the effect should be negligible relative to broad macroeconomic trends.

6.2.2.3   Public Acceptance

Ammonia has a characteristic strong unpleasant odour, but leakages in a properly running plant will be minimal and should not affect neighbouring communities. Given the association of ammonia (but especially ammonium nitrate) with industrial accidents, it is likely that there will be local public backlash against large scale ammonia plants. In addition, the fact that protective gear is indicated when handling ammonia may discourage wider public acceptance, though this could potentially be mitigated by various means, such as assigning dedicated employees to provide pumping services to consumers.

6.3 Renewables-based Ammonia Systems Market Analysis

In the near and medium term we anticipate that the demand for renewables-based ammonia systems will come primarily from the markets for (i) electrical energy storage, and (ii) anhydrous ammonia fertiliser. The total revenues (or 'market potential) that renewables-based ammonia may capture depend on both the size of each of these markets and the relative competitive position of ammonia within each of them. Both market size and competitiveness will also be heavily influenced by whether the ammonia generation is located at an 'islanded' site or not. In particular, 'islanded' locations will favour the competitiveness of locally produced ammonia, whereas the size of such markets will be less at these locations than in better connected areas. It is therefore useful to examine this market according to the separate demands for energy storage and fertiliser, and whether or not these functions are located in an 'islanded' location. These distinct market segments for renewables-based ammonia are illustrated in Figure 6-15, and numbered 1-6. The market potential of each of these six market segments is analysed below.

Figure 6-15: Market Segments for Renewables-based Ammonia

Market Segments

1. **'Islanded' energy storage**
2. **Non-'islanded' energy storage**
3. **'Islanded' fertiliser**
4. **Non-'islanded' fertiliser**
5. **'Islanded' energy storage and fertiliser**
6. **Non-'islanded' energy storage and fertiliser**
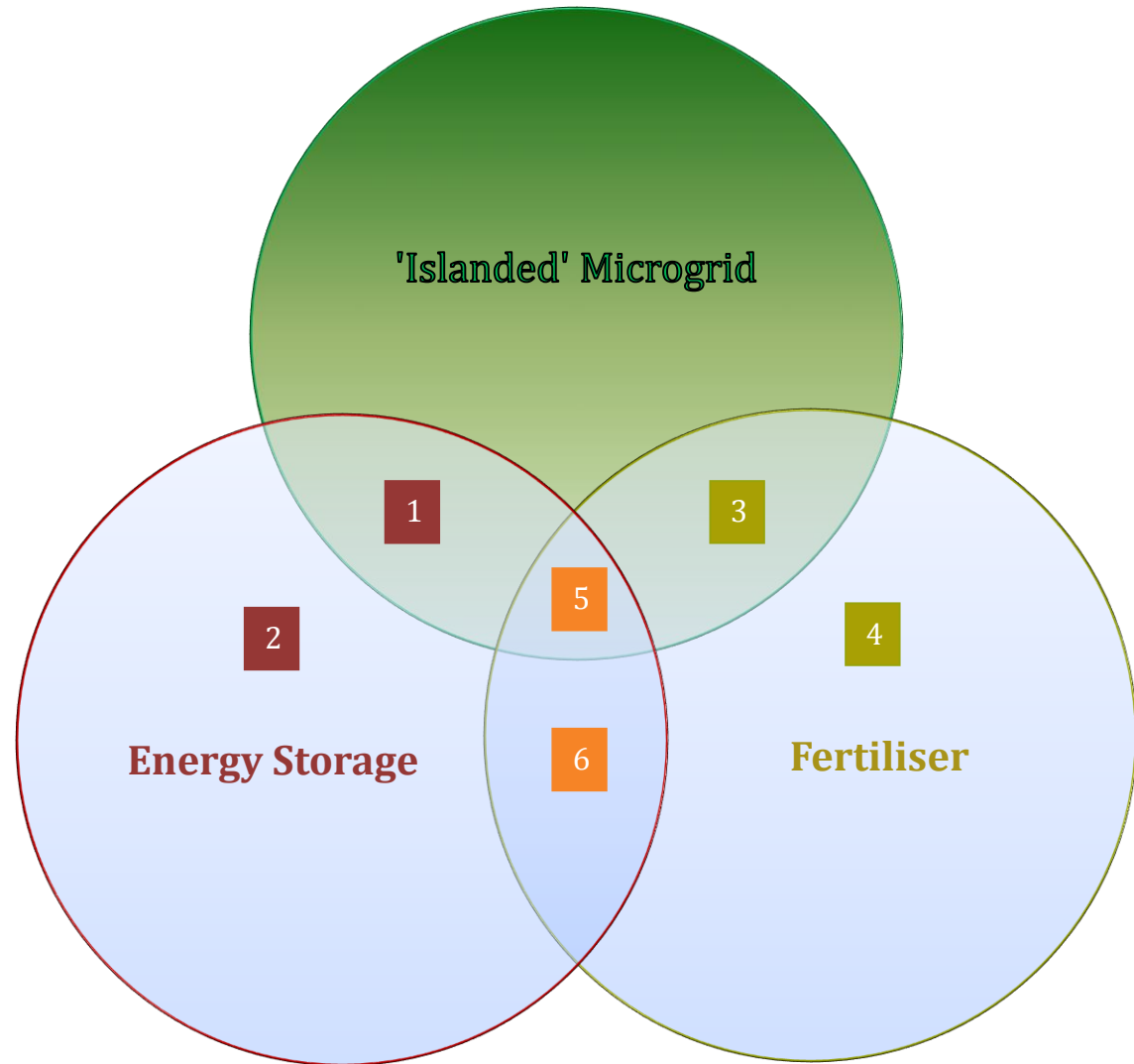
6.3.1 Competing Energy Storage Technologies

There is great and growing need for energy storage, especially at scale. The demand for ammonia-based energy storage in particular will largely depend on its capabilities relative to other competing technologies. The market for energy storage is an emerging one. Existing options tend to have one or more significant limitations, whereas more promising technologies are at an early development or even conceptual phase. In order to better understand ammonia's competitive position, we present a brief overview of the technological options (substitutes) for energy storage and their relative strengths and weaknesses.

As Figure 6-10 illustrates, there are four main energy storage technologies currently available: Mechanical, Electrical, Thermal, and Chemical. When competing with ammonia the key parameters for energy storage technologies are the costs of that storage and round-trip energy efficiency. Round-trip energy efficiency is important because it directly affects the size of the wind-farm/electricity generation plant needed to produce sufficient storage capacity to deliver a given level of continuous electricity output.
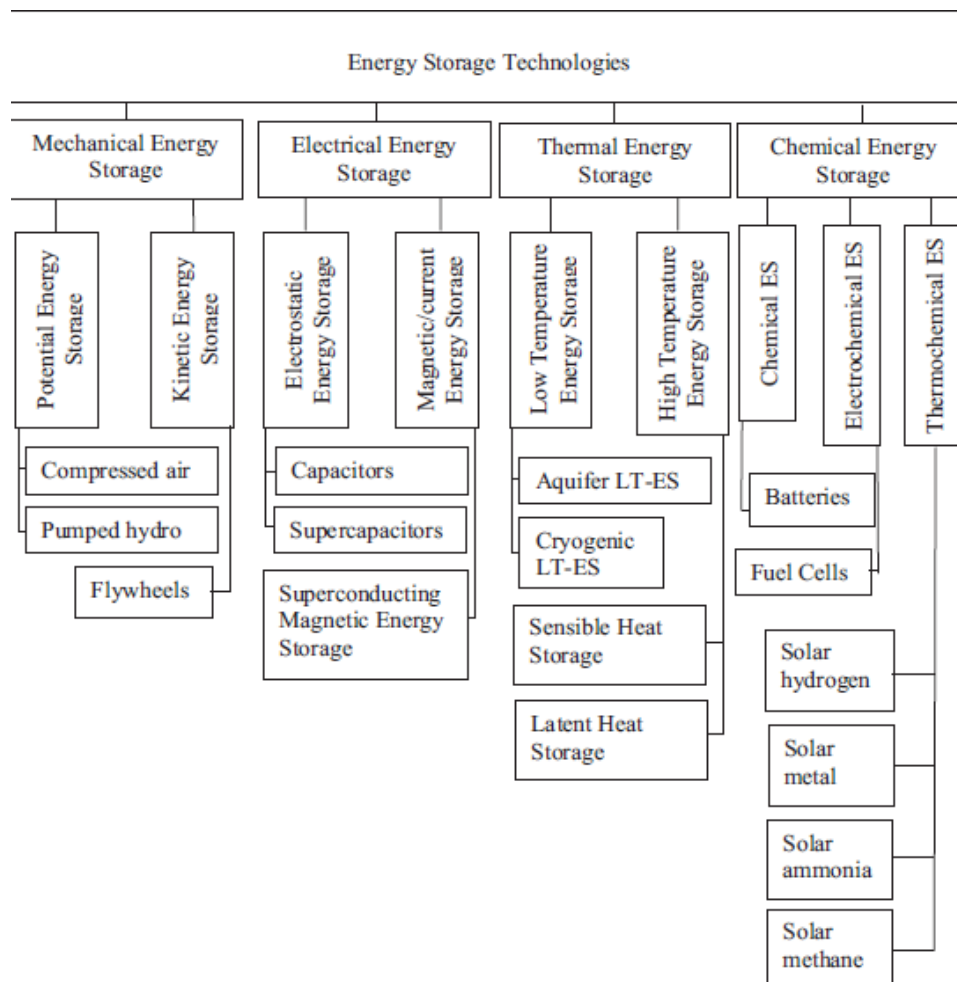
Figure 6-16: Energy storage technologies. Source: Evans, Strezov, and Evans (2012)

6.3.1.1   Mechanical Energy Storage

Pumped Hydro Energy storage

Pumped-hydro energy storage (PHES) is by far the most prevalent method of grid-scale energy storage, with more than 99% of world grid-energy stored by this technology (European Commission, 2014). This technology uses the height differential between two basins to store energy by simply pumping water from the lower to the higher vessel (electricity to potential energy) and back when energy is needed.   The system is highly efficient (round-trip efficiency can reach levels higher than 80%).   The cost of this technology ranges from 5 to 100 USD/kWh. Currently the largest pumped storage scheme in the UK, Dinorwig in North Wales, can store 9.1 GWh of energy, but given its geographical dependency this technology has little potential for new sites in UK.

Main advantages:
virtually unlimited number of charge/discharge cycles
extremely rapid cycle times
high efficiency
Main disadvantages:
expensive
environmental impacts
high fixed costs
bureaucratic difficulties (permissions, authorizations, etc.)
geography dependent

Compressed air energy storage

In Compressed Air Energy Storage (CAES), air is compressed (to around 70 bar), stored under pressure and released when power is needed. Due to high pressure this process has special technical requirements. During the first phase the heat of compression must be extracted (and compensated for during the power generation phase) by the means of inter-coolers/after-coolers. Then, the compressed air must be stored in underground caverns[5] or in surface systems[6].

With respect to the compression/power generation via heat, there are three types of storage systems: diabatic, adiabatic and isothermal. The diabatic process extracts compression heat and uses natural gas to heat up the high pressured air before pumping it into a combustor. Alternatively, the exhaust heat of a combustion gas turbine can be utilized for the power generation phase. The round-trip efficiency of the diabatic storage system is approximately 42% when using natural gas and 55% (with a lower emission of CO_2 of 30-60%) when reutilizing the exhaustion heat. The adiabatic system, by contrast, uses the compressed gas during the power generation phase causing an increase in the round-trip efficiency up to 70% thus increasing the sustainability of the process (no need

---

[5] A storage capacity up to 10 Gwh is possible.
[6] Storage capacity in general limited to 60Mwh due to costs.

for extra natural gas)[7]. Finally, the isothermal storage divides the compression phase into several steps so as to maintain roughly the same temperature at all the steps while storing the compression heat. The round-trip efficiency in this case increases to 70-80% but the process is still technically a challenge.

Currently there are only two examples in the world of CAES: one is in Germany (Huntorf, 290 MW) and the other one is in Alabama, US (110 MW). A much larger project is under construction at the Iowa stored Energy Park: 2700 MW of turbine power in conjunction with a large wind farm.

<u>Main advantages</u>:
use of sustainable materials for large turbines
use of free and easily accessible feedstock (air)
<u>Main disadvantages</u>:
technologically demanding with respect to the storage sites and processes
low round trip efficiency for the diabatic process
requires specific geologic locations in order to store acceptable quantities of energy

Kinetic Energy (Flywheel)

Electricity can be stored also as kinetic energy through a rotor (Flywheel Energy Storage - FES). Based on the principle of conservation of energy the system is able to absorb energy (speeding up) and release it (slowing down).

The most effective FES systems make use of carbon-fibre composite rotors, suspended in magnetic bearings whose spin frequency ranges from 20,000 to 50,000 rpm in a vacuum enclosure. The round-trip efficiency for those advanced devices is extremely high, up to 85%, while the energy density is strictly linked to the shape of the rotor as well as to the materials combination used. This storage system has proven to be very flexible due to its high charge/discharge rates but its self-discharge rate of 20% per hour is a fatal weakness in competing with ammonia for grid-level storage.

 <u>Main advantages</u>:
high power potential
low environmental footprint
low maintenance costs
<u>Main disadvantages</u>:
high self-discharge rate

---

[7] A pilot plant to test new devices for the heat storage in the adiabatic process is due to start in 2018, run by a consortium headed by a German energy company (RWE).

6.3.1.2 Electrical Energy Storage

Superconducting magnetic storage

Superconducting magnetic energy storage systems store electricity by generating high magnetic fields. In a typical process electricity flows into a vessel filled with a superconductive coil. Electricity accumulation and release is almost instantaneous and the amount of energy available is independent from the discharging rate (as opposed to batteries). The most common used material is Niobium-Titanium (NbTi) whose operational temperature is -271°C.

The round-trip efficiency is very high (more than 95%) and the self-discharge rate is 0 at 4K 100% at 140K. Currently there are 30 SMES installations in the USA with a capacity of approximately 50 MW, but for the standard size of the majority of applications the cost would be prohibitive.

Main advantages:
fast charge/discharge time cycle
almost infinite working life
high efficiency
Main disadvantages:
high costs
high storage losses due to the low operating temperatures of the magnet
low energy density

Supercapacitor energy storage

Supercapacitors store electricity electrostatically in an electrical field. Their energy efficiency is very high (85-90%). The cost of this solution is linked to the material used and may decrease as technology improves. Nevertheless, due to their high self-discharge level, they are only suitable for short term storage.

Main advantages:
virtually unlimited number of charge/discharge cycles
extremely rapid cycle times
not susceptible to overcharging
Main disadvantages:
expensive
high self-discharge rate

6.3.1.3   Thermal Energy Storage

Liquid Air Energy Storage

Liquid Air Energy Storage system (LAES) also known as Cryogenic Energy Storage (CES) makes use of air or nitrogen to store energy. Air or nitrogen is cooled and condensed at very low temperatures. The process consists of three main phases: charging, storage and discharging in which electricity is used to run a gas liquefier, then the liquid is stored and finally, when power is needed, it is it is delivered to a turbine that generates electricity from the re-expansion of the gas. The roundtrip efficiency of LAES is 25 – 50% but low-grade heat waste (up to 120 C) can be used to drive the process[8] increasing the efficiency to 25 – 70%.
General Electric Oil & Gas (NYSE: GE) has signed an exclusive global licensing deal with Highview Power Storage, a UK start-up that makes utility-scale liquid air energy storage systems.

In addition, it was announced this April that UK-based Highview Power Storage had been awarded £8 million ($13 million) by the Department of Energy and Climate Change in order to build a commercial-scale plant[9] (5 MWh) based on liquid air technology. The Company claims that with economies of scale they can achieve a cost as low as $500 per kilowatt/hour of storage.

Main advantages:
it does not require mining of (rare) earth elements
the technology of air separation is well known and understood[10]
few requirements in terms of operational conditions and location
small geographical footprint
no downtime for catalyst replacement
zero emissions
no (or very low depending on the liquid used) toxicity
no combustion and therefore much quieter engines
it uses standard industrial components - which reduces commercial risk
Standard storage tanks for liquid nitrogen, oxygen, and LNG can be used to hold GWh of electricity. Storage loss at 0.17%/day
Main disadvantages:
low roundtrip efficiency unless waste heat is used
it cannot be transported in pipelines due to insulation expenses – therefore best for localised production

---

[8] Waste heat at 115 C is very common in many industrial processes.
[9] A pilot plant had been already in place in Slough, UK, since summer 2011 and the cost has been around $ 500 per Kw/h of stored energy, lower than current battery-grid costs.
[10] The first liquid air car was produced in 1899-1902

6.3.1.4   Other thermal energy storage

Thermal Energy Storage (TES) consists of a wide range of technologies aimed at storing electricity as thermal energy. There are several processes to achieve this that have been suggested including heat stored as hot water in rock caverns and directly as "hot-rocks" or molten salt. The heat stored is then combined with water to drive a steam turbine.

The round trip efficiency of the system is high (above 70%) but several projects are attempting to increase the efficiency of this technology. One of the most important projects currently running is the US Department of Energy's SunShot Initiative whose targets for the thermal storage system are:

Improve heat transfer and thermal energy storage media
Thermal energy storage cost < $15/kWh (40% lower than current costs)
Exergetic efficiency > 95%
Material degradation due to corrosion < 15 μm/year.

Main advantages:
high power potential
low environmental footprint
Main disadvantages:
high costs
high water use

6.3.1.5   Chemical Energy Storage

Chemical batteries

Chemical batteries are devices able to store energy by electrochemical reactions through charge (accumulation) and discharge (release) phases. There are different types of batteries depending on the chemical elements involved and the storage process.

The most common storage process is given by the rechargeable technology, also known as Redox Flow Batteries whose name suggests the use of a reduction/oxidation cycle. Several chemical elements combinations are able to obtain this result (e.g. lead–acid, nickel cadmium (NiCd), nickel metal hydride (NiMH), lithium ion (Li-ion), and lithium ion polymer (Li-ion polymer)) and, depending on the chosen configuration, round-trip efficiency is affected.

As a storage device batteries can be very effective reaching a round-trip efficiency of 80%. However, their storage capacity is directly linked to their size and on an industrial scale the cost is prohibitive. On average the costs range from $400 per kilowatt-hour to $1,200 per kilowatt-hour for the Li-ion batteries while a lead-acid battery cost is roughly $170 per kilowatt-hour.

There are currently several projects aimed at increasing the efficiency of batteries as a storage device. The EnerVault experience, for example, choosing an iron-chromium

combination because both materials are abundant and low-cost, says CEO Jim Pape. According to what he says the company projects it can deliver energy for utilities and other users at a cost of less than $250 per kilowatt hour; at that price, energy storage becomes competitive with natural gas plants that provide power at peak hours.

Main advantages:
high efficiency
high power density
Main disadvantages:
too expensive at an industrial scale
limited number of discharge cycles giving limited lifespans of 5-15 years
constant self-discharge
time consuming recharge
use of toxic materials

Hydrogen

Hydrogen can be produced by reforming natural gas with steam or through an electrolysis reaction. It can be, then, re-electrified by the means of a combustion engine or a fuel cell (converting chemical energy to electrical one). The round-trip efficiency on average ranges from 35 to 60%. However, the chemical characteristics of hydrogen make its storage demanding from a technological point of view. It has an extremely low boiling point (-253 C) and to be transported it needs to be compressed at 350 – 700 bar. In case of underground and cryogenic storage, cooling is complex and energy loss is high. Since 2008 the EU Fuel Cells and Hydrogen (FCH) programme has supported research and is aimed at contributing to the goals of Horizon 2020. In the US a similar program from the Department of Energy (DOE) with a budget of $250 million has been running since 2004 developing a large number of specific performance targets.

Finally, depending on the chosen technologies, hydrogen has a levelized cost profile ranging from 6 to 725 $/KWh. It is economically comparable to CAES and chemical batteries but its low round-trip efficiency (around 32%) makes this system hardly competitive.

Main advantages:
high potential in combination with other liquids
no self-discharge
Main disadvantages:
too expensive to store, transport and produce at an industrial scale
security concerns
very low round-trip efficiency

Hydrocarbon synthesis

This technology uses CO_2 and a source of hydrogen to artificially produce hydrocarbons via the Fischer-Tropsch process. Currently applications of these storage methods are still at a development stage. A US company, Doty Energy, claims that strong arguments in favour of this technology include: (a) higher storage density (two times higher than

batteries), (b) the energy stored in liquid fuels can be used within our current transportation infrastructure, and (c) the chemical processes promise scalability. Doty's process electrolyzes water and combines the generated hydrogen with CO in a Fischer-Tropsch process to produce the liquid fuels. Eventually, the CO_2 might come from the atmosphere, though with current technology the energy required for separating CO_2 from the atmosphere is about 15 times greater than from point sources. Currently these costs mean that co-location with an industrial CO_2 source is required in order to compete with other chemical energy storage technologies. This limiting factor will prevent the wide-scale adoption of synthetic hydrocarbon energy storage.

Main advantages:
fuel can be seamlessly used with existing infrastructure
scalable
Main disadvantages:
requires CO_2 source
safety concern due to large scale storage of hydrogen
low round-trip efficiency

	Energy Storage System	Round-Trip Efficiency	Self-Discharge per Day	Suitable Storage Duration	Capital Costs (US $/KWh)	Limited by
Mechanical	Pumped Hydro	74%	Very small	Hours-Months	5-100*	Topography
	Compressed Air	42-70%	Small	Hours-Months	2-50*	Geology
	Flywheel	90%	100%	Seconds-Minutes	1000-5000*	-
Electrical	Lead-acid Battery	70-90%	0.1-0.3%	Minutes-Days	200-400*	-
	Nickel-Cadmium Battery	60-65%	0.2-0.6%	Minutes-Days	800-1500*	-
	Lithium-Ion Battery	85-90%	0.1-0.3%	Hours-Months	600-2500*	-
	Flow Battery	65-70%	Small	Hours-Months	150-1000*	-
	Supercapacitor	90%	20-40%	Seconds-Hours	300-2000*	-
Thermal	Liquid Air	25-70%	0.17%	Hours-Months	500	-
	Pumped Heat	72-80%	-	-	618	-
Chemical	Hydrogen	42%	Almost Zero	Hours-Months	6-725*	Geology
	Hydrocarbon Synthesis	25%	Very small	Hours-Months	-	CO_2 Source
	Ammonia	20-25%	Very small	Hours-Months	-	Water Source

* Costs of operation, maintenance, disposal and other ownership costs are not considered.

Table 6-5: Energy storage systems: techno-economic comparison. Source: Adapted from Chen et al. (2009), Diaz-Gonzales et al. (2012), Hughes (2013) and (Taylor et al., 2012).

6.3.2 'Islanded' energy storage (Market Segment 1)

Microgrids

Energy storage will be required in order to provide energy security for so-called 'microgrids' – electrical grids which can operate independently from main grids. Such microgrids currently number in the thousands worldwide, and usually operate out of necessity as a result of an 'islanded' location. However this need not always be the case.
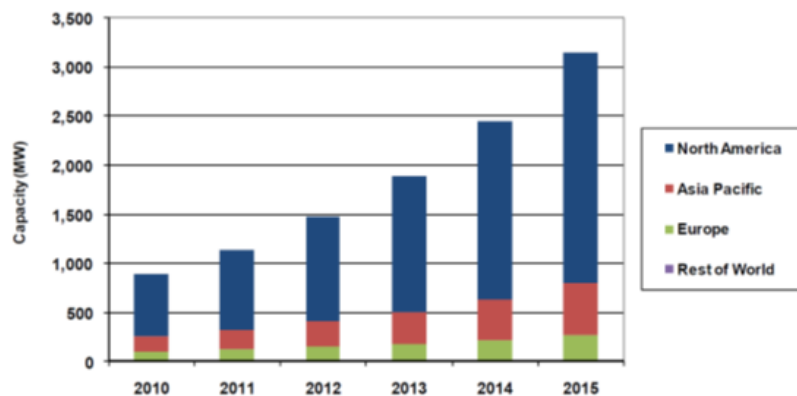
Figure 6-17: Microgrid Capacity, World Markets: 2010-2015. Source: Pike Research (2009)

Universities, hospitals, some industries, and the military may desire to have the capability of functioning independently of an existing central grid. For instance, during the 2012 superstorm Sandy, NYU and Princeton University stayed lit and heated due to their microgrids despite surrounding blackouts. The majority of such systems are powered by diesel generation, but strategic and social image considerations may put pressure on microgrid markets to diversify towards renewables generation combined with energy storage.
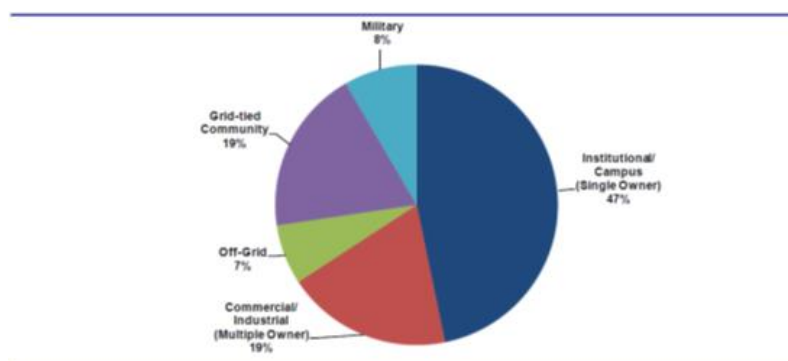
Figure 6-18: Market Sector Revenue Breakdown, North America: 2015. Source: Pike Research (2009)

A key question regarding potential market size for microgrids is the scale at which ammonia energy storage becomes economically and technically feasible. A global survey conducted by the Australian Commonwealth Scientific and Industrial Research Organisation (CSIRO) in early 2009 focused on microgrids that included some level of renewable energy generation. It showed that the largest segment of such microgrids (34%) is between 1 MW and 5 MW in size, with 81% of microgrids at capacities below 5MW)[11]. Therefore the market for microgrids with renewables is likely to be dominated by small-scale generating plants.

The key technical limitation for accommodating levels of ammonia production small enough to meet this demand is the scale of the Haber-Bosch process. A windfarm with nameplate size of 102 MW and a peak demand of 20 MW were assumed, resulting in a feasible ammonia production of 48 ton NH_3/day (smaller than most existing Haber-Bosch ammonia plants). This would be a large windfarm, and permitting would be difficult in Europe except at an offshore site due to planning restrictions and local opposition. Currently the median and average onshore windfarm size in the UK is, respectively, 9 and 11 MW. However, we are aware of private firms which specialise in small-scale ammonia production as an energy storage medium. These firms claim to be able to efficiently produce ammonia at scales as small as 3 tons NH_3/day. If true, this would greatly expand the economic potential market for ammonia across small microgrids. Applied to an 'islanded' ammonia system, roughly 1-20 MW microgrids correspond to what would be considered mini-HB technology.

Unfortunately, because ammonia has such low round-trip energy efficiency (23 to 41%, see Table 5-1), unless energy storage is combined with another desired capability of ammonia, ammonia might be rejected as an energy storage technology in favour of more efficient alternatives. Furthermore, unlike many other technologies, ammonia is limited in where it can be produced by requirements for a water source. Looking decades into the future, the ability of 'islanded' ammonia windfarms to produce synthetic fuel on site could potentially be a valuable service, both because it mitigates transportation costs of fuel and insulates islanders from oil price fluctuations. Assuming a levelised cost of ammonia of 655 US$/ton_NH₃, ammonia would cost 0.40 US$/litre[12], or 0.034 US$/Millijoule, whereas assuming wholesale petrol costs in the UK of 1.78 US$/litre[13] affords 0.057 US$/Millijoule. On this basis ammonia could be seen, in principle, to be an economically viable alternative to petrol not only in locations with high fuel tariffs such as the UK, but also in low fuel tariff nations such as the US. In the US however, taxed petrol prices would have to double for this to be the case[14]. This result differs markedly from (Morgan et al., 2014) which found that variably produced ammonia only becomes competitive at $2.64/litre of diesel fuel: slightly more than twice the current price. The disparity arises due the lower levelised cost of ammonia estimated in our study.

---

[11] http://www.smartgridobserver.com/n6-15-12-1.htm
[12] There are 1,623 litres per metric tonne NH3.
[13] Or £1.10/litre, assuming the petrol is purchased in the UK with applicable taxes included.
[14] (Morgan et al., 2014) also finds that variably produced ammonia becomes competitive at $2.64/litre of diesel fuel: slightly more than twice the current price.

Stranded Renewables

All renewable energy sources are highly location dependent. Rarely is it the case that the best renewable energy sites are collocated with population centres with high energy use. According to Weidou and Zhen (2011), "*currently, difficulty in accessing the power grid is the major bottleneck for the development of wind power*", p.9. Transporting this energy generally requires costly grid expansion. For instance, the Orkney Islands are one of the most favourable locations in Europe to deploy a variety of renewable technologies. However, these islands are extremely remote from industrial areas, and although they have had a 50 MW power connection with mainland Scotland in place since the 1980s, in order to export more power they are currently exploring the possibility of laying a second cable to mainland Scotland capable of exporting 200 MW at a cost of £300 m (Orkney Sustainable Energy, 2014). Given these substantial costs, remote ammonia production and transportation from locations such as the Orkneys, Iceland, Norway, etc. to more populated areas could potentially be a viable alternative to costly grid expansion[15].

Furthermore, it is widely recognised that gaining permission to expand the grid network and capacity (often across multiple jurisdictions) is more difficult and time-consuming than gaining permission to exploit renewable energy sources. As result, renewable energy sources may be effectively 'stranded' from consumers in spite of being located in an otherwise desirable location. This is currently the case in Germany, for instance, where high-voltage transmission lines to link large-scale offshore wind generation in the North with industry in the South have been held up for many years[16]. Similar to the true 'islanded' case, ammonia energy storage and transportation via conventional means could temporarily or even permanently circumvent electricity transmission bottlenecks. Ammonia has a distinct first-mover advantage over other energy storage technologies for dealing with stranded renewables because it is a relatively mature technology[17] and has an existing global support infrastructure for its transportation. In addition, the scale of ammonia production necessary for capturing stranded renewables would generally be large enough for mature standard-scale Haber-Bosch technologies to be employed. Other stranded renewable technologies such as synthetic hydrocarbon manufacture are not practical because they require a low-cost source of CO_2, which will be unlikely to be present in remote locations and would also be less environmentally friendly than ammonia.

An additional advantage of exploiting stranded renewables is the fact that total ammonia storage can be reduced to correspond to a regular or production dependent extraction schedule. Monthly extractions of stranded ammonia, for instance, could thereby reduce total ammonia storage costs to a fraction of the micro-grid case. Furthermore, because capital expenditures on wind turbines could be economised by locating them in areas

---

[15] For instance, Germany's four main grid operators have stated that it needs an additional 3,800 km of new electrical lines at a cost of €20 bn (€5.3 m/km) in order to meets plans to phase out nuclear power by 2022, and €12 bn to connect wind power in the North to the rest of Germany. (http://www.spiegel.de/international/germany/germany-needs-miles-of-new-power-lines-to-make-energy-transition-a-835979.html)

[16] The German government currently wants to build 3800 km of high voltage lines (2100 km direct and 1700 km alternative current) to support 25 GW of wind power in the north of the country, at an estimated cost of €20 bn.

[17] A wind to ammonia stranded renewables plant is currently in operation in Estonia's Pakri islands.

with superior wind profiles, and because the cost of turbines dominates the total cost of a renewables-based ammonia plant (85% of total costs); a stranded ammonia plant in an ideal renewables location could produce ammonia at a significant discount to the onshore Australian case explored here. Each ton of ammonia so produced could then be used to generate 2.6 MWh of electricity on demand, at a levelised cost of $655/2.6 = 251 USD/MWh[18].

Figure 6-19 presents industry forecasts of various markets for energy storage. The green line corresponds to the total market that ammonia market segment (1) in Figure 6-15 would attempt to capture, and the purple line roughly corresponds to the total market targeted by market segments (1) and (2) combined. Figure 6-20 gives a breakdown of the (1) + (2) Wind and Solar Energy Storage market segment (the purple line in Figure 6-19) by technology.
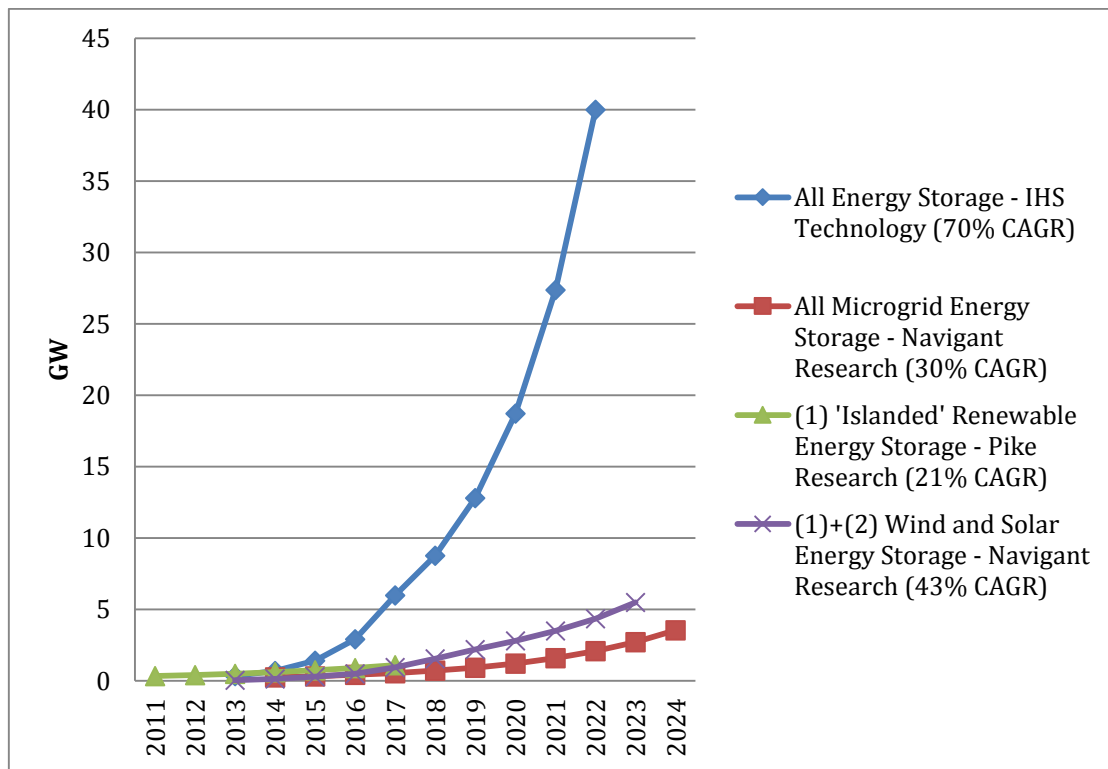
Note: To transform Figure 6-19 into revenues, multiply each GW of energy storage by US$2bn. CAGR refers to Cumulative Average Growth Rate.

Figure 6-19: New Installed Energy Storage Market Global Forecasts

---

[18] Solid oxide fuel cells (SOFC) is a technology currently being researched which should yield 3.9 MWh/ton_NH3. This would provide 124 $/MWh of stored electricity.
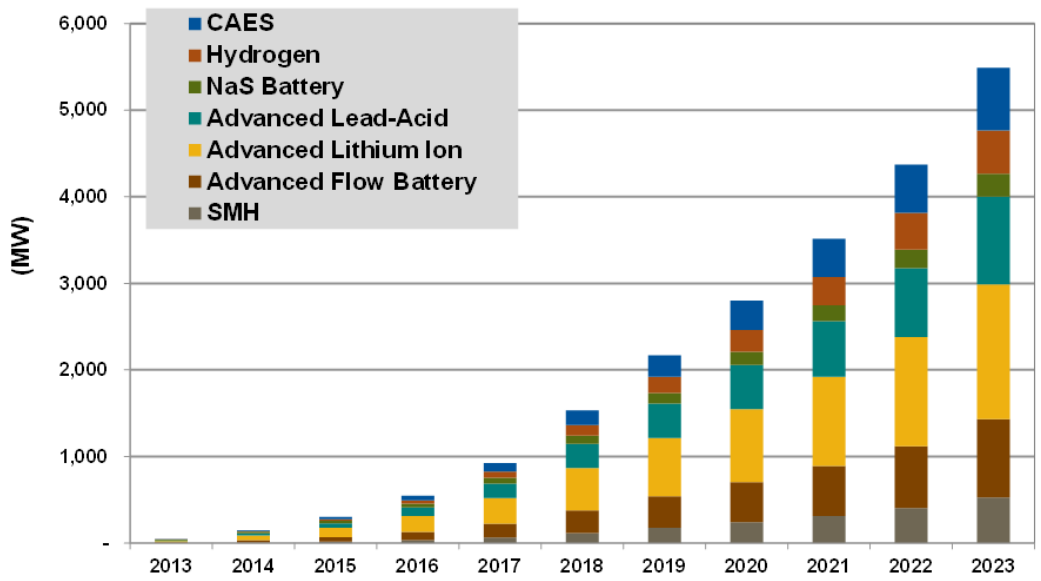
Note: CAES refers to Compressed Air Energy Storage, NaS refers to Sodium-Sulfur, and SMH refers to Sodium Metal Halide.

Figure 6-20: New Installed (1)+(2) Wind and Solar Energy Storage by Technology, World Markets: 2013-2023. Source: (Navigant Research, 2013).

6.3.3   Non-'islanded' energy storage (Market Segment 2)

The amount of intermittent renewable energy a grid can handle before storage becomes absolutely necessary depends upon local wind and grid characteristics. According to a recent white paper published by the Irish government[19], up to 42% of wind power penetration can be accommodated without any need of storage in the Irish system. A similar study conducted by the US Department of Energy (2008) found that wind power up to 20% penetration could be achieved without the need for energy storage capacity. According to the European Commission (2014) the intermittent renewable share is below 15-20%, grid operators are generally able to compensate the intermittency. But when these levels exceed 20-25% this is no longer possible, and surplus generation must be disposed of. Therefore, even with perfect interconnectivity, after the EU achieves 20% renewables penetration by 2020, this will be an upper limit to the penetration renewables can achieve unless additional storage or back-up capacity is installed.

---

[19] Department of Enterprise, Trade and Investment and Department of Communications, Energy and Natural Sources (2008)
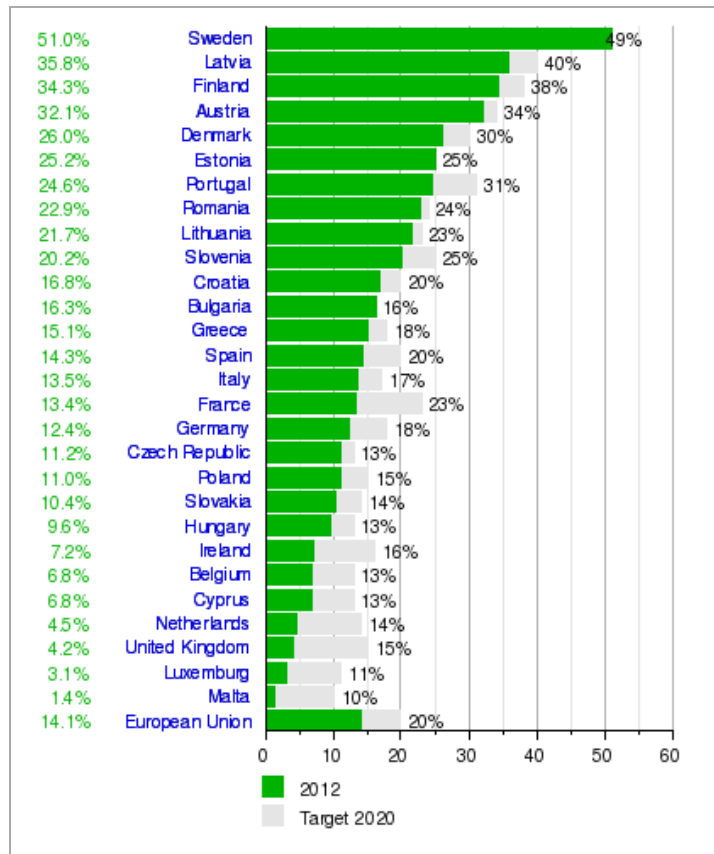
Figure 6-21: Share of renewables in gross final energy consumption in EU-28 as of 2012.
Source: Wikipedia

In practice, however, the threshold of 20% intermittent renewables is already exceeded in many EU countries. For instance, in October 2013, Denmark supplied 122% of the country's power needs via renewable sources. That same month Germany hit a momentary peak of nearly 60% of generation from wind and solar, and in the first 5 months of 2014 actually *payed* consumers to use electricity for a total of 55 hours. Although the EU has an overall goal of 20% final energy consumption from renewables by 2020, currently there is very limited storage in the EU energy system (around 5% of total installed capacity) composed almost exclusively of pumped hydro-storage, which is limited to mountainous areas (Alps, Pyrenees, Scottish Highlands, Ardennes, Carpathians). Other forms of storage – batteries, electric cars, flywheels, hydrogen, chemical storage - are either minimal, or at a very early stage of development. In response some countries such as Germany have enacted policies to specifically encourage the adoption of energy storage for the purpose of integrating variable energy sources into the grid.
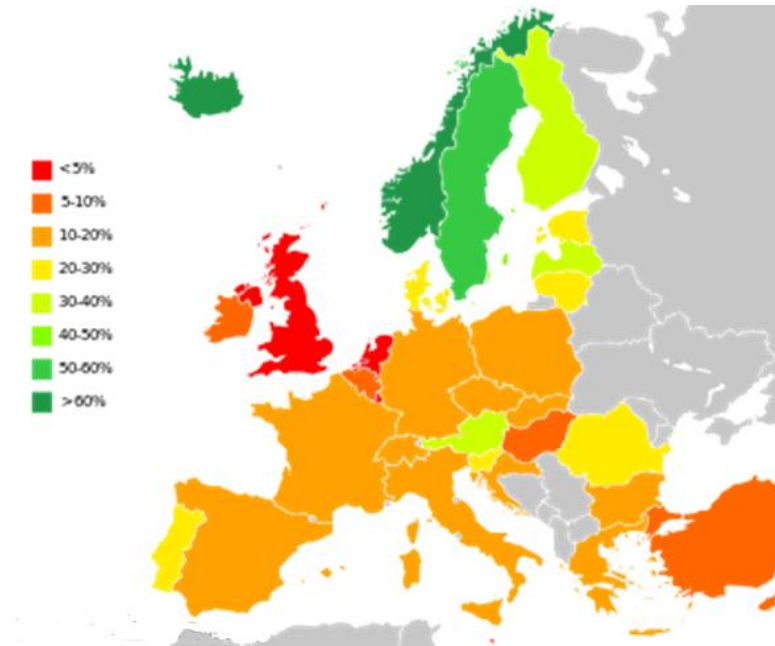
Figure 6-22: Renewable energy as proportion of total consumption 2012. Source: Eurostat 2012, (Iceland, Switzerland, Turkey 2010)
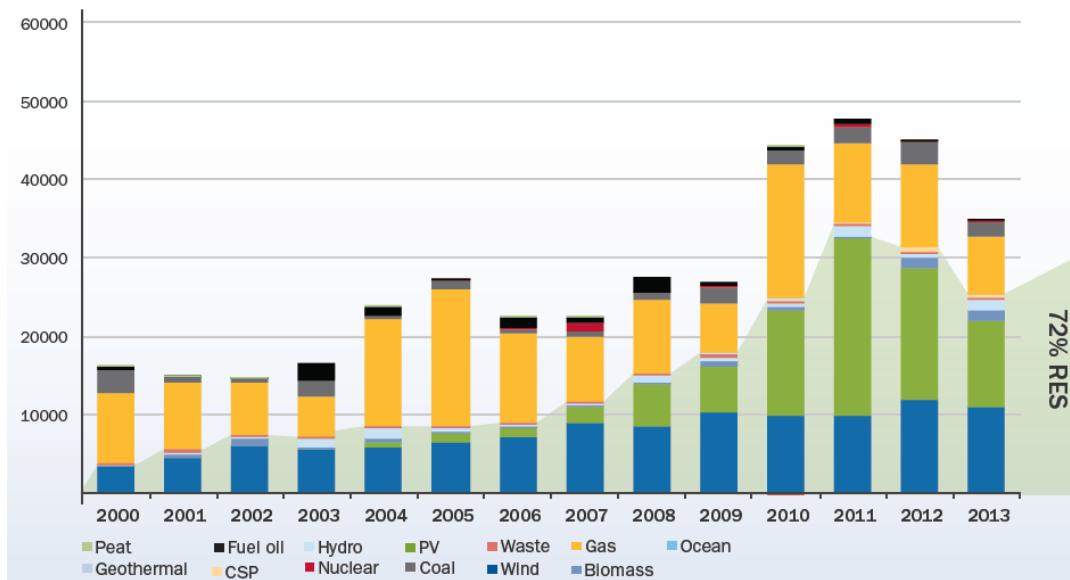
Figure 6-23: Installed Power Generating Capacity per Year in MW and Renewable Energy Share (RES) (%). Source: (EWEA, 2014).

Other countries, such as the UK, have opted instead for back-up fossil fuel plants to be run in concert with renewables. For instance, the UK government has chosen to pay for back-up generation via its so-called 'Capacity Market'. This policy is expected to cost each

household in the UK an additional £15/yr on average to 2030, or £396 m/yr nationwide[20], and intends to secure an estimated 53.3 GW of electricity generating capacity, equating to more than 80% of peak electricity use.
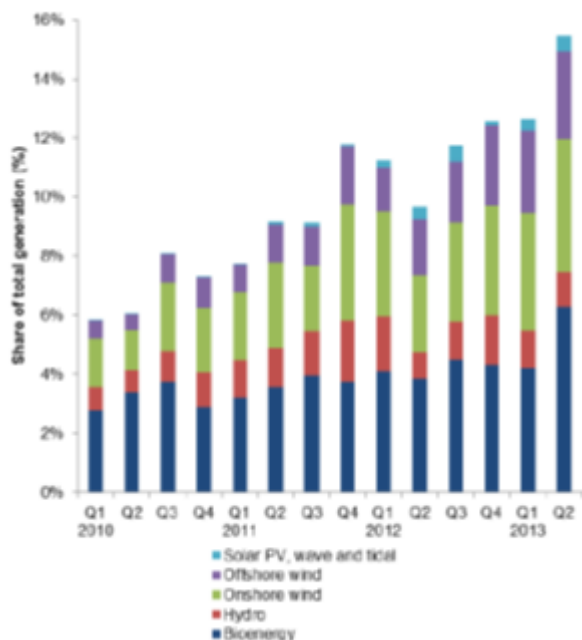
Figure 6-24: UK Renewable Electricity Share of Total Generation. Source: DECC (2014)

Although the potential for growth in the market for grid-scale energy storage is large, it will also be the one of the most competitive markets, with only one or a few technologies eventually dominating all others. As a solution for grid-level storage, ammonia seems a poor choice primarily because of its relatively low round-trip efficiency (23-41%) compared to other emerging technologies such as liquid air (50-70% round-trip efficiency) and pumped heat energy storage (72-80%). Because wind turbines make up such a large portion of stored energy costs, even large differences in the capital and operating costs of storage technologies are relatively immaterial if their round-trip efficiencies are poor. Furthermore, anticipated technology improvements even in the long-term would also be insufficient to make non-'islanded' ammonia-based renewable energy buffering economically viable.

6.3.4   'Islanded' fertiliser (Market Segment 3)

A typical farmer using AA would apply 111-196 kg to every hectare of land. Assuming a farm size of 1,000 ha[21], an average farmer would apply some 150 metric tonnes of AA to their fields annually. At this level of production, a standard-scale Haber-Bosch process would not be feasible at this level of production, but a mini-HB could be, especially on a particularly large farm or with a farm cooperative. One practical difficulty for the use of

---

[20] There are 26.4 m households in the UK as of 2013.
[21] See Figure 6-25 below.

locally produced ammonia in farming however is that since crops are fertilised with AA once or twice a year immediately before planting, roughly a year's worth of ammonia (150+ tonnes) would need to be stored on site. This is a large amount of ammonia for such a small plant, and would approximately add US$250 k to the costs of an identical size plant with standard storage.
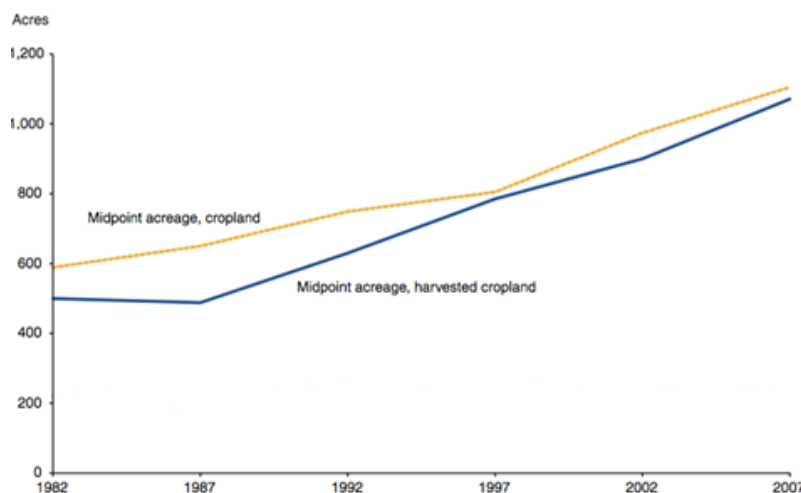
Note: 'Midpoint acreage' defined – half of all cropland acres are on farms with more cropland than the 'midpoint acreage', and half are on farms with less.

Figure 6-25: US Farm Size 1982-2007. Source: ERS calculations from unpublished census of agriculture data

The market for 'islanded' nitrogenous fertiliser that is produced and consumed on site should primarily consist of anhydrous ammonia, which unlike all other synthetic nitrogen-based fertilisers requires no further processing. Given that agricultural markets are among the most competitive markets in the world, the single largest barrier to the wider adoption of renewable-based ammonia fertiliser systems will be the issue of cost[22]. This high degree of competition will mean that even farms would struggle to unilaterally adopt more expensive technologies, such as ammonia produced from renewables.

We estimate that the levelised cost of ammonia would be 655 $/tn, or between 1.5 and 3 times as expensive as ammonia produced from natural gas – depending on location. Western Europe and the Ukraine have the highest ammonia production costs in the world[23]. Unfortunately, in these areas AA is also substantially less popular as a fertiliser than in the US. Among single nutrient fertilisers in Western Europe, ammonium nitrate and urea are the most commonly used. In 1999 anhydrous ammonia comprised only 0.5% of the Western European market (Isherwood, 2005). In order for ammonia's market share to increase in Western Europe, we would likely have to see significant price falls from current levels in order to incentivise farmers to switch. At present levels of relative

---

[22] However, at the national level a great deal of government protection is extended to agriculture, particularly in the developed world. Therefore market competition in agriculture for developed countries will be greatest within nations and free-trade groups.

[23] See Figure 6-4 above.

costs, even substantial technology improvements would be insufficient to make renewables-based ammonia directly competitive with the conventional variety.

Low-carbon regulation is also unlikely to be inadequate to bridge the gap in prices between renewables and fossil fuel-based ammonia fertiliser. Although climate change regulation has increased rapidly over the past decade (see Figure 6-26), this legislation has been weak and full of exemptions for the most polluting industries. For instance, the EU Emissions Trading Scheme has been plagued by a surfeit of permits causing price levels to fall well below intended levels. In an effort to supplement this weak price signal, the UK government introduced a carbon price floor in 2013, which was to gradually increase to 113 $/ton_$CO_2$ by 2030. However in the very next budget all future increases above 24 $/ton were indefinitely suspended. Even if the original price level of 113 $/ton was in effect today, this would barely create a level playing field for renewables and fossil fuel-based ammonia.
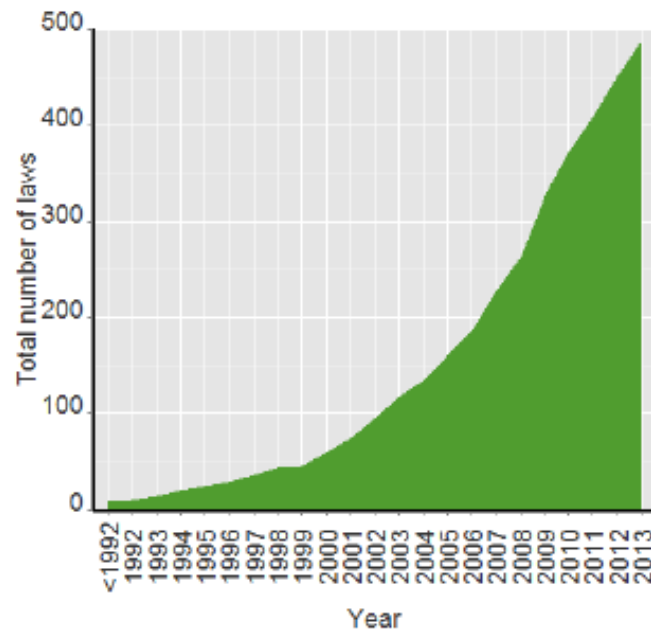
Figure 6-26: Cumulative Global Climate Change Regulations. Source: Globe International (2014)

A further difficulty with the market for ammonia fertiliser in 'islanded' locations is that the majority of industrial scale agricultural activity is located in areas with good transport links, therefore the overall market would be small. Furthermore, transporting ammonia is relatively cheap. Transcontinental shipping of ammonia costs roughly 50 $/ton and can be done with existing ocean-going ships capable of transporting 50,000 tonnes at a time. Ammonia is also cheaply transported by truck and rail. Highway trailers and rail cars are currently in use which, respectively, can hold 26.6 and 77.5 metric tonnes of ammonia (Bartels, 2008). For these reasons it is expected that the market for 'islanded' renewables-based ammonia fertiliser to be consumed on-site would be restricted to a relatively small number of locations. As in the energy storage 'stranded renewables' case, significant cost saving could be achieved by locating plants in areas with superior wind profiles. Because the wholesale price of electricity in the UK is roughly 85 $/MWh, at

current prices ammonia produced in 'islanded' locations would be most profitably sold as fertiliser rather than burned as fuel (~600 $/ton as fertiliser vs 221 $/ton as stored electricity).

6.3.5 Non-'islanded fertiliser (Market Segment 4)

At non-islanded' sites the economics of wind-based ammonia fertiliser production are even worse than the 'islanded' case. The competitiveness of agricultural markets combined with the considerable cost premium on wind-powered ammonia means that over the medium-term the market for renewables-based ammonia fertiliser will be restricted to perhaps a few niche high-end farming markets where social image is paramount.

Over a longer time-frame major corn users such as General Mills and Coca-Cola could also be pressured by consumers to decarbonise their supply chains. In this case, non-'islanded' ammonia fertiliser generated by renewables could become a focal point of broader corporate social responsibility in the agricultural sector. If this were to happen, viable markets for renewables-based ammonia would emerge even in countries with low-cost natural gas such as the US.

6.3.6 'Islanded' and energy storage and fertiliser (Market Segment 5)

This market would consist of remote farms which have a need for both renewable electricity storage _and_ ammonia fertiliser. Electricity demand on farms is generally low except following the harvest when refrigeration may be required. Fortunately, the requirement for energy and the requirement for fertiliser come at opposite ends of the growing cycle. Hence, the ammonia storage capacity necessary to accommodate both uses would be similar to the capacity required for the largest ammonia use alone (most likely as fertiliser). Even though it would still be more expensive to consume wind-generated electricity and ammonia as opposed to conventional alternatives, given the synergies of these products, there may be significant demand for such systems on certain 'islanded' locations which value simplicity. In contrast to the market for stranded renewables (market segment 1), the required size of ammonia plants for combined 'islanded' energy storage and fertiliser production will be relatively small, and likely consist almost exclusively of mini-HB technology.

6.3.7 Non-'islanded' energy storage and fertiliser (Market Segment 6)

Well-connected non-'islanded' locations will suffer higher costs for both energy and ammonia with little gain in supply security or convenience. Hence, the non-'islanded' combination ammonia energy storage and fertiliser market segment is anticipated to have the least economic potential of all the market segments studied.

6.3.8   Market Segment Analysis Summary

Given current technologies and prices, we believe that Figure 6-27 is a fair representation of the present market potential of renewables-based ammonia. The horizontal and vertical axes represent, respectively, the present and future economic competitiveness of renewables-based ammonia. All market segments' competitiveness will increase in future due to technological improvements and greater carbon pricing. From this figure we see that 'islanded' energy storage alone (bubble 1) has the greatest potential of all the relevant markets. This is because even though other technologies will be superior to ammonia as a store of energy, ammonia is the best solution for capturing the output potential of stranded renewables due to its mature transportation infrastructure. Another market (although smaller) where ammonia could have competitive advantage is 'islanded' locations where a combination of energy storage and fertiliser production is required (bubble 5). 'Islanded' ammonia fertiliser on its own (bubble 3) is less likely to be a competitive solution given the high costs of hydrolytic ammonia, and for similar reasons non-'islanded' fertiliser (bubble 4) will have even less market potential. However, should prices for natural gas and coal increase 2-3 times due to scarcity or carbon taxation, the fertiliser markets, particularly 'non-islanded' fertiliser, have the potential to become the largest of the renewables-based ammonia markets. However, this would be unlikely to happen within the next 20 years at a minimum. Non-islanded energy storage (bubble 2) is also unlikely to be an important source of demand given other superior and cheaper technologies. However, this could change if ammonia became a widespread substitute for petrol in automobiles. This is an unlikely scenario and could only come about in the long-term since both ammonia prices relative to fossil fuels would have to fall considerably and ammonia would have to end up outcompeting other automobile power sources such as batteries and biofuels. Finally, non-'islanded' energy storage and fertiliser combinations (bubble 6) represent the worst of worlds, where inefficient energy storage meets expensive fertiliser but with little compensating benefits. Therefore, it will struggle the most to make any market impact.

Only market segment 5 is viable at present, but market segment 1 would be close to viable if a 'stranded renewable' plant was located in a location with excellent wind. Market segment 3 may approach viability if technological advances are sufficient. Market segments 2 and 6 are so uncompetitive that no foreseeable combination of favourable technology improvements or legislation could make them a viable market. Market segment 4 on the other hand could achieve some traction, especially if social pressure forces the hand of large corporations which heavily utilise agricultural products, but this scenario for viability is less likely than the 'islanded' fertiliser case (market segment 3).
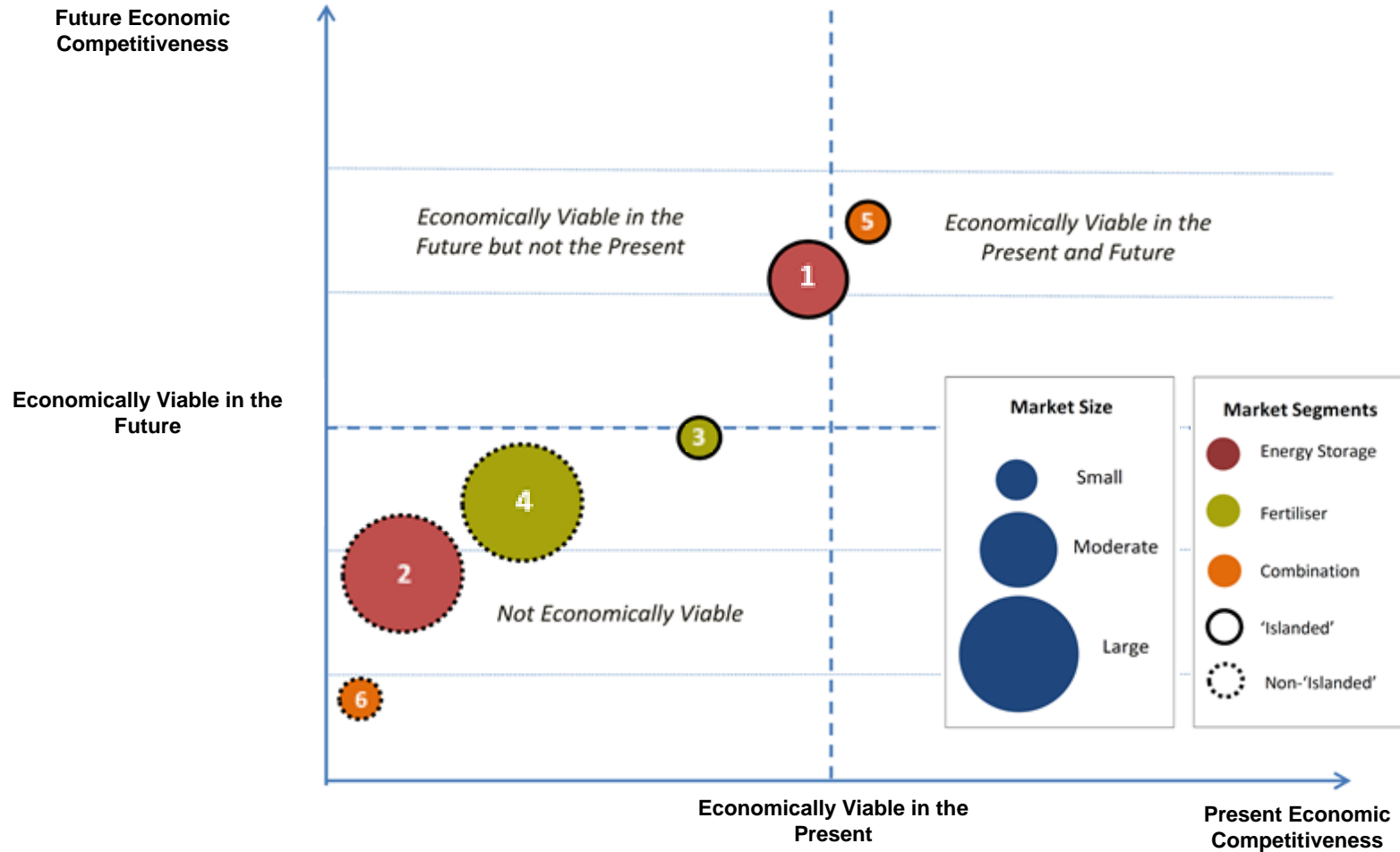
Relative Market Potential

Figure 6-27: Relative Market Potential of Market Segments 1-6

6.3.9 Energy Cost Buffering

It was also examined whether energy cost buffering in the UK could be a potential market for renewables-based ammonia. In the UK firms pay for electricity transmission costs on the national grid partly based on their electricity use during the three highest usage half-hour periods of the year, the so-called 'triad' periods. During these periods they can (ex post facto) be required to pay as much as £30KWh. Currently some energy intensive industries such as steel manufacturing attempt to predict these periods and shut-down in order to reduce this cost. Given that it may be expensive to shut-down production and that there may be synergies in steel production with hydrolysis, it was explored whether there may be potential for ammonia to serve as a profitable source of energy generation during suspected 'triad' periods. However for a number of reasons this use of ammonia would likely be infeasible.

1. In general it is possible to predict the half-hour periods[24] in which energy consumption will be highest, and since steel manufacture is a batch process which can be stopped[25], it is simple to cease production during these periods.

2. In addition, peak charges in the UK at most cost medium sized heavy electricity users a few hundred thousand pounds a year and large users a few million, while such firms would require 150-1200MWh of energy storage capacity. The cost of producing an ammonia plant that could deliver this output daily would be upwards of £100m.

3. The potential for oxygen produced in hydrolysis to be used synergistically in steel manufacturing, is less than might be otherwise anticipated because the type of furnaces which use the most electricity (arc furnaces) are not the same furnaces which use the most oxygen[26] (blast furnaces).

4. There is also a real danger that if firms became very good at reducing peak loads during 'triads' that the national grid would simply change the rules of pricing transmission, and thereby negate previous peak-shaving investments. So even if it made sense for individual firms to invest in energy storage technology, the entire market could not be expected to receive these benefits.

5. Ammonia has poor round-trip energy efficiencies compared to other technologies

---

[24] Between 4-7pm in winter months.

[25] It takes generally 50 minutes to 3 hours to go through a batch depending on the product and the mill (Sheffield Forgemasters, personal communication).

[26] Oxygen is a waste gas in the Haber-Bosch process – generated from either hydrolysis or fractional distillation of air. In steel manufacture 99% purity oxygen at 100-150 psi is used to decarburise molten iron. It is also used in smaller quantities in pulp and paper manufacturing, ceramic creation, glass-making, petroleum processing, chemical manufacturing and welding.

For these reasons the potential for energy-intensive firms to use ammonia for electricity peak-shaving is thought to be negligible.

5.1.1   Transport fuel

Ammonia also has the potential to be utilised as a transport fuel, and in the future this could represent an enormous market for renewables-based ammonia production. The economic feasibility of ammonia as a transport fuel is a complex issue, beyond the immediate scope of this report. Nevertheless what is relevant to this study is the fact that the use of ammonia as a transport fuel could in the future provide synergies with energy storage and fertiliser production, particularly on an 'islanded' case.

5.2 Conclusion

Ammonia is a poor technology for energy storage alone given its low round-trip efficiency and high production costs. Similarly, hydrolytic ammonia fertiliser cannot compete directly with fossil fuel-based ammonia, and will be unable to do so for the foreseeable future. However, ammonia does offer unique advantages in its ability to be readily transported with existing infrastructure, and the fact that its energy storage capabilities can be integrated with fertiliser production. In 'islanded' locations these two characteristics have the potential to make ammonia a viable store of energy for the exploitation of 'stranded' renewables, and a viable source of fertiliser and baseload energy in specific 'islanded' locations which demand both functions. Over the longer term a combination of technological breakthroughs, tighter low-carbon regulations, and increases in fossil fuel prices could eventually create a substantial market for non-fossil fuel-based ammonia fertiliser. But recent advances in hydraulic fracking and perennially soft CO_2 taxation globally threaten to delay such a scenario considerably.

7. Conclusions and recommendations

We conclude the report with a list of key techno-economic observations obtained from the literature review and model-based analysis carried out in this work, as well as several recommendations for future research.

7.1 Conclusions

7.1.1 Technical performance characteristics

7.1.1.1 Energy consumption and efficiency

a. *Comparative energy loss of individual units.*

Within the ranges of exergy efficiencies considered in this work for each system unit, electrolysis and NH_3-to-power conversion are always the largest and the second largest units for energy loss, followed by NH_3 synthesis, regardless of the technology options chosen. The consumption and loss at the air separation unit are very insignificant (~1%) implying little scope for noticeable improvement of the ESS from this unit.

b. *Most efficient system configuration and the key contributing factor*.

The combination of PEM-based electrolysis (lowest power consumption and highest H_2 product pressure), Ru-based NH_3 synthesis (good balance between compression power consumption and loss of materials via purging), and SOFC+GT for power generation (higher efficiency) yields a highest cycle efficiency of 41%.

c. *Opportunities for overall efficiency improvement*.

The ESS will benefit from future improvement in electrolysis and gas turbine (GT) or fuel cell based power generation, likely to be brought about by research on H_2-based energy storage. Improvement of the NH_3 synthesis loop will also contribute due to its quite sizable energy losses; options include materials and power recovery as well as optimisation of operating conditions in connection with catalysts selection for reducing compression work requirements. These options however will need to be considered not only in terms of efficiency but also in the context of a holistic economic assessment.

7.1.1.2 Systems configuration for balancing supply and demand

a. *Implication of supply and demand profiles on NH₃ production scale.*

For fixed wind power inputs and demand outputs, the configuration, size and operating conditions of the ESS are constrained. Energy deficits will result from an oversized or undersized ESS; the former because the ESS will consume too much energy and the latter because it will not produce enough ammonia.

b. *Needs for a sound operating strategy to retain balancing and feasibility.*

The two conditions for feasible operation are that (i) there are no cumulative deficits in any of the intermediate products (H_2, N_2 and NH_3), and that (ii) the demand profile is satisfied.

Given the low energy requirements of air separation in relation to those of electrolysis and the Haber-Bosch processes, the model matches stoichiometrically the production of N_2 to that of NH_3, bypassing the need for N_2 storage in the ESS. However, an overproduction of H_2 from stoichiometric levels is part of the operating strategy because it enables the ESS to bypass hydrogen production when wind power inputs are low. This is desirable because the energy consumption of the electrolysers dominates, and is possible because their wide range of operating loads.

Finally, in order to maximise the lifetime of the HB catalyst, the HB synthesis loop is operated with minimal load variations (in effect, at constant load).

c. *Implication of supply and demand profiles on storage requirement.*

Two types of storage are required as a result of the operating strategy: short-term H_2 storage (to ensure NH_3 production), and NH_3 storage (to ensure demand coverage and ESS operation at minimal loads).

7.1.1.3 Catalysts and catalytic processes

a. *HB-based ammonia synthesis.*

Fused iron catalysts still appear to be the most appropriate catalysts for the industrial Haber-Bosch process. Ru catalysts can be used in industrial practice once problems relating to H_2 poisoning and degradation of the support are solved. For the new generation of Co_3Mo_3N catalysts, further improvement in the activity would render the new process (based on renewable energy and materials) economically more viable.

b. *Non-HB based ammonia synthesis.*

Regarding the electrochemical approach to synthesize ammonia, the potential elimination of the separation and purification steps for H_2 when H_2O is used as the reductant for N_2, along with the input of electrochemical energy at milder conditions, is very attractive. However, the reported production rates are very far away from those of industrial practice using heterogeneous catalysis approaches.

c. *Ammonia decomposition.*

For the ammonia decomposition reaction, potassium promoted, CNTs supported ruthenium catalysts appear to be the most promising candidates at lower temperatures. Considering the high costs of noble metals and their preparations, low cost but highly active catalysts should be developed for the practical conversion of ammonia under industrial applicable conditions.

7.1.2   Economic cost analysis

7.1.2.1   Capital costs

The electrolysis and the NH_3-to-power units dominate the capital cost of the ESS, contributing to 60-85% of the overall CAPEX between the two (the percentage varies with the specific configuration of the ESS). The next most costly unit is the Haber-Bosch synthesis loop (5-25% of CAPEX). In turn, the HB process is dominated by either compression or catalysts costs.

7.1.2.2   Aggregated and levelised costs

The levelised cost of ammonia, LCOA, was estimated as 655 USD/ton_NH_3, i.e. between 1.5 and 3 times as expensive as ammonia from natural gas. In turn, the levelised cost of energy, LCOE, was estimated to be 251 USD/MWh. In both cases it was assumed that the wind energy cost was 50.8 USD/MWh.

7.1.2.3   Opportunities for cost reduction

Results from the sensitivity analyses indicate a number of ways in which costs can be reduced for the configurations that have been explored, all of which use current technologies. The most important opportunities are:

- Increase of catalyst activity, thereby increasing conversion at less extreme operating conditions.

- Operation of electrolisers at higher pressures; this could have significant effects in reducing compression costs in the HB synthesis loop.

145

A number of recommendations for future research (Section 7.2) considers other configurations and the use of new technologies.

7.1.3 Market and industrial analysis

7.1.3.1 Potential market segments and ranking

A ranking in terms of revenue potential is as follows:

A. 'Islanded' energy storage (as stranded renewables).

B. 'Islanded' energy storage and fertiliser production.

C. 'Islanded' fertiliser production.

D. Non-'islanded' fertiliser production.

E. Non-'islanded' energy storage.

F. Non-'islanded' energy storage and fertiliser production.

Electrochemical ammonia synthesis has the greatest potential to expand the first two markets above (A and B). In addition, as fuel costs and carbon taxes rise, this technology may even allow wind-powered ammonia to compete directly with fossil fuel-based ammonia on price alone.

7.1.3.2 Comparison with other energy storage options (excluding efficiency and cost criteria)

Advantages:

- Readily transportable

- Mature storage and transportation infrastructure

- Low discharge rates

- Additional potential uses as fertiliser and fuel

- Does not require exotic materials

Disadvantages:

- Low round-trip energy efficiency

- Deployment limited by water availability (if water input is fresh water)

- Visually imposing due to large H_2 storage tanks

7.1.3.3   Non-economic issues associated with NH_3 from renewables

- Potentially hazardous

- Unpleasant smell

- Requires significant technological improvements in order to realise full market potential

- Technological advances have greater potential than low-carbon legislation to bring renewables-based ammonia costs in line or below that of natural gas.

7.2 Recommendations for future research

1. *In-depth research on catalysts integrated with model-based engineering analysis.*

   The production of NH_3 using renewable energies and non-fossil raw materials results in new challenges (e.g. high energy consumption of electrolysis) and opportunities (e.g. "cleaner" inputs to the HB process).

   These can better be addressed by developing new catalysts and their associated processes optimised to work with them. Thus, the development of new catalysts and processes should be concomitant, with the catalyst operating conditions guiding the process design, and the bottlenecks in the process steering the development of the catalyst.

2. *Electrolysis H_2 outlet pressure optimisation.*

   This should be explored for the integrated electrolysis-NH_3 synthesis system for different operating pressures (in connection with the selection of catalyst), in order to determine the most economical H_2 outlet pressure from the electrolysis unit.

3. *N_2 feed gas purity and purge gas recovery.*

   This should be explored for the integrated ASU-NH_3 synthesis system to consider (a) ASU options leading to different levels of impurities in its N_2 product, and (b) options for recovering valuable reactants (particularly H_2) from the purged stream in the synthesis loop, taking into account both

operational savings and additional capital costs so that the overall economics can be optimised.

4. *Ramping rate limitations of system components.*

   The current study has considered the ranges of operational load of individual units when determining the dispatch/allocation of the wind power. Future research should consider additionally the dynamic limits of ramping for each unit, to devise more realistic operating strategies.

5. *Load- and scale- flexible NH_3 synthesis with electrolytic H_2.*

   In addition to the obvious need for long-term research on electrochemical NH_3 production, further short- to mid-term research on HB-type NH_3 synthesis is required with respect to load and scale flexibility. This study has adopted a rather constant load for the NH_3 synthesis loop to minimise the disturbance to the working conditions of the catalyst, which is considered desirable to maintain the performance of the catalyst. Future work may carry out a more detailed investigation on how the change in the operational load (throughput) would affect the operating conditions such as temperature, pressure, and gas distribution in the catalyst bed, hence exploring the potential of operating NH_3 synthesis with a higher load flexibility. Additional work is also required to assess more closely how changes in production scale may affect the techno-economic characteristics differentially from the power-law based trend as adopted in the current work.

6. *Economics for co-production of power, heat and NH_3.*

   On the demand side, the model-based analysis in this work has only focused power supply. Future work may carry out an economic assessment of a poly-generation system that satisfies local demands for power, heat and NH_3 (as fertiliser) with or without exports.

7. *Integration to the grid.*

   A grid-integrated ESS would most likely be substantially smaller and cheaper than one in isolation because it would not have to handle extreme events (e.g. long periods of low wind or of unusual high demand). The deficit energy could be bought from the grid in these cases. Similarly, surplus energy from the ESS could be exported to the grid instead of being thrown away.

Notation

AA	Anhydrous Ammonia
ASU	Air Separation Unit
CAPEX	Capital expenditure, capital cost
CAES	Compressed Air Energy Storage
CAGR	Cumulative Average Growth Rate
CoMoN	Cobalt/Molybdenum bimetallic Nitride catalyst (Co_3Mo_3N)
CNTs	Carbon Nanotubes
CRF	Capital Return Factor
ESS	Energy Storage System
Fe	Iron
GT	Gas Turbine
H_2	Hydrogen
HB	Haber-Bosch process
HEX	Heat Exchanger
HHV	High Heating Value
LCOA	Levelised Cost of Ammonia
LCOE	Levelised Cost of Energy (in this case onshore wind)
LHV	Low Heating Value
MVC	Mechanical Vapour Compression
N_2	Nitrogen
NaS	Sodium-Sulfur
NH_3	Ammonia
OPEX	Operating expenditure; operating cost
PEM	Proton Exchange Membrane
PSA	Pressure Swing Adsorption
Ru	Ru
SMH	Sodium Metal Halide
STP	Standard Pressure and Temperature

References

Adams II, T.A., Nease, J., Tucker, D., Barton, P.I., 2013. Energy conversion with solid oxide fuel cell systems: A review of concepts and outlooks for the short- and long-term. Ind. Eng. Chem. Res. 52, 3089–3111. doi:10.1021/ie300996r

Amar, I.A., Lan, R., Petit, C.T.G., Tao, S., 2011. Solid-state electrochemical synthesis of ammonia: a review. J. Solid State Electrochem. 15, 1845–1860. doi:10.1007/s10008-011-1376-x

Appl, 2012. Ammonia, 2. Production Processes, in: Ullmann's Encyclopedia of Industrial Chemistry. Wiley-VCH Verlag GmbH & Co. KGaA, Weinheim, Germany.

Appl, M., 1999. Ammonia. Principles and Industrial Practice. Wiley--VCH.

Bakker, R., Pedersen, E., va den Berg, G., Stewart, R., Lok, W., Bouma, J., 2012. Impact of wind turbine sound on annoyance, self-reported sleep disturbance and psychological distress. Sci. Total Environ. 425, 42–51.

Bartels, J., 2008. A feasibility study of implementing an Ammonia Economy.pdf.

Benner, J., van Lieshout, M., Croezen, H., 2012. Identifying Breakthrough Technologies for the Production of Basic Chemicals. A Long Term View on the Sustainable Production of Ammonia, Olefins and Aromatics in the European Region. University of Delft, CE Delft.

Bensmann, B., Hanke-Rauschenbach, R., Peña Arias, I.K., Sundmacher, K., 2013. Energetic evaluation of high pressure PEM electrolyzer systems for intermediate storage of renewable energies. Electrochimica Acta 110, 570–580. doi:10.1016/j.electacta.2013.05.102

Bradford, M., 1997. Kinetics of NH3Decomposition over Well Dispersed Ru. J. Catal. 172, 479–484. doi:10.1006/jcat.1997.1877

Brown, D.E., Edmonds, T., Joyner, R.W., McCarroll, J.J., Tennison, S.R., 2014. The Genesis and Development of the Commercial BP Doubly Promoted Catalyst for Ammonia Synthesis. Catal. Lett. 144, 545–552. doi:10.1007/s10562-014-1226-4

Carmo, M., Fritz, D.L., Mergel, J., Stolten, D., 2013. A comprehensive review on PEM water electrolysis. Int. J. Hydrog. Energy 38, 4901–4934. doi:10.1016/j.ijhydene.2013.01.151

Castle, W.F., 2002. Air separation and liquefaction: recent developments and prospects for the beginning of the new millennium. Int. J. Refrig. 25, 158–172.

Center for European Policy Studies, 2014. Study on Composition and Drivers of Energy Prices and Costs in Energy Intensive Industries: The Case of the Chemical Industry - Ammonia.

Chellappa, A.., Fischer, C.., Thomson, W.., 2002. Ammonia decomposition kinetics over Ni-Pt/Al2O3 for PEM fuel cell applications. Appl. Catal. Gen. 227, 231–240. doi:10.1016/S0926-860X(01)00941-3

Chen, C., Ma, G., 2009. Proton conduction in BaCe1−xGdxO3−α at intermediate temperature and its application to synthesis of ammonia at atmospheric pressure. J. Alloys Compd. 485, 69–72. doi:10.1016/j.jallcom.2009.05.108

Chen, H.-B., Lin, J.-D., Cai, Y., Wang, X.-Y., Yi, J., Wang, J., Wei, G., Lin, Y.-Z., Liao, D.-W., 2001. Novel multi-walled nanotubes-supported and alkali-promoted

Ru catalysts for ammonia synthesis under atmospheric pressure. Appl. Surf. Sci. 180, 328–335. doi:10.1016/S0169-4332(01)00374-9

Chen, H., Cong Ngoc, T., Yang, W., Tan, C., Li, Y., Ding, Y., 2009. Progress in electrical energy storage system: A critical review. Prog. Nat. Sci. 19.

Choudhary, T.V., Sivadinarayana, C., Goodman, D.W., 2001. Catalytic ammonia decomposition: COx-free hydrogen production for fuel cell applications. Catal. Lett. 72, 197–201.

Chung, Y., Na, B.-K., Song, H.K., 1998. Short-cut evaluation of pressure swing adsorption systems. Comput. Chem. Eng. 22, S637–S640.

Dahl, S., Logadottir, A., Egeberg, R., Larsen, J., Chorkendorff, I., Törnqvist, E., Nørskov, J., 1999. Role of Steps in N2 Activation on Ru(0001). Phys. Rev. Lett. 83, 1814–1817. doi:10.1103/PhysRevLett.83.1814

Dahl, S., Sehested, J., Jacobsen, C., Tornqvist, E., Chorkendorff, I., 2000. Surface science based microkinetic analysis of ammonia synthesis over ruthenium catalysts. J. Catal. 192, 391–399. doi:10.1006/jcat.2000.2857

David, W.I.F., Makepeace, J.W., Callear, S.K., Hunter, H.M.A., Taylor, J.D., Wood, T.J., Jones, M.O., 2014. Hydrogen Production from Ammonia Using Sodium Amide. J. Am. Chem. Soc. 140622080101000. doi:10.1021/ja5042836

DECC, 2014. UK Renewable Energy Roadmap: Update 2013.

Department of Enterprise, Trade and Investment and Department of Communications, Energy and Natural Sources, 2008. All Island Grid Study.

Diaz-Gonzales, F., Sumper, A., Gomis-Bellmunt, O., Villafafila-Robles, R., 2012. A review of energy storage technologies for wind power applications. Renew. Sustain. Energy Rev. 16, 2154–2171.

Dincer, I., Rosen, M., 2007. Exergy. Energy, Environment and Sustainable Development. Elsevier.

Energy Information Administration (EIA), 2013. Updated Capital Cost Estimates for Utility Scale Electricity Generating Plants. U.S. Department of Energy, Washington, DC.

Erisman, J.W., Sutton, M.A., Galloway, J., Klimont, Z., Winiwarter, W., 2008. How a century of ammonia synthesis changed the world. Nat. Geosci. 1, 636–639. doi:10.1038/ngeo325

European Commission, 2014. The Future Role and Challenges of Energy Storage.

Evans, A., Strezov, V., Evans, T., 2012. Assessment of utility energy storage options for increased renewable energy penetration. Renew. Sustain. Energy Rev. 6. doi:10.1016/j.rser.2012.03.048

EWEA, 2014. Wind in Power: 2013 European Statistics.

Farbouda, A., Crunkhorna, R., Trinidadea, A., 2013. "Wind turbine syndrome": fact or fiction? J. Laryngol. Otol. 127, 222–226.

Fernández, C., Sassoye, C., Debecker, D.P., Sanchez, C., Ruiz, P., 2014. Effect of the size and distribution of supported Ru nanoparticles on their activity in ammonia synthesis under mild reaction conditions. Appl. Catal. Gen. 474, 194–202. doi:10.1016/j.apcata.2013.09.039

Feyen, M., Weidenthaler, C., Güttel, R., Schlichte, K., Holle, U., Lu, A.-H., Schüth, F., 2011. High-Temperature Stable, Iron-Based Core-Shell Catalysts for Ammonia Decomposition. Chem. - Eur. J. 17, 598–605. doi:10.1002/chem.201001827

Finlayson, B.A., 2012. Introduction to Chemical Engineering Computing, 2nd Edition edition. ed. Wiley-Blackwell, Hoboken, N.J.

Gibbons, S., 2014. Gone with the Wind: Valuing the Visual Impacts of Wind Turbines through House Prices. SERC Discuss. Pap. April.

Giddey, S., Badwal, S.P.S., Kulkarni, A., 2013. Review of electrochemical ammonia production technologies and materials. Int. J. Hydrog. Energy 38, 14576–14594. doi:10.1016/j.ijhydene.2013.09.054

Globe International, 2014. The GLOBE Climate Legislation Study: A Review of Climate Change Legislation in 66 Countries, 4th ed.

Grundt, T., Christiansen, K., 1982. Hydrogen by water electrolysis as basis for small scale ammonia production. A comparison with hydrocarbon based technologies. Int. J. Hydrog. Energy 7, 247–257.

Guan, S., Liu, H.Z., 2000. Effect of an Iron Oxide Precursor on the N_2 Desorption Performance for an Ammonia Synthesis Catalyst †. Ind. Eng. Chem. Res. 39, 2891–2895. doi:10.1021/ie990695g

Guthrie, K.M., 1974. Process Plant Estimating Evaluation and Control. Craftsman Book Company of America.

Gutiérrez-Martín, F., Confente, D., Guerra, I., 2010. Management of variable electricity loads in wind – Hydrogen systems: The case of a Spanish wind farm. Int. J. Hydrog. Energy 35, 7329–7336. doi:10.1016/j.ijhydene.2010.04.181

Gutiérrez-Martín, F., García-De María, J.M., Baïri, A., Laraqi, N., 2009. Management strategies for surplus electricity loads using electrolytic hydrogen. Int. J. Hydrog. Energy 34, 8468–8475. doi:10.1016/j.ijhydene.2009.08.018

Hagen, S., 2003. Ammonia synthesis with barium-promoted iron–cobalt alloys supported on carbon. J. Catal. 214, 327–335. doi:10.1016/S0021-9517(02)00182-3

Hansen, T.W., Hansen, P.L., Dahl, S., Jacobsen, C.J., 2002. Support effect and active sites on promoted ruthenium catalysts for ammonia synthesis. Catal. Lett. 84, 7–12.

Harrison, K.W., Martin, G.D., Ramsden, T.G., Kramer, W.E., Novachek, F.J., 2009. The wind-to-hydrogen project: operational experience, performance testing, and systems integration. Natl. Renew. Energy Lab. Gold. CO2009 Mar Rep. No NRELTP55044082 Contract No DEAC3608G028308 200–211.

Hellman, A., Baerends, E.J., Biczysko, M., Bligaard, T., Christensen, C.H., Clary, D.C., Dahl, S., van Harrevelt, R., Honkala, K., Jonsson, H., Kroes, G.J., Luppi, M., Manthe, U., Nørskov, J.K., Olsen, R.A., Rossmeisl, J., Skúlason, E., Tautermann, C.S., Varandas, A.J.C., Vincent, J.K., 2006. Predicting Catalysis: Understanding Ammonia Synthesis from First-Principles Calculations. J. Phys. Chem. B 110, 17719–17735. doi:10.1021/jp056982h

Hildmann, H., Saffre, F., 2011. Influence of variable supply and load flexibility on Demand-Side Management, in: Energy Market (EEM), 2011 8th International Conference on the European. Presented at the Energy Market (EEM), 2011 8th International Conference on the European, pp. 63–68. doi:10.1109/EEM.2011.5952980

Honkala, K., 2005. Ammonia Synthesis from First-Principles Calculations. Science 307, 555–558. doi:10.1126/science.1106435

Huazhang, L., Caibo, L., Xiaonian, L., Yaqing, C., 2003. Effect of an Iron Oxide Precursor on the H$_2$ Desorption Performance for an Ammonia Synthesis Catalyst. Ind. Eng. Chem. Res. 42, 1347–1349. doi:10.1021/ie0202524

Hughes, 2013. Project Proposal: Green NH3 for a Post Fossil Economy (Internal report).

Hwang, D.-Y., Mebel, A.M., 2003. Reaction Mechanism of N$_2$/H$_2$ Conversion to NH$_3$: A Theoretical Study. J. Phys. Chem. A 107, 2865–2874. doi:10.1021/jp0270349

IMechE, 2014. Energy Storage: The Missing Link in the UK's Energy Commitments. Institution of Mechanical Engineers.

Isherwood, K., 2005. Fertilizer Use in Western Europe: Types and Amounts. Encycl. Life Support Syst., Agricultural Sciences.

Itoh, M., Masuda, M., Machida, K., 2002. Hydrogen Generation by Ammonia Cracking with Iron Metal-Rare Earth Oxide Composite Catalyst. Mater. Trans. 43, 2763–2767. doi:10.2320/matertrans.43.2763

Ivanova, S., Lewis, R., 2012. Producing Nitrogen via Pressure Swing Adsorption.

Jacobsen, C.J.., 2001. Boron Nitride: A Novel Support for Ruthenium-Based Ammonia Synthesis Catalysts. J. Catal. 200, 1–3. doi:10.1006/jcat.2001.3200

Jacobsen, C.J.., Dahl, S., Hansen, P.L., Törnqvist, E., Jensen, L., Topsøe, H., Prip, D.V., Møenshaug, P.B., Chorkendorff, I., 2000. Structure sensitivity of supported ruthenium catalysts for ammonia synthesis. J. Mol. Catal. Chem. 163, 19–26. doi:10.1016/S1381-1169(00)00396-4

Jacobsen, C.J.H., 2000. Novel class of ammonia synthesis catalysts. Chem. Commun. 1057–1058. doi:10.1039/b002930k

Jacobsen, C.J.H., Dahl, S., Clausen, B.S., Bahn, S., Logadottir, A., Nørskov, J.K., 2001. Catalyst Design by Interpolation in the Periodic Table: Bimetallic Ammonia Synthesis Catalysts. J. Am. Chem. Soc. 123, 8404–8405. doi:10.1021/ja010963d

Jensen, J.O., Bandur, V., Bjerrum, N., Jensen, S.H., Ebbesen, S., Mogesen, M., Tophøj, N., Yde, 2008. Pre-Investigation of Water Electrolysis (No. PSO-F&U 2006-1-6287). Technical University of Denmark (DTU), Department of Chemistry.

Kitano, M., Inoue, Y., Yamazaki, Y., Hayashi, F., Kanbara, S., Matsuishi, S., Yokoyama, T., Kim, S.-W., Hara, M., Hosono, H., 2012. Ammonia synthesis using a stable electride as an electron donor and reversible hydrogen store. Nat. Chem. 4, 934–940. doi:10.1038/nchem.1476

Knorr, B., 2014. Weekly fertilizer.

Kojima, R., Aika, K., 2000. Cobalt Molybdenum Bimetallic Nitride Catalysts for Ammonia Synthesis. Chem. Lett. 514–515. doi:10.1246/cl.2000.514

Kojima, R., Aika, K., 2001a. Cobalt molybdenum bimetallic nitride catalysts for ammonia synthesis. Appl. Catal. Gen. 215, 149–160. doi:10.1016/S0926-860X(01)00529-4

Kojima, R., Aika, K., 2001b. Cobalt molybdenum bimetallic nitride catalysts for ammonia synthesis. Appl. Catal. Gen. 218, 121–128. doi:10.1016/S0926-860X(01)00626-3

Kojima, R., Aika, K., 2001c. Cobalt molybdenum bimetallic nitride catalysts for ammonia synthesis. Appl. Catal. Gen. 219, 157–170. doi:10.1016/S0926-860X(01)00678-0

Kowalczyk, Z., Jodzis, S., 1990. Activity and thermoresistance of fused iron catalysts for ammonia synthesis. Appl. Catal. 58, 29–34. doi:10.1016/S0166-9834(00)82276-9

Kowalczyk, Z., Jodzis, S., Raróg, W., Zieliński, J., Pielaszek, J., Presz, A., 1999. Carbon-supported ruthenium catalyst for the synthesis of ammonia. The effect of the carbon support and barium promoter on the performance. Appl. Catal. Gen. 184, 95–102. doi:10.1016/S0926-860X(99)00090-3

Liang, C., Li, W., Wei, Z., Xin, Q., Li, C., 2000. Catalytic Decomposition of Ammonia over Nitrided MoNx/α-Al $_2$ O $_3$ and NiMoNy/α-Al $_2$ O $_3$ Catalysts. Ind. Eng. Chem. Res. 39, 3694–3697. doi:10.1021/ie990931n

Liang, C., Wei, Z., Xin, Q., Li, C., 2001. Ammonia synthesis over Ru/C catalysts with different carbon supports promoted by barium and potassium compounds. Appl. Catal. Gen. 208, 193–201. doi:10.1016/S0926-860X(00)00713-4

Li, L., Zhu, Z.H., Wang, S.B., Yao, X.D., Yan, Z.F., 2009. Chromium oxide catalysts for COx-free hydrogen generation via catalytic ammonia decomposition. J. Mol. Catal. Chem. 304, 71–76. doi:10.1016/j.molcata.2009.01.026

Li, L., Zhu, Z.H., Yan, Z.F., Lu, G.Q., Rintoul, L., 2007. Catalytic ammonia decomposition over Ru/carbon catalysts: The importance of the structure of carbon support. Appl. Catal. Gen. 320, 166–172. doi:10.1016/j.apcata.2007.01.029

Liu, H.-Z., Li, X.-N., Hu, Z.-N., 1996. Development of novel low temperature and low pressure ammonia synthesis catalyst. Appl. Catal. Gen. 142, 209–222. doi:10.1016/0926-860X(96)00047-6

Liu, R., Xie, Y., Wang, J., Li, Z., Wang, B., 2006. Synthesis of ammonia at atmospheric pressure with Ce0.8M0.2O2−δ (M=La, Y, Gd, Sm) and their proton conduction at intermediate temperature. Solid State Ion. 177, 73–76. doi:10.1016/j.ssi.2005.07.018

Li, Y., Liu, S., Yao, L., Ji, W., Au, C.-T., 2010. Core-shell structured iron nanoparticles for the generation of COx-free hydrogen via ammonia decomposition. Catal. Commun. 11, 368–372. doi:10.1016/j.catcom.2009.11.003

Li, Z., Liu, R., Wang, J., Xu, Z., Xie, Y., Wang, B., 2007. Preparation of double-doped BaCeO $_3$ and its application in the synthesis of ammonia at atmospheric pressure. Sci. Technol. Adv. Mater. 8, 566–570. doi:10.1016/j.stam.2007.08.009

Lu, A.-H., Nitz, J.-J., Comotti, M., Weidenthaler, C., Schlichte, K., Lehmann, C.W., Terasaki, O., Schüth, F., 2010. Spatially and Size Selective Synthesis of Fe-Based Nanoparticles on Ordered Mesoporous Supports as Highly Active and Stable Catalysts for Ammonia Decomposition. J. Am. Chem. Soc. 132, 14152–14162. doi:10.1021/ja105308e

Malavasi, L., Fisher, C.A.J., Islam, M.S., 2010. Oxide-ion and proton conducting electrolyte materials for clean energy applications: structural and mechanistic features. Chem. Soc. Rev. 39, 4370. doi:10.1039/b915141a

Marnellos, G., 1998. Ammonia Synthesis at Atmospheric Pressure. Science 282, 98–100. doi:10.1126/science.282.5386.98

Marnellos, G., Kyriakou, A., Florou, F., Angelidis, T., Stoukides, M., 1999. Polarization studies in the Pd|SrCe0.95Yb0.05O2.975|Pd proton conducting solid electrolyte cell. Solid State Ion. 125, 279–284. doi:10.1016/S0167-2738(99)00186-1

Marnellos, G., Sanopoulou, O., Rizou, A., Stoukides, M., 1997. The use of proton conducting solid electrolytes for improved performance of hydro- and dehydrogenation reactors. Solid State Ion. 97, 375–383. doi:10.1016/S0167-2738(97)00088-X

Mary, S., Kappenstein, C., Balcon, S., Rossignol, S., Gengembre, E., 1999. Monopropellant decomposition catalysts. I. Ageing of highly loaded Ir/Al2O3 catalysts in oxygen and steam. Influence of chloride content1These results have been originally published at the 34th AIAA/ASME/SAE/ASEE Joint Propulsion Conference of the American Institute of Aeronautics and Astronautics, Cleveland, OH, July 1998 (Paper 98-3666).1. Appl. Catal. Gen. 182, 317–325. doi:10.1016/S0926-860X(99)00019-8

Mini Ammonia Production Unit Presentation, 2010.

Morgan, E., 2013. Techno-Economic Feasibility Study of Ammonia Plants Powered by Offshore Wind (PhD). University of Massachusetts - Amherst.

Morgan, E., Manwell, J., McGowan, J., 2014. Wind-powered ammonia fuel production for remote islands: A case study. Renew. Energy 72, 51–61. doi:10.1016/j.renene.2014.06.034

Navigant Research, 2013. Energy Storage for Wind Solar Integration: Market Issues, Business Case Analysis, Technology Issues, and Forecasts for Energy Storage Systems for Wind and Solar Applications.

Orkney Sustainable Energy, 2014. Personal Communicaton.

Panagos, E., Voudouris, I., Stoukides, M., 1996. Modelling of equilibrium limited hydrogenation reactions carried out in H+ conducting solid oxide membrane reactors. Chem. Eng. Sci. 51, 3175–3180. doi:10.1016/0009-2509(96)00216-3

Pan, C., Li, Y., Jiang, W., Liu, H., 2011. Effects of Reaction Conditions on Performance of Ru Catalyst and Iron Catalyst for Ammonia Synthesis. Chin. J. Chem. Eng. 19, 273–277. doi:10.1016/S1004-9541(11)60165-1

Patel, H.C., Woudstra, T., Aravind, P.V., 2012. Thermodynamic Analysis of Solid Oxide Fuel Cell Gas Turbine Systems Operating with Various Biofuels. Fuel Cells 12, 1115–1128. doi:10.1002/fuce.201200062

Peters, M.S., Timmerhaus, K.D., West, R.E., 2003. Plant Design and Economics for Chemical Engineers, 3 edition. ed. McGraw-Hill Higher Education, New York.

Pike Research, 2009. Microgrids: Islanded Power Grids and Distributed Generation for Community, Commercial, and Institutional Applications.

Potashcorp, 2013. Overview of Potashcorp and its Industry.

Proton OnSite, n.d. C Series. Hydrogen Generation Systems.

Roy, A., Watson, S., Infield, D., 2006. Comparison of electrical energy efficiency of atmospheric and high-pressure electrolysers. Int. J. Hydrog. Energy 31, 1964–1979. doi:10.1016/j.ijhydene.2006.01.018

Salvatore, J., 2013. World Energy Perspective. Cost of Energy Technologies. World Energy Council, London.

Sankararao, B., Gupta, S.K., 2007. Multi-Objective Optimization of Pressure Swing Adsorbers for Air Separation. Ind. Eng. Chem. Res. 46, 3751–3765. doi:10.1021/ie0615180

Seetharamulu, P., Siva Kumar, V., Padmasri, A.H., David Raju, B., Rama Rao, K.S., 2007. A highly active nano-Ru catalyst supported on novel Mg–Al hydrotalcite precursor for the synthesis of ammonia. J. Mol. Catal. Chem. 263, 253–258. doi:10.1016/j.molcata.2006.08.071

Skodra, A., Stoukides, M., 2009. Electrocatalytic synthesis of ammonia from steam and nitrogen at atmospheric pressure. Solid State Ion. 180, 1332–1336. doi:10.1016/j.ssi.2009.08.001

Smith, A.R., Klosek, J., 2001. A review of air separation technologies and their integration with energy conversion processes. Fuel Process. Technol. 70, 115–134.

Spencer, N., 1982. Iron single crystals as ammonia synthesis catalysts: Effect of surface structure on catalyst activity. J. Catal. 74, 129–135. doi:10.1016/0021-9517(82)90016-1

Staffell, I., 2011. The Energy and Fuel Data Sheet.

Step, G.K., Petrovichev, M.V., 2002. Pressure swing adsorption for air separation and purification. Chem. Pet. Eng. 38, 154–158.

Stoll, R.E., von Linde, F., 2000. Hydrogen - what are the costs? Hydrocarb. Process. 42–46.

Strongin, D., 1987. The importance of C7 sites and surface roughness in the ammonia synthesis reaction over iron. J. Catal. 103, 213–215. doi:10.1016/0021-9517(87)90109-6

Taylor, P., Bolton, R., Stone, D., Zhang, X.-P., Martin, C., Upham, P., 2012. Pathways for energy storage in the UK.

The Fertilizer Institute, 2013. The History of Ammonia to 2012.

Turton, R., Bailie, R.C., Whiting, W.B., Shaeiwitz, J.A., 2008. Analysis, Synthesis and Design of Chemical Processes, 3 edition. ed. Prentice Hall, Upper Saddle River, N.J.

Ulrich, G.D., 1984. A Guide to Chemical Engineering Process Design and Economics. John Wiley & Sons, New York.

Ursúa, A., Marroyo, L., Gubía, E., Gandía, L.M., Diéguez, P.M., Sanchis, P., 2009. Influence of the power supply on the energy efficiency of an alkaline water electrolyser. Int. J. Hydrog. Energy 34, 3221–3233. doi:10.1016/j.ijhydene.2009.02.017

US Department of Energy, 2008. 20 Percent Energy by 2030 Report. Technical Report DOE/GO-102008-2567, July.

Wang, B.H., Wang, J.D., Liu, R., Xie, Y.H., Li, Z.J., 2006. Synthesis of ammonia from natural gas at atmospheric pressure with doped ceria–Ca3(PO4)2–K3PO4 composite electrolyte and its proton conductivity at intermediate temperature. J. Solid State Electrochem. 11, 27–31. doi:10.1007/s10008-005-0042-6

Wang, Z., Liu, B., Lin, J., 2013. Highly effective perovskite-type BaZrO3 supported Ru catalyst for ammonia synthesis. Appl. Catal. Gen. 458, 130–136. doi:10.1016/j.apcata.2013.03.037

Wang, Z., Ma, Y., Lin, J., 2013. Ruthenium catalyst supported on high-surface-area basic ZrO2 for ammonia synthesis. J. Mol. Catal. Chem. 378, 307–313. doi:10.1016/j.molcata.2013.07.003

Weidou, N., Zhen, C., 2011. Synergistic utilization of coal and other energy - Key to low carbon economy. Energy 5, 1–19.

Wiessner, F.G., 1988. Basics and industrial applications of pressure swing adsorption (PSA), the modern way to separate gas. Gas Sep. Purif. 2, 115–119.

Worrell, Price, L., Neelis, M., Galitsky, C., Zhou, N., 2007. World best practice energy intensity values for selected industrial sectors.

Xu, G., Liu, R., 2009. Sm $_{1.5}$ Sr $_{0.5}$ MO $_4$ (M=Ni, Co, Fe) Cathode Catalysts for Ammonia Synthesis at Atmospheric Pressure and Low Temperature. Chin. J. Chem. 27, 677–680. doi:10.1002/cjoc.200990111

Xu, Q.-C., Lin, J.-D., Fu, X.-Z., Liao, D.-W., 2008. Effects of solvent stabilizer in the preparation of highly active potassium-promoted Ru/MgO catalysts for ammonia synthesis. Catal. Commun. 9, 1214–1218. doi:10.1016/j.catcom.2007.11.005

Yang, X.-L., Zhang, W.-Q., Xia, C.-G., Xiong, X.-M., Mu, X.-Y., Hu, B., 2010. Low temperature ruthenium catalyst for ammonia synthesis supported on BaCeO3 nanocrystals. Catal. Commun. 11, 867–870. doi:10.1016/j.catcom.2010.03.008

Yin, S., 2004. Nano Ru/CNTs: a highly active and stable catalyst for the generation of COx-free hydrogen in ammonia decomposition. Appl. Catal. B Environ. 48, 237–241. doi:10.1016/j.apcatb.2003.10.013

Yin, S.F., Xu, B.Q., Zhou, X.P., Au, C.T., 2004. A mini-review on ammonia decomposition catalysts for on-site generation of hydrogen for fuel cell applications. Appl. Catal. Gen. 277, 1–9. doi:10.1016/j.apcata.2004.09.020

Yin, S.-F., Zhang, Q.-H., Xu, B.-Q., Zhu, W.-X., Ng, C.-F., Au, C.-T., 2004. Investigation on the catalysis of COx-free hydrogen generation from ammonia. J. Catal. 224, 384–396. doi:10.1016/j.jcat.2004.03.008

YouGov, 2010. Wind Power, survey conducted on behalf of Scottish Power.

Zhang, L., Lin, J., Ni, J., Wang, R., Wei, K., 2011. Highly efficient Ru/Sm2O3-CeO2 catalyst for ammonia synthesis. Catal. Commun. 15, 23–26. doi:10.1016/j.catcom.2011.08.003

Zheng, W., Zhang, J., Xu, H., Li, W., 2007. NH3 Decomposition Kinetics on Supported Ru Clusters: Morphology and Particle Size Effect. Catal. Lett. 119, 311–318. doi:10.1007/s10562-007-9237-z

Zheng, Y., Zheng, Y., Li, Z., Yu, H., Wang, R., Wei, K., 2009. Preparations of C/SiC composites and their use as supports for Ru catalyst in ammonia synthesis. J. Mol. Catal. Chem. 301, 79–83. doi:10.1016/j.molcata.2008.11.009